The Influence of Center of Mass Velocity Redirection on Mechanical and Metabolic Performance During Walking

by

Peter Gabriel Adamczyk

A dissertation submitted in partial fulfillment
of the requirements for the degree of
Doctor of Philosophy
(Mechanical Engineering)
in The University of Michigan
2008

Doctoral Committee:

Associate Professor Arthur D. Kuo, Chair
Professor Gregory M. Hulbert
Professor Sridhar Kota
Associate Professor Daniel P. Ferris

© Peter Gabriel Adamczyk, 2008

Acknowledgements

My most special thanks go to my wife Marianne, who told me I was going to make it even when I almost gave up, and to my daughter Cecilia, who did her best to distract but inspired me instead. I Love You both!

Thank you also to Professor Kuo for the careful mentorship throughout the Ph.D. program, and for strategic boosts of confidence when I needed them most. Thanks to my fellow Kuolings, especially Steve and Shawn, for the in-depth criticism and robust support you provided all along. And thanks to Professor Ferris and the Ferrisites for allowing me to take up so much lab space and time, and for providing effective guidance from a more clinical perspective.

Finally, thank you to my family. Mom and Dad, thank you for your encouragement and generous support all the way, and for believing in me since I was little. Thanks to Mark for reminding me to “be a finisher!” Thanks to Mandy for emotional support at all the tough spots. And thanks to Max for keeping up good humor and high spirits all the way!

Table of Contents

List of Figures

Figure

Abstract

The Influence of Center of Mass Velocity Redirection
on Mechanical and Metabolic Performance During Walking

by

Peter Gabriel Adamczyk

Chair: Arthur D. Kuo

The work the legs perform on the body center of mass (COM) is an important determinant of the metabolic cost of walking. Much COM work is performed to redirect the center of mass from a downward to an upward velocity during transitions between successive stance legs, termed *step-to-step transitions*. We elucidate the links between COM velocity fluctuation, COM work, and metabolic cost through several experimental manipulations of gait.

We show that foot length and foot bottom curvature affect COM work and metabolic cost in fixed-ankle walking. In dynamic walking models, longer feet lead to decreased work requirements for gait. We measured COM work and metabolic cost while subjects walked with locked ankles and artificial foot bottom shapes. COM work decreases with increasing foot length, because longer feet reduce the angular redirection of COM

velocity during the step-to-step transition. Foot bottom curvature has no significant effect for humanlike foot sizes. In this range, COM work using arc shapes is less than for normal walking, though metabolic cost is higher. Metabolic cost is minimized by feet having length 28% of leg length.

We also show that COM work for mechanically unconstrained walking depends on COM speed and angular redirection of COM velocity during the step-to-step transition. We measured variations in COM velocity while subjects walked at a wide range of speeds and step lengths. COM work scales quadratically with COM speed at heel strike times angular redirection of COM velocity. We introduce a sagittal plane plot of COM velocity trajectory, called a hodograph, to visualize these variables and understand abnormal gait.

We use these hodographs to show that unilateral transtibial amputees walk asymmetrically with respect to several kinetic variables of gait. Amputees exhibit higher mid-stance COM speed and weaker push-off on the prosthetic side, and more positive and negative step-to-step transition COM work on the intact side.

Finally, we introduce the Rock'N'Lock foot, a reconfigurable foot prosthesis that implements a rigid foot bottom shape with the goal of reducing metabolic cost. In preliminary results this foot has cost equal to other prostheses', but forthcoming design improvements may lower the cost further.

Chapter 1

Introduction

This dissertation is a story about work. Specifically, it is another chapter in our understanding of how the body performs mechanical work to move itself around, and how that work contributes to the metabolic cost of motion. Among the variety of mechanical functions the body performs, work performed against the rest of the universe is relatively easy to measure, but relatively difficult to understand. Because work is linked to force, motion and changes in energy, all of these are often mistaken for it. But far from having identical roles, these three interact with the work the body performs to accomplish a person's many tasks with minimum metabolic cost. We have chosen to study the body's work against the outside world in a few very simple cases of walking locomotion, in the hope that we would learn how to economically restore or substitute for these interactions when they are lost or impaired in different individuals. We have found, to our surprise, that in the special case of lost ankle motion a passive force can eliminate the need for some of the body's usual work, and could potentially reduce the cost of walking. This dissertation describes our findings, and our latest efforts to implement the

principles we have learned in a prosthetic foot designed to save energy for amputees in walking.

Some systems of two or three linked pendulums, if put in motion with appropriate position and velocity, will progress through a trajectory that is very similar to the motion of the human legs during walking (Mochon, 1980). Within stricter limits, some such systems can also repeat the movement after the heel strikes the ground, resetting their initial conditions automatically based on collision dynamics. These machines, called *passive dynamic walkers*, walk cyclically down a shallow slope under only the force of gravity, mimicking the action of the human legs in walking (McGeer, 1990a, 1990b). In computer models and in physical robots, this walking motion is purely passive – the machines roll on the ground with circular feet while the various links pivot at the joints without actuation. The downhill force of gravity adds just enough energy during each step to offset the kinetic energy lost when the swing leg collides with the ground. This sequence of events – a passive rolling and swinging motion, followed by a dissipative transition to the next step – resembles human gait so well that it is a useful and insightful paradigm under which to consider mechanical energy use in human walking.

The amount of energy used to power such a model at a given speed and step length is greatly reduced if the power comes from an impulsive push-off force under the trailing leg just before opposite heel strike instead of from gravity (Kuo, 2002). This pattern of activity, in which one leg pushes off just before the other leg lands is characteristic of human gait as well. Trends in the amount of work performed by the human legs on the body's center of mass in this *step-to-step transition* are well-predicted by the mechanics of a dynamic walker for variations in speed, step length and step width (Donelan, 2002a,

2002b). Longer and wider steps lead to greater collisions at each heel strike, with an accompanying greater push-off by the trailing leg. However, there is great nuance to the underlying principles that control how much work actually occurs, and it is on these principles that we focused our experiments.

Chapter 2 describes our first human study, which was inspired by revisitation of one of the original discoveries about passive dynamic walkers from McGeer's (1990a) early work. In his simulations, passive dynamic walkers showed that the slope required for walking – which defines the rate of gravitational potential energy input to the motion – is sensitive to the radius of curvature of the circular foot. As the radius of curvature increases toward leg length, the slope required grows less, approaching a limit of zero slope and zero cost (McGeer, 1990a). This result is intuitive – a rolling link with a curvature radius equal to its length is equivalent to a wheel, which ideally can roll without energy loss. Feet of large radius give the model's center of mass (COM) a smooth forward motion, with relatively little vertical motion and very soft collisions at heel strike. We investigated whether the same trend would occur in humans modified to walk on fixed-shape circular arcs. If large-radius arcs could reduce the amount of work performed by the legs on the center of mass (COM work), there might be a corresponding decrease in metabolic cost. Our results show that there is a substantial savings in work when using large-radius feet as in the model. The results of this study inspired us to design of a rigid foot prosthesis (see Chapter 5) to exploit the lower work cost achieved with favorable arc-shaped feet. However, the results did not demonstrate clearly whether the work savings was caused by the curvature of the large-radius feet or by their

correspondingly long heel and toe. This question is addressed in a follow-up study in Chapter 6.

In Chapter 3 we describe our second experiment, in which we revisited normal (i.e., structurally unmodified) walking across a wide range of walking speeds and step lengths to clarify our understanding of how these parameters lead to changes in cost. Using a dynamic walking model as a guide, Donelan (2002a) abstracted the model's step-to-step transition mechanics to a prediction that work performed for gait should grow in proportion to the square of walking speed times the square of step length. However, this high-level understanding did not explain the results of the arc foot study described in Chapter 2. In that study speed and step length were both constant, yet COM work and metabolic cost changed dramatically. In Chapter 3 we look deeper into the model to demonstrate that variations in COM work previously attributed to changing step length are actually mediated by changes in the COM velocity vector during the step-to-step transition. Higher walking speed increases overall velocity change for a given angle of COM velocity redirection. Large steps and small arc feet both lead to steeper direction changes in COM velocity during the transition and result in increased work, as well as increased metabolic cost. We also introduce a new tool, the COM *hodograph* (Greenwood, 1988), for evaluating normal and pathological gait quantitatively based on changes in COM velocity throughout the course of a step or a stride. Viewing the entire gait motion as fluctuations in an otherwise steady COM velocity promotes understanding of how work is performed during gait: to increase or decrease the COM velocity, or to change its direction.

In Chapter 4 we address the gait of amputees for the first time. Amputees are widely known to have a considerably higher metabolic cost for walking than non-amputees. The increase in cost ranges from about 20% for unilateral transtibial amputees to as much as 100% for transfemoral amputees (Waters, 1999). This increase persists across a variety of prosthetic feet that could be used, including modern dynamic elastic response feet, in spite of the widespread preference for such feet among amputees due to increased comfort (e.g., Barth, 1992). It has been suggested that the loss of some of the leg muscles, especially plantarflexors, is a fundamental functional deficit that increases cost and cannot be overcome with a passive prosthesis (Nolan, 2003; Zmitrewicz, 2007). In Chapter 4 we apply our COM velocity analysis to compare asymmetry in COM motion between amputees and non-amputees, in order to better understand the deviations of amputee gait from normal with respect to motion of the whole body. We show that amputees' COM velocity is different in prosthetic *versus* intact limb stance phases, and changes in different ways during the step-to-step transition on either side. These asymmetries suggest that the amputees are using a different strategy for powering gait with the two legs. We show that this difference in strategies causes the two sides perform different amounts of COM work, but it need not necessarily imply a higher overall cost for gait. By studying changes in the asymmetry due to changes in a subject's prosthesis, it may yet be possible to design a passive prosthetic foot that circumvents any cost-increasing properties of existing prostheses.

We describe in Chapter 5 a prosthesis that attempts to use a smooth rolling foot action to reduce mechanical and metabolic costs through a different strategy than current commercial prostheses use. During normal walking, the human foot and ankle flex and

deform in such a way that the center of pressure under the foot moves with respect to the leg as though the foot were an arc, rolling on the ground (Hansen, 2004a, 2004b, 2005). Existing commercially-available prostheses behave similarly, bending and compressing under load and emulating a rolling action (Hansen, 2000). However, a flexible prosthesis only achieves this shape under specific loading conditions, which may not always be met in daily use, and may not represent the best forces to apply to the body. Based on our study of the energetics of walking on arc-shaped feet (Chapter 2), we designed a new rigid foot prosthesis to exploit the mechanics of a favorable arc-shaped foot in walking, without relying on the compliance of commercial prostheses. However, an arc-shaped foot is neither stable for standing nor aesthetically pleasing. Therefore, we also made the prosthesis reconfigurable, to provide a smooth, rigid arc for walking and a stable base of support during standing. We report our prosthesis, dubbed the Rock'N'Lock foot, as well as the COM hodographs and metabolic results from a pilot test of four amputees walking with it. Our results show that the Rock'N'Lock has a different effect on COM motion than the subjects' everyday prostheses. Results also give us hope that with training and design improvement, the Rock'N'Lock foot may be able to lower the metabolic cost of walking for amputees.

In Chapter 6 we describe a followed up study addressing additional questions raised by the original arc foot study (Chapter 2) and by the Rock'N'Lock foot pilot study (Chapter 5). The original arc foot study (Chapter 2) showed that increasing the length and radius of curvature of foot arcs leads to relative decreases in COM work and metabolic cost. However, it did not resolve whether this result was driven more by curvature or by foot length. The follow-up study of Chapter 6 addresses the difference between these two

parameters, and at the same time seeks to determine the optimal arc radius and foot length for a rigid foot. The results from this study show that the length of the foot has a much stronger influence on the COM work and metabolic cost of gait than the foot radius of curvature. We also find that there exists a combination of foot length and radius of curvature that leads to minimum metabolic cost of walking. Our findings will be applied to future generations of the Rock'N'Lock foot, which we hope will ultimately achieve our goal of reducing the cost of walking for amputees.

References

Barth, D. G. (1992). Gait analysis and energy cost of below- knee amputees wearing six different prosthetic feet. *Journal of Prosthetics and Orthotics* **4**, 63-75.

Donelan, J. M., R. Kram and A. D. Kuo. (2002a). Mechanical work for step-to-step transitions is a major determinant of the metabolic cost of human walking. *Journal of Experimental Biology* **205**, 3717-27.

Donelan, J. M., R. Kram and A. D. Kuo. (2002b). Simultaneous positive and negative external work in human walking. *Journal of Biomechanics* **35**, 117-24.

Hansen, A. D. (2000). Prosthetic foot roll-over shapes with implications for alignment of trans-tibial prostheses. *Prosthetics and Orthotics International* **24**, 205-215.

Hansen, A. D., and D. S. Childress. (2004a). Effects of shoe heel height on biologic rollover characteristics during walking. *Journal of Rehabilitation Research and Development* **41**, 547-54.

Hansen, A. D., and D. S. Childress. (2005). Effects of adding weight to the torso on roll-over characteristics in walking. *Journal of Rehabilitation Research and Development* **42**, 381-90.

Hansen, A. D., D. S. Childress and E. H. Knox. (2004b). Roll-over shapes of human locomotor systems: effects of walking speed. *Clinical Biomechanics* **19**.

Kuo, A. D. (2002). Energetics of actively powered locomotion using the simplest walking model. *Journal of Biomechanical Engineering* **124**, 113-20.

Kuo, A. D., J. M. Donelan and A. Ruina. (2005). Energetic consequences of walking like an inverted pendulum: step-to-step transitions. *Exercise Science and Sports Reviews* **33**, 88-97.

McGeer, T. (1990a). Passive dynamic walking. *International Journal of Robotics Research* **9**, 68-82.

McGeer, T. (1990b). Passive walking with knees. In *Proceedings of the 1990 IEEE Robotics and Automation Conference*, pp. 1640-5. Cincinnati, OH.

Mochon, S., and T. McMahon. (1980). Ballistic walking. *Journal of Biomechanics* **13**, 49-57.

Nolan, L. et al. (2003). Adjustments in gait symmetry with walking speed in TF and TT amputees. *Gait and Posture* **17**, 142-151.

Waters, R. L. and S. Mulroy (1999). The energy expenditure of normal and pathologic gait. *Gait & Posture* 9(3):207-231.

Zmitrewicz R. J., R. R. Neptune, J. G. Walden, W. E. Rogers, and G. W. Bosker. (2006). The effect of foot and ankle prosthetic components on braking and propulsive impulses during transtibial amputee gait. *Archives of Physical Medicine and Rehabilitation* **87**, 1334-1339.

Chapter 2

The Advantages of a Rolling Foot in Human Walking

Introduction

During each step of human walking, the center of pressure exerted against the ground progresses forward from heel to toe. This progression is similar to the rolling of a wheel, with the complex actions of the ankle, foot, and shoe somehow resulting in an overall motion analogous to that of a rigid curved surface. Rolling contact of the entire foot with the ground is characteristic of plantigrade gaits, and is unique to humans among bipeds. Other bipeds such as birds employ a digitigrade gait that allows for long stride lengths because the foot can be extended during ground contact. The relatively flexed, plantigrade foot need not, however, be at a disadvantage. The effective shape or curvature emulated by the rolling foot may, for example, offer mechanical or energetic benefits. Here we examine the mechanical and metabolic consequences of different rolling foot curvatures during human walking.

Empirical evidence indicates that humans normally produce a particular effective foot curvature. The forward progression of the center of pressure is similar to that of a rolling wheel with radius equal to 30% of leg length (McGeer, 1990a). Hansen et al (2004b) proposed another method for evaluating the effective “roll-over shape” of the

knee-ankle-foot complex, by transforming successive center-of-pressure locations during a step into a limb-fixed coordinate system and fitting a curve to these locations. They found that a simple circular shape matched empirical data well, with a radius of curvature agreeing closely with McGeer's (1990a) 30% of leg length. They also found human effective roll-over shape to be remarkably invariant to factors such as walking speed, shoe height, and carried load (Hansen, 2004a; 2005; 2004b).

Curvature of the foot bottom has long been exploited in rehabilitation applications. Therapeutic shoes are designed with curved, rocker-bottom surfaces for patients with peripheral neuropathy, diabetic ulcers, or transmetatarsal amputation. These shoes reduce plantar pressure under the forefoot and improve walking performance (e.g., (Schaff, 1990)). For persons wearing a rigid lower limb cast that immobilizes the ankle, cast shoes provide a rocker bottom shape, promoting a more natural gait (Dhalla, 2003; Wu, 2004). However, despite the clear benefits provided by these aids, there is little understanding of how rolling foot curvature affects the mechanics and energetics of walking.

The rolling foot may be studied with dynamic walking models. These models liken the stance leg to an inverted pendulum and the swing leg to a swinging pendulum (Mochon, 1980). McGeer (1990a) showed that the coupled pendulums, with a collisional ground contact for the stance foot, can produce a passive dynamic walking gait. Modeling the feet with circular arcs rigidly attached to the legs, McGeer (1990a) found that the cost of transport decreased as the arcs' radius of curvature increased. One might expect the curved foot's advantage to arise from a greater distance traveled during the stance phase. However, a radius of curvature of 30% of leg length (McGeer, 1990a) confers negligible distance advantage compared to a point foot. Nor is there an advantage

in the pendulum motion of either leg, which is conservative of mechanical energy for either curved or point feet. This suggests little advantage to the rolling itself.

The advantage of curved feet may be from their effect on step-to-step transitions. Step-to-step transitions refer to the work performed to redirect the body's center of mass (COM) velocity from one step to the next (Donelan, 2002b). The leading leg performs negative work and the trailing leg positive work as the COM velocity is redirected from the pendular arc prescribed by the stance leg to the corresponding arc for the next step (Kuo, 2002). In normal human walking, much of this work occurs simultaneously during double support (Donelan, 2002b), with an approximately proportional metabolic cost (Donelan, 2002a). In dynamic walking models, curved feet reduce the directional change that the COM velocity must undergo (McGeer, 1990a; Ruina, 2005), reducing step-to-step transition work. The magnitude of step-to-step transition work theoretically will decrease with increasing radius of curvature of the feet, potentially leading to decreases in metabolic cost with the amount of work.

The purpose of this study was to quantify the effects of an imposed rolling foot curvature on the work performed on the COM during human walking, and on the associated metabolic cost. We imposed a rigid, curved foot surface on human subjects, manipulating the radius of curvature experimentally. We counteracted the human tendency to preserve a single effective roll-over shape by rigidly constraining the ankles. Subjects therefore rolled forward on the foot surface much like dynamic walking models, e.g., (Kuo, 1999; McGeer, 1990a). We hypothesized that curved feet of small radius would result in high step-to-step transition costs, in terms of both work performed on the COM and metabolic energy consumption. We expected these costs to decrease with

increasing radius of curvature. However, the theoretical dependency cannot apply to all radii, because it predicts the lowest cost at an impractically large radius of curvature equal to leg length. We therefore sought to test the hypothesis of step-to-step transitions, and to evaluate the limitations of the theory as applied to actual humans.

Methods

We designed an experiment to rigidly constrain ankle motion and impose different foot curvatures on subjects, and observed the impact of these changes on COM work and metabolic cost of walking. We constructed a simple boot apparatus to fix subjects' ankle joints in a neutral position. This allowed us to restrict the ankle's dynamic action and impose different static curvatures that could be manipulated experimentally. We measured ground reaction forces while subjects walked over force plates wearing different curves. We also measured metabolic rate during matched trials of treadmill walking. Finally, we compared the two data sets to elucidate how changes to curvature affect the work performed on the body center of mass (COM), and in turn how this work affects the metabolic cost of walking. Before describing the experiments in more detail, we use a simple model of walking to predict the effects of changes to radius of curvature.

Model

A simple walking model illustrates the influence of foot curvature on step-to-step transitions (Figure 2.1). This model is based on the Simplest Model of walking on level ground (Kuo, 2001), with the addition of arc-shaped feet. The model has a point mass at the pelvis, with infinitesimally small point masses at the bases of the feet (Figure 2.1a).

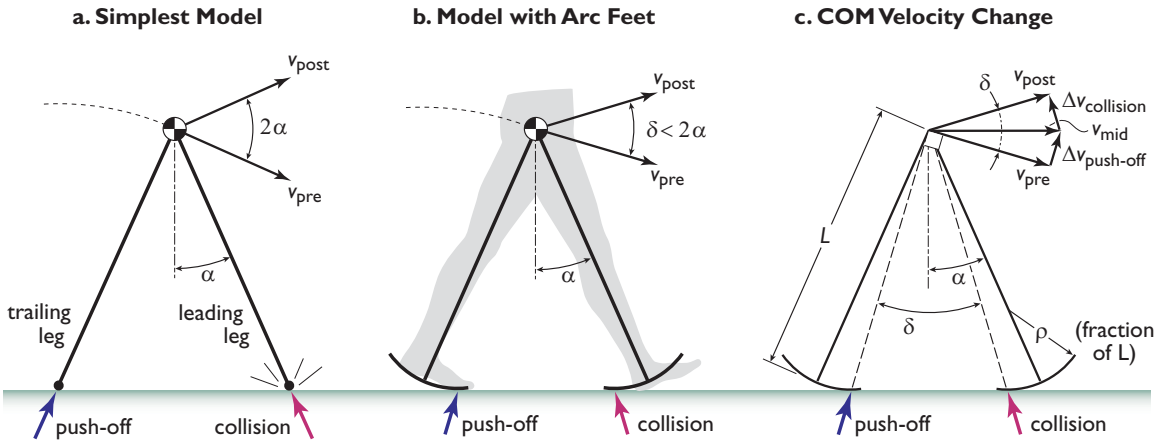

Figure 2.1: A simple model demonstrates how a rolling foot can affect walking energetics. (a.) Modeling the legs as pendulums supporting the body center of mass (COM), a step can be produced by passive limb dynamics with no energy input (McGeer, 1990a). Work is required, however, in the step-to-step transition to redirect the COM velocity. This can be accomplished with positive push-off work performed by the trailing leg, and negative collision work by the leading leg (Kuo, 2002). These leg actions redirect the pre-transition COM velocity v_{pre} to a post-transition velocity v_{post}. For point feet, the net directional change in velocity is equal to the angle between the legs, 2α. (b.) A model with arc feet applies collision at the heel of the leading leg, and push-off at the toe of the trailing leg. This reduces the directional change δ in COM velocity and therefore the step-to-step transition work. (c.) COM velocity change may be understood geometrically. The pre-transition velocity v_{pre} is directed perpendicular to the line from the trailing leg's rolling point of ground contact to the COM. Push-off, directed along this line (angle $\delta/2$ from vertical), causes a change in velocity ($v_{mid} = v_{pre} + \Delta v_{push\text{-}off}$). A periodic gait is achieved if push-off and collision velocity changes ($\Delta v_{push\text{-}off}$ and $\Delta v_{collision}$, respectively) are of the same magnitude, so that v_{post} is equal in magnitude to v_{pre} but directed according to rolling of the leading leg. Work is proportional to the square of each velocity change. As the arc foot radius (ρ, defined as a fraction of leg length L) increases, less step-to-step transition work is needed. There is no redirection of COM velocity for a radius equal to leg length, $\rho = 1$.

The model can be powered by an instantaneous push-off impulse applied under the stance foot just before contralateral heelstrike (Kuo, 2001). This push-off impulse performs positive work on the COM, of magnitude W^+. Immediately thereafter, the collision of swing leg with ground performs negative work, of magnitude W^-. For a periodic gait at steady speed, $W^+ = W^-$.

The step-to-step transitions may be computed as a function of the foot's radius of curvature, ρ. Push-off and heelstrike impulses are directed from the ground contact points to the COM. These impulses successively redirect the COM velocity. The push-off impulse redirects the COM from its pre-transition velocity v_{pre} to a mid-transition

velocity v_{mid}; then the heelstrike impulse redirects the COM to a post-transition velocity v_{post}. A curved foot reduces the directional change in COM velocity, and the work performed to redirect the COM (see Figure 2.1b). For a leg at angle α with respect to vertical at the step-to-step transition, and a positive radius of curvature ρ, the pre-to-post angular direction change δ in COM velocity is less than the angle between the legs 2α. A periodic gait is produced (Kuo, 2002) if this net directional change is shared equally between the push-off and collision impulses (see Figure 2.1c). From the geometry of these impulses,

$$\tan\frac{\delta}{2} = \frac{(1-\rho)\sin\alpha}{\rho + (1-\rho)\cos\alpha}. \qquad (2.1)$$

A small angle approximation for α yields

$$\tan\frac{\delta}{2} \approx \alpha(1-\rho). \qquad (2.2)$$

The magnitude W^- of the negative work performed each step by the heelstrike collision is equal to the change in kinetic energy:

$$W^- = \frac{1}{2}M v_{mid}^2 - \frac{1}{2}M v_{post}^2. \qquad (2.3)$$

The geometric relationship between v_{mid} and v_{post} (see Figure 2.1c) yields

$$W^- = \frac{1}{2}M v_{post}^2 \tan^2\frac{\delta}{2}. \qquad (2.4)$$

The overall trend is revealed by substituting Equation 2.2 into Equation 2.4:

$$W^- \approx \frac{1}{2}M v_{post}^2 \alpha^2 (1-\rho)^2. \qquad (2.5)$$

The model therefore predicts the trends in COM velocity change and step-to-step transition work as a function of foot radius of curvature ρ. Keeping step length fixed, the

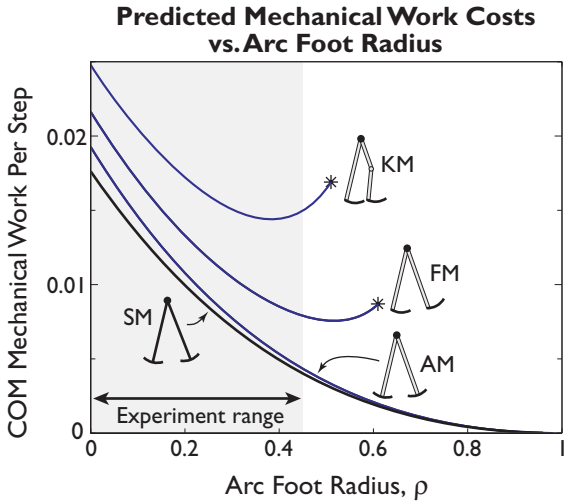

Figure 2.2: Work performed on COM as a function of foot radius of curvature ρ, from various dynamic walking models. Models are powered by push-off to walk on level ground: the *Simplest Model* (SM) with point mass pelvis and feet (Kuo, 2001), the *Anthropomorphic Model* (AM) with human-like mass distribution (Kuo, 2001), the *Forward-foot Model* (FM) with feet facing forward from the legs, and the *Kneed Model* (KM) with knees and forward feet (after (McGeer, 1990b)). All simulations generally predict decreasing step-to-step transitions with increasing arc foot radius, roughly in proportion to $(1-\rho)^2$ as in Equation 2.7. However, FM and KM have a slight upward trend for larger values of ρ, due to different foot geometry and introduction of knees. The SM is used as a prediction for experimental results. Over the range of arc radii studied experimentally, all other models match the trend of Equation 2.7 reasonably well, with r^2 ranging 0.940 – 0.998.

step-to-step transition leg angle α is nearly constant (varying only by a few percent over the range of ρ applied in our experiment). Keeping walking speed fixed, the post-transition velocity v_{post} is also approximately constant. Again assuming small angles, the angular direction change δ in COM velocity then decreases approximately linearly with foot radius of curvature ρ:

$$\delta \propto (1-\rho). \qquad (2.6)$$

The trend in the magnitude of negative COM work performed is

$$W^- \propto (1-\rho)^2. \qquad (2.7)$$

For a constant-speed gait, $W^+ = W^-$, allowing Equation 2.7 to predict the trend for positive COM work as well. This prediction forms the basis for comparisons to measured data.

We used numerical simulations to verify the analytical prediction of Equation 2.7, and to quantify how well it holds for more realistic models (Figure 2.2). The *Simplest Model* (SM) analyzed above neglects leg mass and inertia to allow our closed-form energetic analysis. An *Anthropomorphic Model* (AM) introduces more human-like mass distribution, but retains straight legs and curved feet that extend fore and aft from the legs (Kuo, 2001; McGeer, 1990a). A *Forward-foot Model* (FM) moves the anthropomorphic model's feet forward from the leg axis, more like human feet (similar to (McGeer, 1990b), but without knees). Finally, a *Kneed Model* (KM) introduces a hinged knee joint to the forward-foot model, with a stop to prevent hyperextension (McGeer, 1990b). The anthropomorphic and kneed models (AM and KM) both resemble physical machines constructed by McGeer (1990a; 1990b). All of these models include springs about the joints in order to produce human-like step frequencies (Dean, 2005; Kuo, 2001). We examined the gaits of all of these models as a function of ρ, keeping speed, step length, and other parameters fixed.

These models have different absolute step-to-step transition costs, but all exhibit a net decrease in cost over the range of ρ explored in our human experiment (Figure 2.2). However, the decrease is monotonic only for SM and AM. Simulations show that SM closely follows the curve of Equation 2.7 to a minimum of zero cost at $\rho = 1$. AM follows the same trend remarkably well despite the different mass distribution of the legs. The other models—FM and KM—exhibit a U-shaped curve, where step-to-step transition costs increase beyond a certain radius of curvature. FM has a minimum cost at approximately $\rho = 0.52$, with an increasing cost due to the unfavorable mass distribution of the leg relative to the point of collision with ground. KM has a minimum at $\rho = 0.38$

for the same reason, but with even higher costs due to increasing energy lost during knee lock. These latter models also do not yield walking gaits at larger radii ($\rho > 0.61$ and $\rho > 0.51$, respectively, marked with asterisks in Figure 2.2), without a change in other parameters. Despite these significant differences in actual behavior, the simple trend of Equation 2.7 applies remarkably well to all models over the experimental range of ρ (up to 0.45), with an r^2 value of at least 0.94. For this reason, we compared experimental data against the same single trend, predicting a general decrease in step-to-step transition work proportional to $(1-\rho)^2$.

We hypothesized that the mechanical work of step-to-step transitions would be accompanied by an approximately proportional metabolic cost. Work performed actively by muscle would be expected to exact a proportional metabolic cost. Indeed, both step-to-step transition work and metabolic cost measured in humans undergo changes proportional to the work predicted by models as a function of step length and step width (Donelan, 2001; Donelan, 2002a; Kuo, 2005).

There are, of course, many other factors likely to contribute to overall cost. Muscles incur metabolic cost due to their use in supporting body weight, controlling posture and stability, moving the legs, and moving other parts of the body such as the arms and trunk (Doke, 2005; Kuo, 2001). We assume that these other costs are relatively constant when only radius of curvature ρ is varied, and step length and frequency are fixed. Any relatively constant costs would contribute to an offset in mechanical work rate or metabolic rate, but would not affect the general trend of Equation 2.7.

We also considered an alternative explanation that the metabolic cost of walking reflects work performed by muscles to raise the COM during each step (Saunders, 1953).

Following this hypothesis, metabolic cost should be proportional to vertical displacement of the COM, with a muscular efficiency of approximately 25% relative to work against gravity (Margaria, 1976). The application of different radii ρ is predicted to cause small changes in vertical COM displacement, yet large changes in COM velocity direction. If raising the COM, rather than redirecting its velocity, is a more important contributor to metabolic cost, we would therefore expect much smaller changes in metabolic rate than predicted by Equation 2.7. We therefore compared metabolic cost measured in subjects against their measured vertical COM displacement.

Experimental Procedure

We measured mechanical work performed on the COM and metabolic rate while 10 adult human subjects walked in rigid boots with soles of different curvature. Walking speed was fixed at 1.3 $m \cdot sec^{-1}$ and step frequency was fixed across conditions for each subject. All subjects (5 male, 5 female; body mass 67.5 ± 9.6 kg, mean ± standard deviation, SD; leg length 0.94 ± 0.07 m, floor to greater trochanter) were healthy and had no known gait abnormalities. The study was approved by the local Institutional Review Board and subjects gave their informed consent to participate prior to the experiment.

The experimental apparatus consisted of a pair of rigid walking boots modified to accept circular foot surfaces in place of their standard soles (see Figure 2.3). The boots were Aircast Pneumatic Walkers (Aircast, Inc.; Summit, NJ, USA), with the bottom surface replaced by an aluminum plate with a pyramidal prosthesis adapter. These adapters allowed attachment of foot surfaces (referred to as *arcs*), circular segments as viewed in the sagittal profile, cut from pine wood 0.086 m wide. Pairs of arcs were

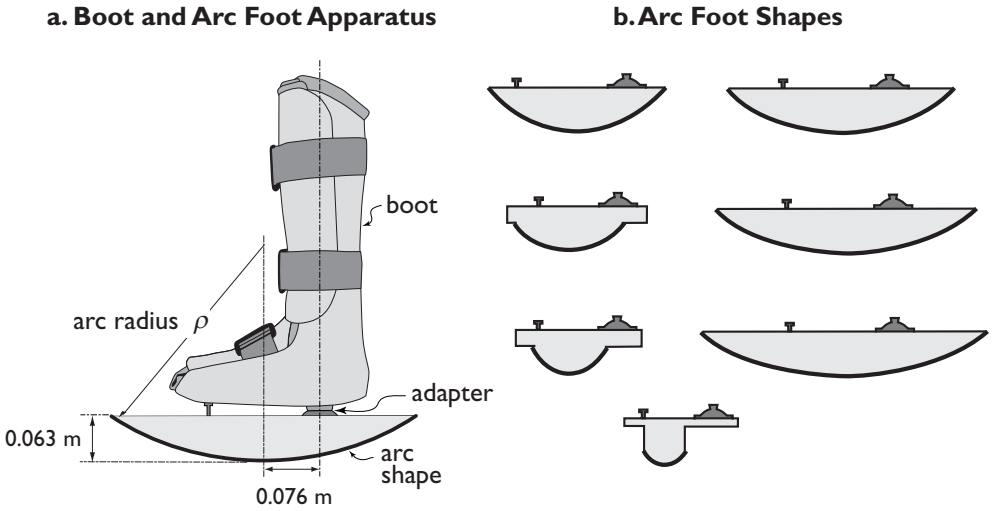

Figure 2.3: Apparatus used to rigidly restrict human ankle motion and control rolling characteristics of the foot. (a.) Subjects wore a boot and arc apparatus bilaterally, each consisting of a rigid walking boot modified to accept wooden arc shapes of varying radius. (b.) *Arc foot* shapes of varying arc radius ρ (defined as fraction of leg length) were rigidly attached with pyramidal prosthesis adapters. Arcs ranged in radius 0.02 – 0.40 m in absolute dimensions, and each subtended a sufficient range of angles to ensure continuous rolling ground contact throughout the stance phase. Arcs had matched mass of 1.1 ± 0.1 kg, and boots had mass 0.85 or 1.05 kg, depending on size.

constructed with seven different radii of curvature (0.02, 0.05, 0.10, 0.15, 0.225, 0.30, and 0.40 m; see Figure 2.3b). All arcs had sufficient fore-aft extent to ensure rolling contact with the ground throughout a normal stance phase. Arcs were matched in weight (1.1 ± 0.1 kg each) and standing height (0.11 m), although moment of inertia could not be matched over this range of sizes. All arcs were attached to the same boots (0.85 kg medium, 1.05 kg large). Subjects walked with each pair of arcs and in normal street shoes (*normal walking*), with the order of arc conditions randomized for each subject.

Arcs were positioned relative to the leg so that the arc center was 0.076 m anterior to the tibial axis (Figure 2.3a). Through trial and error experimentation we determined that the offset could affect walking comfort and metabolic cost. A zero offset (aligning the arc center directly with the tibial axis) caused the ground reaction force to pass behind the knee early in the stance phase. To prevent the knee from buckling, subjects counteracted this flexion moment with high quadriceps activity. A forward offset reduced the buckling

moment, but larger offsets led to increasing discomfort due to a knee extension moment late in the stance phase. The offset of 0.076 m was found to provide reasonable compromise between these two factors.

Walking speed was held constant at 1.3 meters per second for all trials, with a subject-specific fixed step frequency. Step frequency was fixed to control for the cost of moving the legs, which increases with step frequency (Doke, 2005), and to match our constant step frequency simulations. The particular value chosen was dependent on each subject's preferred step frequency for large arcs. Subjects briefly practiced walking over ground and on a treadmill (Star-Trac; Irvine, CA) with each arc until they felt comfortable with their gait. Prior to experimental trials, we measured each subject's preferred step frequency while they walked with the largest arcs, which were expected to be the most difficult to move quickly due to their inertia. We then tested whether subjects could comfortably maintain this same frequency on the smallest arcs. If not, we measured the lowest frequency they could achieve and used that as the enforced frequency. The mean step frequency thus chosen was 1.74 ± 0.09 Hz (SD), slightly slower than the typical normal walking step frequency of about 1.8 Hz (Donelan, 2002a).

Trials were performed both over ground and on a treadmill for the same conditions. We measured ground reaction forces (GRFs, see Figure 2.4) in the over-ground walking trials. Subjects walked across two sequential force plates (AMTI; Watertown, MA, USA) at the same speed and step frequency used in treadmill walking. Speed was measured using two photogates, positioned 2.5 m apart around the force plates, and the chosen step frequency was regulated by a metronome. Trials were discarded if speed was not within 5% of the nominal 1.3 m/s speed. We assessed the net change in speed per trial to be

+0.012 ± 0.050 m/s (mean ± SD) for normal walking and +0.017 ± 0.052 m/s for arc foot conditions. Both were statistically insignificantly different from zero ($p > 0.05$), indicating that subjects walked at relatively steady speed. We recorded ten successful trials for each subject on each pair of arcs, and averaged the GRF from all ten trials. A step was defined as beginning with heelstrike and ending with opposite heelstrike.

We used GRF data to estimate the COM velocity changes and the average rate of negative mechanical work performed on the COM over the step cycle. We calculated COM kinematics (linear acceleration, velocity, and position) from three-dimensional GRF data, assuming periodic gait (Donelan et al., 2002b). The velocity data were then used to derive the maximum angular change δ_{COM} in the direction of COM velocity in the sagittal plane (see Figure 2.5). The instantaneous rate of mechanical work performed by each leg on the COM was calculated according to the *individual limbs method* of Donelan et al (2002b), as the dot product of each leg's GRF and the COM velocity (Figure 2.6). We integrated the combined negative portions of the individual limbs' work rate (Figure 2.6, shaded area) to find the total negative work W^{-}_{mech} (J) performed during one step. Finally, we multiplied this work by step frequency (Hz) to yield the average rate of negative mechanical work $\dot{W}^{-}_{\mathrm{mech}}$ (in W) performed by the subject on the COM. For comparison purposes, we also calculated the average rate of negative COM work performed during double support alone, $\dot{W}^{-}_{\mathrm{DS}}$.

We estimated metabolic energy expenditure rate from respiratory gas exchange data collected during treadmill trials. Subjects walked on the treadmill for at least 7 minutes while we collected data. Steps were again regulated by a metronome set to the chosen step frequency. We used an open-circuit respirometry system (Physio-Dyne Instrument

Corp., Quogue, NY) to measure the volume rates of oxygen consumption and carbon dioxide production ($\dot{V}_{O_2}$ and $\dot{V}_{CO_2}$, mL·sec^{-1}). Following a 3.5-minute transient period to allow subjects to reach steady state, we collected and averaged volume rates over at least 3 minutes of each trial. Metabolic energy expenditure rate $\dot{E}_{\text{met}}$ was estimated using the formula

$$\dot{E}_{\text{met}}\left(\text{W}\right) = 16.48\,\tfrac{\text{J}}{\text{ml}}\cdot\dot{V}_{O_2} + 4.48\,\tfrac{\text{J}}{\text{ml}}\cdot\dot{V}_{CO_2}, \quad (2.8)$$

after Brockway (1987) and Weir (1949). Finally, we calculated net metabolic rate by subtracting the metabolic rate of quiet standing. The quiet standing data collection procedure was similar to that of the walking tests, except that it was administered after at least five minutes of seated rest. Two subjects reported discomfort when walking on some arcs. These conditions were terminated early, and data were not collected for a total of five trials.

Data Analysis

We used angular change in COM velocity, average COM work rate, and metabolic rate to test the simple model's predictions for changes in arc radius. First, we performed a least-squares fit to the model of Equation 2.6, regressing velocity direction change δ_{COM} against arc radius ρ according to

$$\delta_{\text{COM}} = c_{\text{COM}}\left(1-\rho\right) + d_{\text{COM}}. \quad (2.9)$$

Coefficients c_{COM} and d_{COM} accommodate differences between humans and the model, such as knee flexion and duration of step-to-step transition, that can affect measured δ_{COM}.

We regressed subjects' mechanical and metabolic costs against arc radius according to

Simplest Model Fit: $C(1-\rho)^2 + D$. (2.10)

C is an unknown scaling coefficient, and *D* is a constant offset due to costs not affected by arc radius. We applied the same form of fit to three costs: $\dot{W}^{-}_{\text{mech}}$, $\dot{W}^{-}_{\text{DS}}$ and $\dot{E}_{\text{met}}$, applying subscripts "mech," "DS," and "met" respectively to *C* and *D* to distinguish the various coefficients.

We also performed a more general quadratic fit for metabolic rate $\dot{E}_{\text{met}}$. To allow for a minimum cost not occurring at $\rho = 1$, we performed a least squares fit to a general quadratic,

Empirical Fit: $\dot{E}_{\text{met}} = C_{\text{EF}}\left(B_{\text{EF}} - \rho\right)^2 + D_{\text{EF}}$, (2.11)

where the minimum occurs at $\rho = B_{\text{EF}}$. Unlike Equation 2.10, which is based on the dynamic walking model of Equation 2.7, the Empirical Fit is a purely mathematical curve fit.

We also tested the hypothesis that metabolic cost will increase in proportion to step-to-step transition work. We predicted the metabolic cost of step-to-step transitions by scaling the Simplest Model Fit to COM work rate according to the 25% maximum expected efficiency of muscle work (Margaria, 1976) with an arbitrary offset. We then compared this prediction against the observed Empirical Fit, using the difference between the two as an indication of residual costs not predicted by the simple model.

We compared our results against the idea that metabolic cost arises from work performed against gravity in raising the COM. We calculated the vertical displacement of

the COM as the difference between its highest and lowest positions during the step. We multiplied vertical displacement by body weight (Mg) to determine the work performed against gravity during each step, and multiplied this work by step frequency to estimate the average rate of work ostensibly performed to raise the COM, $\dot{W}_{\text{raise}}$. We then formed a predicted metabolic cost due to COM raising. We computed a best-fit line to the $\dot{W}_{\text{raise}}$ versus ρ data, and divided this by the expected 25% efficiency to obtain a prediction of metabolic rate according to the COM raising explanation.

To account for differences in subjects' body size, we performed all analyses with non-dimensionalized variables. We used base units of total mass *M* (body plus apparatus), gravitational acceleration *g*, and total standing leg length *L* (including boots and arc feet). Work rate and energy rate were therefore made dimensionless by the divisor $Mg^{1.5}L^{0.5}$, work and energy by *MgL*, and force by *Mg*. Arc radius was non-dimensionalized by *L*. Work rate and energy rate graphs and model fits are presented in both dimensionless units and in the more common units of $\text{W}\cdot\text{kg}^{-1}$. Conversion between these units was performed with the mean factor $g^{1.5}L^{0.5} \approx 29.8\ \text{W}\cdot\text{kg}^{-1}$. We also accounted for inter-subject kinematic and energetic variations by computing offsets d_{COM}, D and D_{EF} separately for each subject and then averaging them.

Results

The mechanics and energetics of walking changed significantly as a function of arc radius of curvature. The angular direction change in COM velocity occurring each step decreased with increasing radius ρ. The average rate of negative mechanical work performed on the COM also decreased significantly with increasing ρ. Net metabolic rate

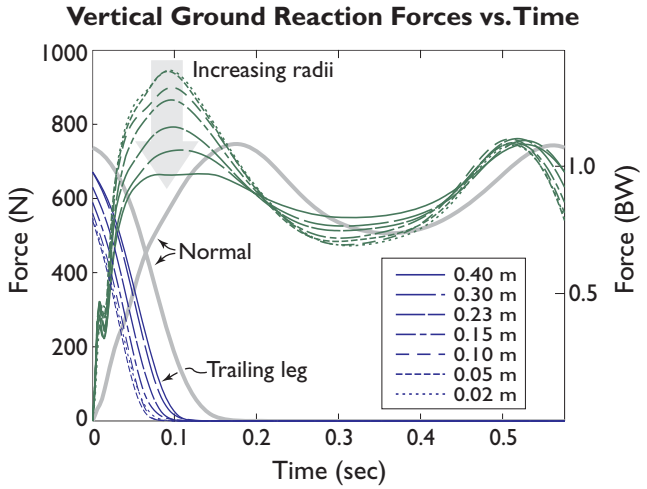

Figure 2.4: Vertical ground reaction forces vs. time over one step, measured during walking with arcs of different radius and in normal shoes. Larger arc radii resulted in smoother collisions during the step-to-step transition. Small arc radius resulted in very large initial peaks in ground reaction force. With larger arcs this peak decreased to below its magnitude in normal walking, but it always occurred earlier in the step. Walking on arcs resulted in shorter double-support times, decreasing with smaller radii. Arc radius had little effect on the second peak in vertical force. Data shown are averaged over all subjects, each subject's data averaged for their particular fixed step period, and then plotted over the mean step period. A step begins at heelstrike and ends at opposite heelstrike, with double support occurring over the first 0.10 – 0.15 sec. BW = body weight.

decreased with small increasing values of ρ, but increased again after reaching a minimum. Results for ground reaction forces, COM velocity direction change, COM work rate, and metabolic rate during normal walking and walking with arcs are compared below.

We first verified that the measured mechanical work rate and metabolic rate of normal walking were comparable to values found in previous literature. In normal walking at 1.3 m/s with preferred step frequency, the angular direction change δ_{COM} in COM velocity was 19.7 deg. Subjects performed negative COM work at an average rate of 0.595 $W \cdot kg^{-1}$ (non-dimensional value, 0.020). This is equivalent to 0.343 $J \cdot kg^{-1}$ per step, comparable to estimates of 0.33 and 0.38 $J \cdot kg^{-1}$ per step from two previous studies (Donelan, 2002a; 2002b). Average net metabolic rate for normal walking was 2.71 $W \cdot kg^{-}$

[1] (non-dimensional value, 0.091), also comparable to previously published results (Donelan, 2002a).

Measured ground reaction forces changed with arc radius, and differed from those of normal walking. Vertical forces (Figure 2.4) exhibited greater overlap with higher radius, expanding the duration of double support from about 6.5% of the stride (two steps) for 0.02 m arcs to 10% for 0.40 m arcs. The early force peak, about 1.4 BW (body weight) for small arcs, decreased to about 1.0 BW for large arcs, possibly because the opposite leg contributed higher forces throughout double support. The second peak's magnitude was about 1.1 BW for all experimental conditions and for normal walking, but its duration was longer for larger arcs. Reflecting the relative rigidity of the boot-arc apparatus compared to a normal foot and ankle, loading of each new stance limb occurred very quickly. Peak load was reached in as little as 8.5% of a stride, compared with about 15% for normal walking.

The observed angular direction change δ_{COM} in COM velocity decreased with increasing arc foot radius ρ ($P < 0.05$, Figure 2.5). These data were fit well ($r^2 = 0.89$) by the linear prediction of Equation 2.9, with coefficients $c_{COM} = 19.6 \pm 3.0$ deg (mean ± 95% Confidence Interval, CI), $d_{COM} = 6.0 \pm 2.8$ deg. The COM direction change for normal walking intersected with the observed trend at an arc radius of about 0.3.

The relative distribution of COM work throughout the step also changed with arc radius (Figure 2.6). We define the collision as the first phase of negative COM work in a step, and push-off as the first phase of positive work starting near the end of the preceding step and extending until the end of double support (Kuo, 2005). There was a dramatic increase in collision negative work with decreasing ρ, occurring over a

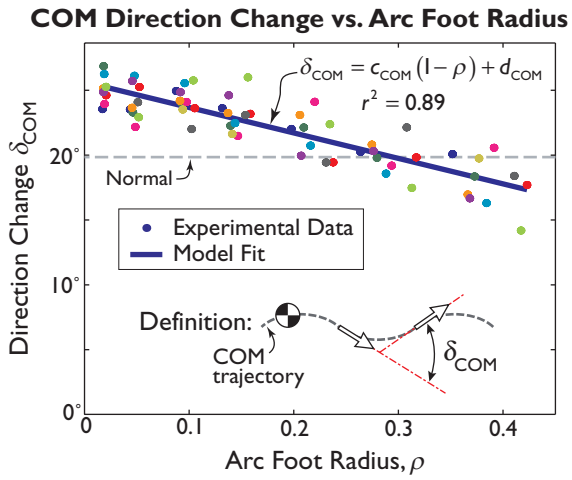

Figure 2.5: The angular direction change δ_{COM} in COM velocity decreased with increasing arc foot radius ρ. COM direction change was estimated as the angle between the steepest upward and downward velocities of the COM in the sagittal plane (defined in inset; compare to Figure 1b). The relationship between δ_{COM} and ρ is described well by the linear fit of Equation 2.9, $r^2 = 0.89$.

relatively fixed duration of about 0.13 sec. But the duration of double support decreased with smaller arcs, so that the collision tended to extend beyond double support in those conditions. The amount of push-off COM work remained relatively fixed, but tended to occur earlier before heelstrike with smaller arcs. Subjects performed less work during push-off than during collision, making up for the deficit with more positive work in the single-support leading leg prior to mid-stance.

In relation to normal walking, walking on arc feet resulted in a roughly comparable average COM work rate but a considerably higher metabolic rate. COM work rate with arcs at 1.3 m/s ranged from a high of 0.774 W·kg^{-1} (dimensionless 0.026) for the smallest arcs to a low of 0.327 W·kg^{-1} (0.011) for the largest arcs (Figure 2.7). Arcs of radius 0.225 m and greater actually resulted in lower average negative COM work rates than normal walking. However, the Empirical Fit to metabolic rate for walking on arcs was always at least 45% higher than the rate for normal walking (Figure 2.8). Net metabolic

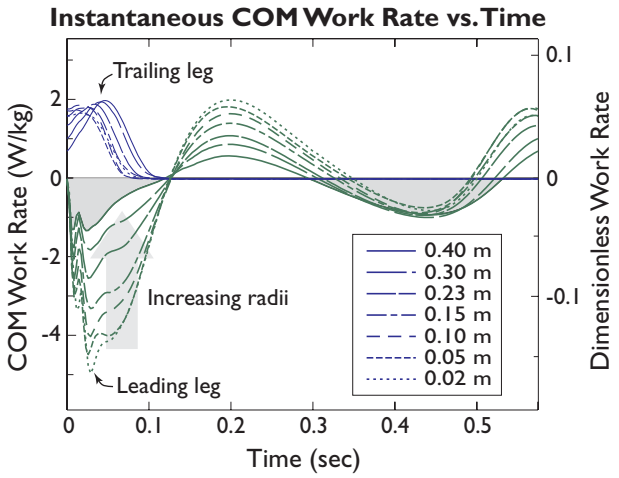

Figure 2.6: Instantaneous COM mechanical work rate for each leg over one complete step, measured with arcs of different radii. The trailing leg performed positive work and the leading leg negative work to redirect the COM during the step-to-step transition. Leading leg negative work rate was highest in magnitude for small-radius arcs. Work rate magnitudes decreased with increasing arc radius for the leading leg during double support, and through most of single support. Average rate of negative work was computed by integrating the magnitude of negative regions of instantaneous work rate (shaded areas for 0.40 m arc) and dividing by step period. Data shown are averaged from all subjects and plotted over the mean step period.

rate ranged from 6.25 W·kg^{-1} (0.210) for the smallest arcs to 3.93 W·kg^{-1} (0.132) for the second-largest arcs, and demonstrated a minimum near $\rho = 0.300$.

The amount of negative COM work performed ($\dot{W}^{-}_{\text{mech}}$) agreed well with the decreasing trend predicted by the Simplest Model (Figure 2.7). Overall negative work rate decreased with increasing ρ ($P < 0.05$), fitting the Simplest Model Fit of Equation 2.10 with an r^2 value of 0.95. The model fit showed a decline in overall negative COM work rate from 0.774 to 0.327 W·kg^{-1} (dimensionless 0.026 to 0.011) as arc radius increased from 0.02 to 0.42 (Figure 2.7). The coefficients are C_{mech} = 0.700 ± 0.050 W·kg^{-1} and D_{mech} = 0.110 ± 0.047 W·kg^{-1} (mean ± CI, dimensionless 0.024 ± 0.001 and 0.004 ± 0.001, respectively). A similar trend was observed for double-support work rate $\dot{W}^{-}_{\text{DS}}$ (r^2 = 0.92), with coefficients C_{DS} = 0.617 ± 0.059 W·kg^{-1} and D_{DS} = -0.093 ± 0.055 W·kg^{-1} (dimensionless 0.0207 ± 0.0020 and -0.0031 ± 0.0019, respectively).

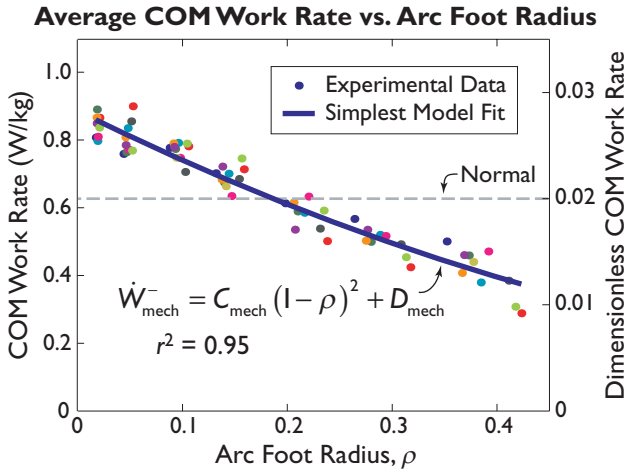

Figure 2.7: The average rate at which negative work is performed on the COM ($\dot{W}^{-}_{mech}$, see shaded areas in Figure 2.6) fell with increasing arc foot radius ρ. The Simplest Model Fit of Equation 2.10 predicted the trend well (r^2 = 0.95). The magnitude of work rate was greater for small arcs than for normal walking (dashed line), and lower for arcs of approximately ρ > 0.2. Less work is needed to redirect the COM velocity with larger arcs, due to a smaller directional change during the step-to-step transition. The work rate observed with smallest arcs was 2.37 times that for the largest arcs.

Metabolic rate $\dot{E}_{met}$ also fell with increasing radius of curvature (P < 0.05), although with a U-shaped rather than a monotonically decreasing curve (Figure 2.8). The Simplest Model (Equation 2.10) predicted a decreasing curve with minimum at $\rho = 1$, but the resulting fit to data for $\dot{E}_{met}$ gave a relatively poor r^2 = 0.77. Metabolic rate was matched better by the purely Empirical Fit of Equation 2.11, r^2 = 0.86. The coefficients are B_{EF} = 0.300 ± 0.108 (mean ± CI), C_{EF} = 32.02 ± 9.40 W·kg^{-1} (dimensionless 1.074 ± 0.316), and D_{EF} = 3.81 ± 1.65 W·kg^{-1} (0.128 ± 0.055).

The predicted metabolic cost for the COM raising hypothesis was far below the observed metabolic cost. Vertical COM displacement decreased approximately linearly from 0.045 m (dimensionless 0.048) for ρ = 0.02 to 0.035 m (0.037) for ρ = 0.42. The rate of work $\dot{W}_{raise}$ needed to raise the COM through these displacements therefore ranged from 0.831 W·kg^{-1} (.028) to 0.614 W·kg^{-1} (0.021). This yields expected metabolic rates of

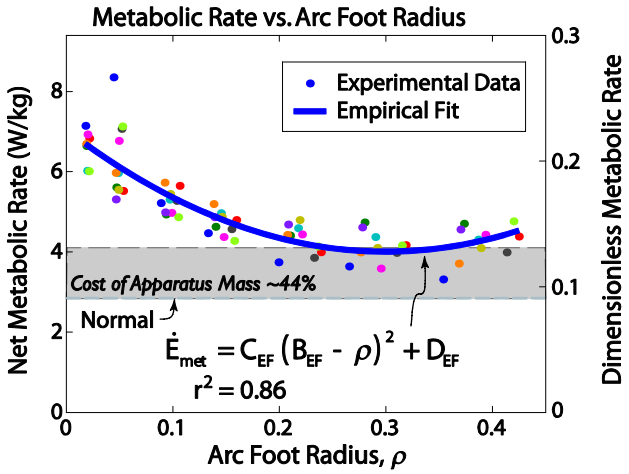

Figure 2.8: Net metabolic rate $\dot{E}_{met}$ exhibited a U-shaped curve as a function of arc radius ρ. For small radii, metabolic rate decreased with ρ much as predicted by the Simplest Model (Figure 2). However, metabolic rate reached a minimum at ρ = 0.30 according to the Empirical Fit of Equation 2.11, r^2 = 0.86, and began to increase with larger ρ. The energetic cost of walking was 59% higher for the smallest arcs than the minimum, and higher for all arc radii compared to normal walking (dashed line). The shaded region indicates the added cost expected due to apparatus mass and mass distribution, about 44% of the normal walking cost.

3.3 W·kg^{-1} (0.111) to 2.5 W·kg^{-1} (0.083), far below the range observed (Figure 2.8). The change in vertical COM displacement could only account for about 24% of the observed change in metabolic rate.

Discussion

We investigated the effects of arc foot radius ρ on the mechanical and metabolic costs of walking. Our model of walking with arc-shaped feet predicted an energetic cost based on the work performed on the center of mass (COM) in each step-to-step transition. We predicted that the average rate of COM work would fall with increasing arc radius according to Equation 2.7. We also predicted that metabolic cost would change in proportion to mechanical work.

The observed downward trend in negative COM work (Figure 2.7) indicates that arc radius influences step-to-step transition mechanics much as predicted (Equation 2.7). Even with no change in walking speed or step length, less work is needed to walk on

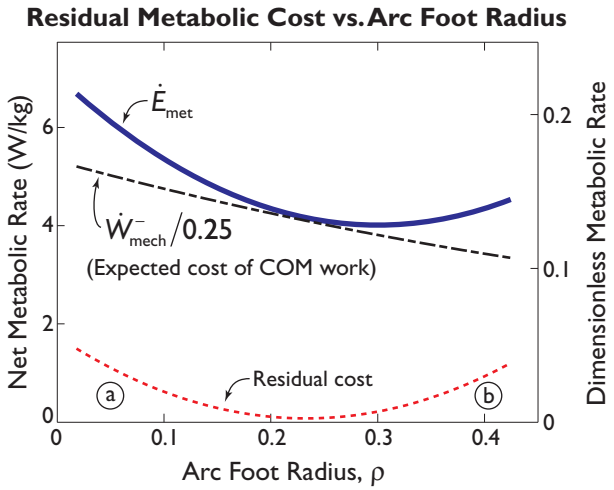

Figure 2.9: Comparison of net metabolic rate $\dot{E}_{met}$ with expected cost based on step-to-step transition work. Assuming a peak efficiency of 25%, the observed work performed on the COM (Figure 7) would be expected to yield a strictly decreasing metabolic rate with increasing ρ. Subtracting the expected cost from observed yields a residual cost not explained by the Simplest Model. The residual cost is substantial for arcs of smallest and largest radii. (a.) The high cost for small radii may be caused by the effort of balancing on a small contact patch through large collisions in the step-to-step transition. (b.) The cost for large radii may be associated with stabilizing the knee joint against a hyperextension moment caused by the ground reaction force late in single support.

larger-radius arcs. This is due to the smaller angular direction change in COM velocity for step-to-step transitions associated with larger radii (Figure 2.5). Small radii result in larger directional changes, greater impact forces and more negative work. Subjects compensated for collisions with more positive work, not during double support but during single support (see Figure 2.6), perhaps by performing positive work with the hips. Regardless of when work was performed, overall work rate decreased in proportion to the predicted $(1-\rho)^2$ trend.

Curiously, larger-radius arcs actually resulted in less step-to-step transition work than occurred in normal walking. COM work rate was lower for all radii greater than about $\rho = 0.2$; the trend exhibited the greatest difference of about 45% at the upper limit of radius, $\rho = 0.42$. By the criterion of center of pressure progression, human walking may appear to have an effective roll-over radius of $\rho = 0.3$, but by the criterion of step-to-

step transition work, normal walking is closer to $\rho = 0.2$. The actions of the human ankle-foot complex appear not to perfectly mimic a static arc. Some of the difference reflects active motion in the normal ankle and foot articulations, performed with mechanical work. Passive deformation of soft tissues may also contribute to normal COM work, with inelastic deformations dissipating energy. Passive elastic deformation, for example in the Achilles tendon, may also contribute to normal COM work (Donelan, 2002b; Kuo, 2005) without dissipating energy. These ankle and foot motions, whether active or passive, elastic or inelastic, are reduced considerably by the arc foot apparatus used in this experiment.

Metabolic rate generally decreased with increasing arc radius, but only to about $\rho = 0.3$ (Figure 2.8). For larger radii, $\dot{E}_{\text{met}}$ increased with ρ. The measured metabolic rate exceeded that predicted by COM work (assuming 25% muscle efficiency) for both low and high values of ρ (Figure 2.9). It appears that changes in metabolic cost were largely proportional to COM work rate, but with additional costs that are not captured by the step-to-step transition model. These unmodeled factors affect the cost of walking on unusually large and small arcs. Subjective observations suggest that there may be separate explanations for the increased metabolic cost measured for small or large arcs.

We consider two possible explanations for the unexpectedly high metabolic cost of walking on small-radius arc feet (Figure 2.9, region a). First, subjects found it difficult to balance while walking with all arcs, especially the smallest ones. The small radius afforded a small ground contact patch and resulted in short impact durations with little time spent in double support (see Figure 2.4). More effort may have been expended to maintain balance, with an added metabolic cost. Second, small arcs resulted in greater

collisions at heelstrike, which subjects found jarring and uncomfortable. Their preference would have been to walk at faster step frequencies, had frequency not been controlled. Faster and shorter steps would have reduced the collisions, trading high step-to-step transition costs for forced motion of the legs (Kuo, 2002). Instead, subjects appeared to expend effort to maintain joint stability, particularly for the knee, through the greater collisions. The additional muscle activity for co-contraction or other stabilizing actions may have incurred a metabolic cost.

Other explanations may apply to the high cost of walking on large-radius arc feet (Figure 2.9, region b). Late in stance, larger arcs produced a longer moment arm between the knee joint axis and the ground reaction force's line of action, resulting in an extension moment tending to hyperextend the knee during late stance. Subjects reported high activity in knee flexors, presumably to counteract hyperextension. Some subjects also reported high activity in plantarflexor muscles, which may have been used to counteract the bending moment the boot applied to the shank, as well as to stabilize the foot within the boot. Stabilization of the knee and ankle may have contributed to the higher metabolic cost on large arcs.

We also consider the higher rotational moments of inertia of larger arcs. Larger arcs might theoretically require greater effort to swing through a step, depending on their contribution to overall moment of inertia about the medio-lateral axis. The arcs had central moments of inertia of about 0.002 – 0.013 $kg \cdot m^2$ (despite all being matched in mass), compared to a total inertia of about 0.90 $kg \cdot m^2$ for the entire lower leg and boot-arc apparatus about an axis passing through the knee. Even the largest arcs therefore

contributed less than 2% to overall rotational inertia. This difference cannot explain the cost of walking with large arcs.

Higher step-to-step transition costs for walking with large arcs were also observed indirectly in models with knees. Forward-facing feet (FM and KM of Figure 2.2) and a passive knee joint (KM) alter the collision geometry, resulting in higher step-to-step transition costs for larger foot radii. These costs are a function of joint spring stiffnesses in the models. If KM were given infinite knee stiffness, its step-to-step transition work would be identical to that of FM. For a human to stiffen a joint in the same manner, muscle activity would presumably incur some metabolic cost. KM also loses more energy at heelstrike for larger arcs. These phenomena may have affected the human subjects metabolically without appearing in COM work rate estimates.

There was also an overall higher metabolic cost of walking on arc feet independent of arc radius. The constant offset was such that metabolic rate was at least 45% higher for arc foot walking than for normal walking (see Figure 2.8), despite the arcs' advantage in terms of mechanical work. One constant factor is that the weight-matched arcs and boot apparatus added about 2.0 kg at the end of the leg in each arc condition. Many studies (Burse, 1979; Inman, 1981; Martin, 1997; Miller, 1987; Skinner, 1990) have quantified the metabolic impact of adding mass to the ankles, measuring increases equivalent to 11-24% over normal walking per kilogram added. One study (Royer, 2005) incrementally varied the location of the mass, and found steadily increasing metabolic costs with more distal placement due to changes in moment of inertia. In our current experiment, the added mass is greater, and it is placed more distally than in any of these studies. Extrapolating from these and other studies' (Griffin, 2003) results, a hypothetical 2.0 kg

mass centered near the bottom of the foot may increase the net metabolic cost of normal walking by up to 44%.

An additional factor may have been the novelty of walking on arc feet. After brief practice sessions, subjects may not have fully adapted to the added mass, restricted ankle motion, smaller ground contact patch, and rigid arcs. We performed a repeatability test on two subjects, and found roughly a 10% decline in cost from their first arc condition to a post-experiment re-test of the same condition. Practice may help subjects to improve balance and control, reducing metabolic cost. Novelty may therefore have contributed to the overall cost of walking on arcs, but not to the observed trends in cost due to randomized trial order. Factors such as added mass, increased moment of inertia, decreased double-support time, difficulty of balancing on the arcs, the need to compensate for restricted ankle motion, and incomplete adaptation could all contribute to the higher overall cost we measured for walking with arc feet.

The metabolic cost of walking on arc feet is not well explained by the alternative hypothesis of raising the COM against gravity. Based on the measured changes in vertical displacement of the COM, work performed against gravity (at 25% efficiency) would account for only about 24% of the observed changes in metabolic rate as a function of ρ. This hypothesis is also at odds with the inverted pendulum analogy for the stance leg, because a pendulum can conserve mechanical energy, gaining height by conversion of kinetic energy to potential energy. Work is therefore not needed to raise a pendulum, which will have the same energy and speed at the beginning and end of single support. Even with a conservative pendulum, however, work is needed to restore energy lost in

collisions. We find the explanation based on step-to-step transitions to be more helpful than that based on raising the COM.

Arc feet allow rolling during single support and reduce step-to-step transition costs. For rolling, a rigid convex curved shape will dissipate less energy than one that is deformable, because deformations cause rolling resistance. Polygonal or concave shapes (e.g. a rigid cast without a cast shoe) are poor choices because each corner produces a collision as it contacts the ground (Ruina, 2005). However, the circular shape we examined is not necessarily optimal. An inverted pendulum can theoretically roll atop any smooth convex curve. Longer (fore-aft) curves reduce the directional change in COM velocity and therefore step-to-step transition work (Equations 6 and 7). For longer curves, some attention must be paid to alignment with respect to the tibial axis, and to induced moments about the knee. Such factors would warrant further study for possible application to rocker bottom shoes, which evidently already employ them to advantage but without quantitative, energetics-based design principles.

The human plantigrade gait appears to use the feet to behave approximately like rigid arcs. The effective roll-over shape ($\rho = 0.3$ based on center of pressure progression) appears to take advantage of reduced step-to-step transition costs compared to a point foot ($\rho = 0$), subject to the limitations apparent with larger arc radii. The disadvantages of larger arcs might stem from side effects such as moments induced about the knee. For animals that walk exclusively on flat ground, it might be preferable to have rigid legs with curved feet of radius equal to leg length, and without ankles or knees. However, animals that wish to sit, stand, climb, or use ankles or knees for any other purpose must

compromise the efficiency of high-radius rolling gait with the body's structural limits and versatility constraints.

Acknowledgements

This work was originally published in very similar form as:

Adamczyk, P. G., S. H. Collins and A. D. Kuo. (2006). The advantages of a rolling foot in human walking. *Journal of Experimental Biology* **209**, 3953-3963.

This work was supported in part by NIH R21DC6466. The authors thank K. Schneider for contributing to experimental measurements, and D. P. Ferris for sharing laboratory facilities.

References

Brockway, J. M. (1987). Derivation of formulae used to calculate energy expenditure in man. *Human Nutrition: Clinical Nutrition* **41C**, 463-471.

Burse, R. L., and K. B. Pandolf. (1979). Physical conditioning of sedentary young men with ankle weights during working hours. *Ergonomics* **22**, 69-78.

Dean, J. C., and A. D. Kuo. (2005). Powering the kneed passive walker with biarticular springs. In *Proceedings of the International Society of Biomechanics XXth Congress and the American Society of Biomechanics Annual Meeting*, pp. #719. Cleveland, OH.

Dhalla, R., J. E. Johnson, and J. Engsberg. (2003). Can the use of a terminal device augment plantar pressure reduction with a total contact cast? *Foot and Ankle International* **24**, 500-505.

Doke, J., J. M. Donelan and A. D. Kuo. (2005). Mechanics and energetics of swinging the human leg. *Journal of Experimental Biology* **208**, 439-445.

Donelan, J. M., R. Kram and A. D. Kuo. (2001). Mechanical and metabolic determinants of the preferred step width in human walking. *Proceedings of the Royal Society of London, Series B* **268**, 1985-92.

Donelan, J. M., R. Kram and A. D. Kuo. (2002a). Mechanical work for step-to-step transitions is a major determinant of the metabolic cost of human walking. *Journal of Experimental Biology* **205**, 3717-27.

Donelan, J. M., R. Kram and A. D. Kuo. (2002b). Simultaneous positive and negative external work in human walking. *Journal of Biomechanics* **35**, 117-24.

Griffin, T. M., T. J. Roberts and R. Kram. (2003). Metabolic cost of generating muscular force in human walking: insights from load-carrying and speed experiments. *Journal of Applied Physiology* **95**, 172-83.

Hansen, A. D., and D. S. Childress. (2004a). Effects of shoe heel height on biologic rollover characteristics during walking. *Journal of Rehabilitation Research and Development* **41**, 547-54.

Hansen, A. D., and D. S. Childress. (2005). Effects of adding weight to the torso on roll-over characteristics in walking. *Journal of Rehabilitation Research and Development* **42**, 381-90.

Hansen, A. D., D. S. Childress and E. H. Knox. (2004b). Roll-over shapes of human locomotor systems: effects of walking speed. *Clinical Biomechanics* **19**.

Inman, V. T., H. J. Ralston and F. Todd. (1981). Human Walking. Baltimore: Williams and Wilkins.

Kuo, A. D. (1999). Stabilization of lateral motion in passive dynamic walking. *International Journal of Robotics Research* **18**, 917-30.

Kuo, A. D. (2001). A simple model predicts the speed - step length relationship in human walking. *Journal of Biomechanical Engineering* **123**, 264-9.

Kuo, A. D. (2002). Energetics of actively powered locomotion using the simplest walking model. *Journal of Biomechanical Engineering* **124**, 113-20.

Kuo, A. D., J. M. Donelan and A. Ruina. (2005). Energetic consequences of walking like an inverted pendulum: step-to-step transitions. *Exercise Science and Sports Reviews* **33**, 88-97.

Margaria, R. (1976). Biomechanics and energetics of muscular exercise. Oxford, England: Clarendon Press.

Martin, P. E., T. D. Royer and S. J. Mattes. (1997). Effect of symmetrical and asymmetrical lower extremity inertia changes on walking economy. *Medicine and Science in Sports and Exercise* **29**, 86.

McGeer, T. (1990a). Passive dynamic walking. *International Journal of Robotics Research* **9**, 68-82.

McGeer, T. (1990b). Passive walking with knees. In *Proceedings of the 1990 IEEE Robotics and Automation Conference*, pp. 1640-5. Cincinnati, OH.

Miller, J. F., and B. A. Stamford. (1987). Intensity and energy cost of weighted walking vs. running for men and women. *Journal of Applied Physiology* **62**, 1497-1501.

Mochon, S., and T. McMahon. (1980). Ballistic walking. *Journal of Biomechanics* **13**, 49-57.

Royer, T. D., and P. E. Martin. (2005). Manipulations of leg mass and moment of inertia: effects on energy cost of walking. *Medicine and Science in Sports and Exercise* **37**, 649-56.

Ruina, A., J. E. A. Bertram and M. Srinivasan. (2005). A collisional model of the energetic cost of support work qualitatively explains leg sequencing in walking and galloping, pseudo-elastic leg behavior in running and the walk-to-run transition. *Journal of Theoretical Biology* **237**, 170-92.

Saunders, J. B., V. T. Inman and H. D. Eberhart. (1953). The major determinants in normal and pathological gait. *Journal of Bone and Joint Surgery* **35A**, 543-58.

Schaff, P. S., and P. R. Cavanagh. (1990). Shoes for the insensitive foot: the effect of a "rocker bottom" shoe modification on plantar pressure distribution. *Foot and Ankle* **11**, 129-140.

Skinner, H. B., and R. L. Barrack. (1990). Ankle weighting effect on gait in able-bodied adults. *Archives of Physical Medicine and Rehabilitation* **71**, 112-5.

Weir, J. B. de V. (1949). New methods for calculating metabolic rate with special reference to protein metabolism. *Journal of Physiology* **109**, 1-9.

Wu, W. L., D. Rosenbaum, and F. C. Su. (2004). The effects of rocker sole and SACH heel on kinematics in gait. *Medical Engineering and Physics* **26**, 639-646.

Chapter 3

Center of Mass Velocity Redirection Predicts Center of Mass Work in Walking

Introduction

The ability to predict the work the legs perform on the center of mass (COM) during walking is a valuable component of any theory of gait. This *COM work* is a major determinant of variations in the metabolic cost of walking when gait is perturbed from normal (Donelan, 2002a). As gait parameters step length, speed and step width increase, measured COM work also increases and incurs a proportional metabolic cost (Donelan, 2002a). The cost of COM work is likely a driving factor in humans' development of a preferred gait that minimizes energy expenditure.

A simple dynamic walking model predicts COM work variations in perturbed gait based on analysis of the transition between single-stance phases, called the *step-to-step transition* (Kuo, 2005). In the step-to-step transition, positive COM work is performed by the trailing leg in push-off, and negative COM work is performed as the leading leg collides with the ground and stops the body's descent (Kuo, 2001; Kuo, 2002). These two actions change the COM velocity from falling to rising, redirecting it from the arc of one pendular stance phase to the next. The geometry of leg configuration and COM velocity redirection shows that COM work W performed by the legs depends on the square of

both walking speed $\bar{v}$ and step length s, $W \propto \bar{v}^2 s^2$. In experiments varying these gait parameters independently, this prediction described trends in measured COM work very well (Donelan, 2002a; Donelan, 2002b).

Unfortunately, these gait parameter studies did not validate their own assumptions about the COM velocity changes underlying measured COM work. Speed and step length do not affect COM work directly, but rather through their influence on the COM velocity change that takes place during each step-to-step transition (Donelan, 2002a). Nor is COM velocity change uniquely related to speed and step length. For example, in a study of walking with fixed ankles and circular arcs on the bottoms of the feet, both parameters were held constant but step-to-step COM velocity change (and the resulting COM work) still decreased as the foot bottom curvature radius increased (Chapter 2). A model capturing the effect of foot radius on COM velocity change predicts the trends, whereas the relationship of COM work to speed and step length alone (e.g., Donelan, 2002a) incorrectly predicts no change in COM work. This result suggests that COM velocity change is the key to predicting COM work, and is more versatile than the prior relationship among work, speed and step length. However, the conclusion is not general because the study did not address normal gait.

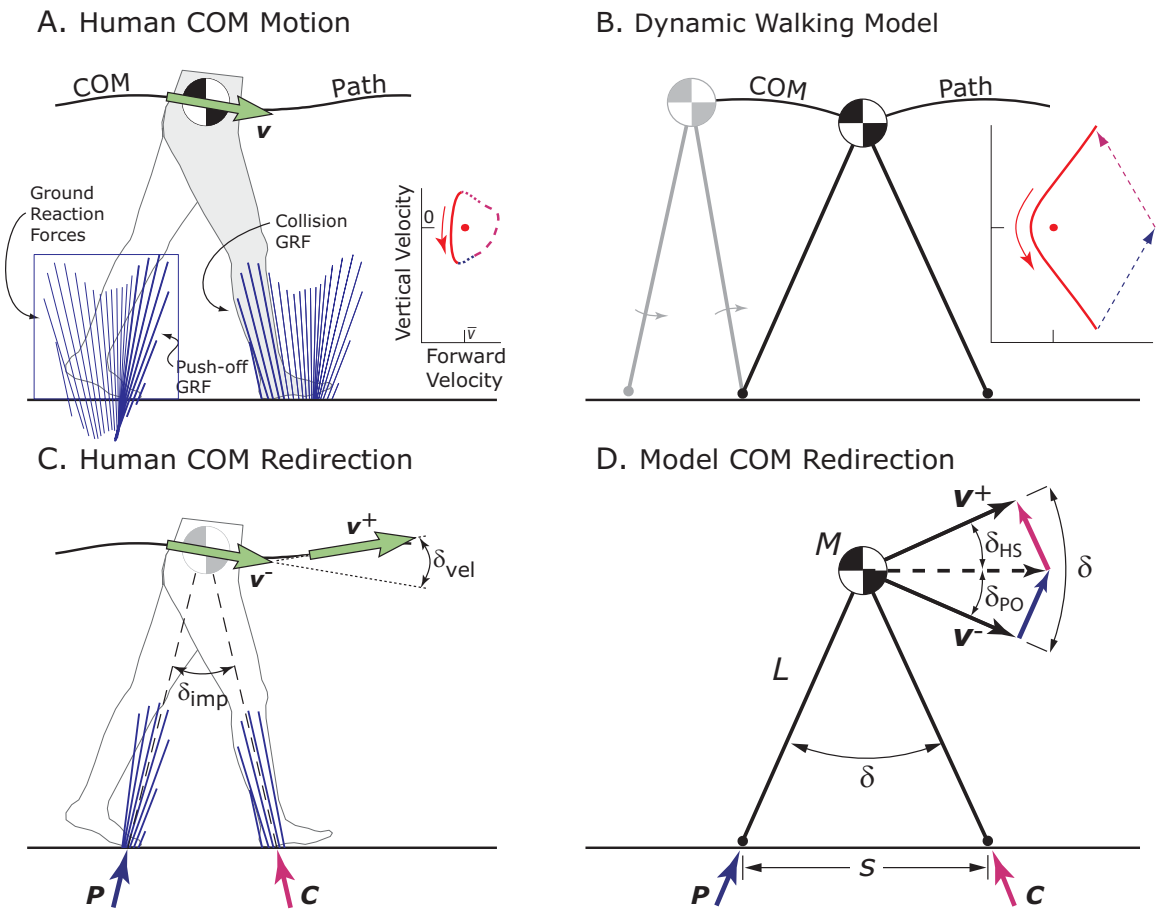

Figure 3.1: A: The path of the human COM is driven cyclically by ground reaction forces and gravity. At each *step-to-step transition*, push-off forces from the trailing leg are directed forward and up while collision forces from the leading leg are directed back and up. These forces redirect the COM velocity from a downward to an upward direction. During the single support time, the body passes up and over the leg and begins to fall again. Inset: a plot of vertical *versus* forward components of COM velocity forms a loop each step, showing fluctuations in COM velocity during different phases of gait. B: A simple dynamic walking model exhibits similar dynamics. The COM passes up and over each stance leg passively, then is redirected during an instantaneous double-support phase. C: The angle of COM redirection δ_{vel} is an important determinant of how much work the legs must perform on the COM. At steeper angles, the collision force performs more work because it is more opposed to COM velocity. The angle of the legs δ_{imp} determines the direction of leg forces. Both δ_{vel} and δ_{imp} increase with step length. D: Push-off (*P*, causing velocity redirection δ_{PO}) and collision (*C*, causing velocity redirection δ_{HS}) in the dynamic walking model act sequentially to redirect the model's COM velocity most economically. The work performed by the legs in the model can be used to predict COM work in humans.

During normal walking a human can exploit the complexity of the body to alter COM work in ways even the model's COM velocity change analysis cannot capture. For example, a human leg can contribute to COM work through off-axis force components,

which the model explicitly disallows. Also, motion of the human torso and arms can help decouple COM motion from leg motion, whereas the model's COM always follows the hip joint. In addition, free knees and ankles allow the effective shape or length of the leg to be changed. Because of such differences between humans and the model, it is uncertain whether COM velocity change dominates COM work in the human step-to-step transition as the model suggests it should.

The purpose of the present study was to measure COM velocity change during walking and to test its relationship to COM work performed by the legs. We varied the gait parameters walking speed and step length in four condition families to determine their unique effects on two aspects of COM velocity change: velocity magnitude and angular redirection. We hypothesized that COM velocity magnitude at the step-to-step transition would increase with increasing walking speed (as intuition suggests), and angular redirection of the COM velocity would increase with increasing step length. We further hypothesized that negative COM work in the step-to-step transition would increase quadratically with both magnitude and redirection of the COM velocity, as in our model. We therefore sought to test the intermediate mechanisms of our step-to-step transition model and examine the limits of its applicability to humans.

Methods

Model

The "powered model" of walking (Figure 3.1, (Kuo, 2002); closely related to the "simplest model" (Garcia, 1998) allows us to make energetic predictions about walking based on a system with well-understood mechanical behavior. This model consists of a

single point mass (M, also the locus of the system COM) supported by a rigid, massless stance leg (length L), and a swing leg with a foot of infinitesimal mass. The stance leg maintains contact with the ground at a single point. When a foot is on the ground, the force acting through it is directed from the ground contact point to the COM – directly along the leg axis.

The stance leg moves like an inverted pendulum about its foot, while gravity acts to slow and speed the COM and causes a pendular motion of the swing leg (Figure 3.1B). When the swing leg contacts the ground, the model has completed a step of length s, corresponding to the angle δ between the legs (see Figure 3.1D):

$$\delta = 2\sin^{-1}\left(s/2L\right). \tag{3.1}$$

In less-simplified models with arc feet, δ and s conform roughly to a scaled version of the same relationship (Chapter 2).

In order to switch to the next leg, the model is subject to impulsive step-to-step transition dynamics. The step-to-step transition involves a preemptive push-off of controlled magnitude along the trailing leg followed by an impulsive collision of the leading leg with the ground (Kuo, 2002). The push-off and collision impulses sequentially redirect the COM from its forward-and-down velocity ($\mathbf{v}^-$) at the end of one step to a forward-and-up velocity ($\mathbf{v}^+$) for the next. Figure 3.1D shows that the net direction change in COM velocity $\mathbf{v}$ is the same as the angle between the legs, δ.

The work W_{PO} performed by the push-off impulse on the model's COM is found from the impulse magnitude P,

$$W_{\mathrm{PO}} = P^2 \big/ 2M \cdot \tag{3.2}$$

Impulse magnitude P relates in turn to the direction change δ_{PO} caused by push-off (Figure 3.1D),

$$P = Mv^{-} \tan\left(\delta_{\mathrm{PO}}\right), \tag{3.3}$$

where $v^{-} = \left\|\mathbf{v}^{-}\right\|$ is the COM velocity magnitude just before the step-to-step transition. Equations 3.2 and 3.3 can be combined to predict push-off COM work from step-to-step transition geometry:

$$W_{\mathrm{PO}} = \tfrac{1}{2} M \left(v^{-} \tan\left(\delta_{\mathrm{PO}}\right)\right)^2. \tag{3.4}$$

A similar expression relates work performed in the collision at heel-strike to the angle of redirection through collision, δ_{HS} (Figure 3.1D):

$$W_{\mathrm{HS}} = -\tfrac{1}{2} M \left(v^{+} \tan^2\left(\delta_{\mathrm{HS}}\right)\right)^2. \tag{3.5}$$

Model geometry dictates that $v^{+} \approx v^{-}$, and the small angle approximation applies to both δ_{PO} and δ_{HS} (accurate to about 4% in the experimental range). Both angles are also proportional to overall COM redirection angle δ, so the trend dominating both push-off and collision work is hypothesized to be:

$$W \propto (v^{-} \cdot \delta)^2. \tag{3.6}$$

Variations on the model such as arc-shaped feet, legs with significant mass and downhill walking change the scaling of Equation 3.6, but they do not alter the dominant trend. For this reason, we use Equation 3.6 to predict energetic trends in humans.

Prior studies (Donelan, 2002a; Donelan, 2002b) made the further assumptions that COM redirection δ is proportional to step length s (see Equation 3.1) and pre-transition

COM velocity v^- is proportional to average walking speed $\bar{v}$. They predicted a simple trend for the work performed in a single step based on the gait parameters speed and step length:

$$W \propto (\bar{v} \cdot s)^2 . \tag{3.7}$$

In the present study, we examine these assumptions to determine the validity of this simplified form.

Experiment

We imposed different combinations of speed and step length on walking human subjects (5 male, 5 female; body mass $M = 68.7 \pm 11.9$ kg, mean $\pm$ s.d.; leg length $L = 0.93 \pm 0.05$ m), and observed the impact of changes to these gait parameters on center of mass (COM) redirection angle, angle between leg impulses, pre-transition COM speed, and work performed on the COM by the two legs. We measured ground reaction forces (GRF) while subjects walked over ground. We used these GRF data to compute the COM trajectory over the course of a step (heel-strike to opposite heel-strike). The simple model captures both COM redirection angle and leg force angle in the single measure δ, but the non-instantaneous step-to-step transition of human gait allows the two quantities to differ. We computed the angular change in sagittal plane COM velocity (δ_{vel}) and the angle between the ground reaction impulses provided by the two legs (δ_{imp}) during the step-to-step transition, as well as the pre-transition COM speed (v^-). We also computed the positive push-off work and the negative collision work performed on the COM (W_{PO} and W_{HS}) during the step-to-step transition. We compared this COM work to

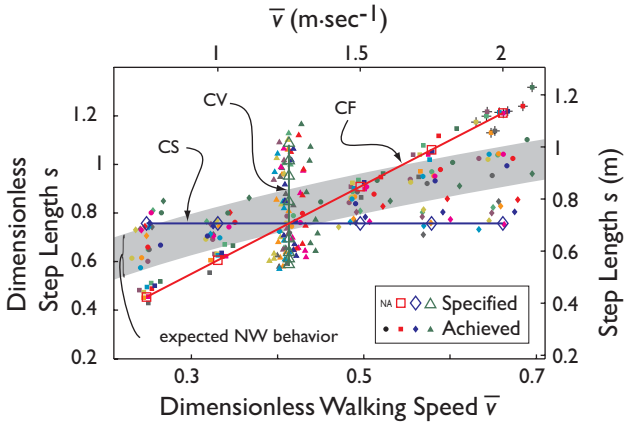

Figure 3.2: Speeds and step lengths specified (open symbols) and achieved (closed symbols) for the four experiments. Circles: conditions NW, free walking with varied speed (located near the gray band (Grieve, 1968)). Squares: CF, constant step frequency with varied speed. Diamonds: CS, constant step length with varied speed. Triangles: CV, constant speed with varied step length and step frequency. Note that the highest specified step lengths occurred in constant-step-frequency walking, and resulted in a very unnatural gait; these trials (marked +) were excluded as outliers from analyses of COM work.

the simple model's predictions (Equations 3.6 and 3.7) according to measured δ_{vel}, $\bar{v}$, s and $\bar{v}$.

We used four different families of conditions to map each subject's performance across a range of speeds and step lengths surrounding normal walking (Figure 3.2). First, each subject walked on a treadmill at 1.25 $\text{m}\cdot\text{sec}^{-1}$ (designated $\bar{v}^*$) while we measured his preferred step frequency (f^*) and step length ($s^* \triangleq \bar{v}^* / f^*$). In the first family of experimental conditions (natural walking, NW; Figure 3.2, circles), subjects walked over ground at speed $\bar{v}^*$ with step length s^* and step frequency f^*, and at 0.75, 1.00, 1.50, 1.75 and 2.00 $\text{m}\cdot\text{sec}^{-1}$ (0.6 to 1.6 times $\bar{v}^*$) with no constraint on step length or frequency (see (Donelan, 2002b)). In the second condition family (constant step frequency, CF; Figure 3.2, squares), each subject stepped to a metronome at his preferred step frequency f^*, while walking at each of the six speeds above (Donelan, 2002a). Because speed equals step length times step frequency, this protocol resulted in step

lengths from 0.6 to 1.6 times s^*. The third family of conditions (constant step length, CS; Figure 3.2, diamonds) was complementary to the second: each subject maintained his preferred step length s^* across the same range of speeds by stepping to a metronome at frequencies from 0.6 to 1.6 times f^*. In the final family of conditions (constant speed, CV; Figure 3.2, triangles), subjects maintained a constant 1.25 $m \cdot sec^{-1}$ walking speed while we adjusted step frequency from 0.70 to 1.30 times f^*. This protocol provided inverse changes in step length and step frequency without affecting overall walking speed. All the data we analyzed were originally collected by Donelan et al for their earlier studies, (Donelan, 2002a) and (Donelan, 2002b). We combined the four data sets in order to observe universal trends across a wide range of speeds and step lengths.

Calculations

We used GRF data to estimate COM velocity and work performed on the COM over the course of each step. We calculated COM kinematics (linear acceleration and velocity, $\mathbf{v}$) from three-dimensional GRF data (Cavagna, 1975; Donelan, 2002b). We used velocity and force data to calculate the instantaneous rate of work performed by each leg on the COM according to the Individual Limbs Method (ILM) (Donelan, 2002b). From ILM work rate, we integrated to find the positive and negative COM work performed by each leg during the step-to-step transition (see Figure 3.8C).

Unfortunately, the step-to-step transition is not as clearly defined in humans as it is in the simple model. In the model, sequential steps on rigid legs have arched COM trajectories whose steepest points intersect at the instant when both feet are on the ground (Figure 3.1B). The COM trajectory instantaneously changes from its steepest downward

angle to its steepest upward angle, and the push-off work and collision work that affect walking economy are both performed impulsively (Kuo, 2002). These step-to-step transition behaviors – double-support, COM velocity redirection and push-off and collision COM work – all occur at different times in humans. Previous researchers have used double-support (Donelan, 2002b) and rate of COM work (Donelan, 2002a; Kuo, 2005) to denote the step-to-step transition based on the principles of locomotion under investigation. In the present study we considered all three definitions (see Appendix). However, since our primary focus was COM velocity redirection, we defined the step-to-step transition as the period between the steepest downward angle of the COM velocity in the sagittal plane ($\mathbf{v}^-$ in Figures 3.1C, 3.4A, 3.6A and 3.8A) and its subsequent steepest upward angle ($\mathbf{v}^+$, same figures). The time span resulting from this definition for humans typically extended from shortly before heel-strike to shortly after toe-off.

We computed the intermediate metrics describing COM velocity change, as well as the COM work performed by the two legs, during the step-to-step transition. We defined pre-transition COM velocity $\mathbf{v}^-$ as the COM velocity vector at the instant the step-to-step transition begins. Similarly, post-transition COM velocity $\mathbf{v}^+$ was the COM velocity at the end of the transition. The directional change in COM velocity (δ_{vel}) was measured as the angle between $\mathbf{v}^-$ and $\mathbf{v}^+$ in the sagittal plane (Figures 3.1C and 3.4A). We also calculated the sagittal plane angle (δ_{imp}) between the net trailing leg and leading leg impulses (time integrals of GRF) during the step-to-step transition as a second correlate of COM redirection angle δ (Figures 3.1C and 3.4B). For comparison to energetics, we integrated ILM work rate to find the COM work performed during the step-to-step transition (Figure 3.8C). Push-off work W_{PO} was defined as the time integral of the

positive portions of the trailing leg COM work rate curve during the step-to-step transition. Heel-strike collision work W_{HS} was the time integral of the negative portions of the leading leg COM work rate curve during the step-to-step transition. Finally, we integrated total negative COM work over a step as the time integral of the negative portions of the whole leading leg work rate curve. For periodic gait, this quantity is identical to total positive COM work.

Data Analysis

We used COM velocity change metrics and COM work to evaluate the predictions of Equations 3.6 and 3.7. We performed least-squares linear fits of the COM velocity change metrics v^-, δ_{vel}, and δ_{imp} to their predictor gait parameters $\bar{v}$ and s, excluding condition families in which these parameters were held constant (CV and CS, respectively; see Figures 3.3 and 3.4):

$$v^- = C_8\bar{v} + D_8 \tag{3.8}$$

$$\delta_{vel} = C_9 s + D_9 \tag{3.9}$$

$$\delta_{imp} = C_{10} s + D_{10} \tag{3.10}$$

We also performed least-squares linear fits of the estimated step-to-step transition COM work to its nonlinear and linearized predictor quantities, per Equations 3.6 and 3.7, excluding the highest-step-length condition as an outlier (see Figures 3.2 and 3.5):

$$W_{HS} = C_{11}(v^- \cdot \delta_{vel})^2 + D_{11} \tag{3.11}$$

$$W_{PO} = C_{12}(v^- \cdot \delta_{vel})^2 + D_{12} \tag{3.12}$$

$$W_{HS} = C_{13}(\bar{v} \cdot s)^2 + D_{13} \tag{3.13}$$

$$W_{PO} = C_{14}(\bar{v} \cdot s)^2 + D_{14} \tag{3.14}$$

Our main work measure is W_{HS}, because it varies more consistently across conditions than W_{PO} (Donelan, 2002b).

We performed all regressions using dimensionless variables to account for differences in subjects' body size. We used base units of subject mass M, gravitational acceleration g, and standing leg length L. Velocity was therefore made dimensionless by the divisor $(gL)^{0.5}$, and work and energy by MgL. Step length was non-dimensionalized by leg length L. Angles δ_{vel} and δ_{imp} are naturally dimensionless. Work graphs and model fits are presented in dimensionless units, but also include axes in Joules. Conversion to dimensional units was performed with the mean factor $MgL = 628.5$ J. We also accounted for inter-subject variations in kinematics and energetics by computing the offset in each equation (D) separately for each subject and then averaging across subjects.

Results

The kinematics and kinetics of walking changed significantly with changes in walking speed and step length, according to the trends predicted by analysis of COM velocity change during the step-to-step transition of our dynamic walking model. Pre-transition COM velocity v^- increased approximately linearly with walking speed $\bar{v}$ (Figure 3.3). COM velocity direction change δ_{vel} and the angle between leg impulses δ_{imp} both increased approximately linearly with step length (Figure 3.4). Negative (W_{HS})

and positive (W_{PO}) COM work performed during the step-to-step transition also increased, in proportion to both predictors, $(v^{-} \cdot \delta_{vel})^2$ and $(\overline{v} \cdot s)^2$ (Figure 3.5). Results for pre-transition COM velocity, COM velocity direction change, and step-to-step transition work during walking at various speeds and step lengths are compared below.

We first established a baseline value for the three outcome variables under normal walking conditions. In normal walking at a speed of 1.27 ± 0.01 m·sec^{-1} (mean ± 95% standard deviation (SD); dimensionless speed 0.419 ± 0.004 for mean subject parameters) with preferred step length 0.707 ± 0.033 m (dimensionless step length 0.757 ± 0.036), the COM velocity direction change δ_{vel} was 0.322 ± 0.054 radians (18.4 ± 3.1 degrees), and the mean angle between leg impulses δ_{imp} was 0.332 ± 0.033 rad (19.0 ± 1.9 deg). These values are comparable to the 0.344 rad (19.7 deg) we previously reported for δ_{vel} in normal walking at 1.3 m·sec^{-1} (Chapter 2). Mean pre-transition COM velocity v^{-} was 1.24 ± 0.02 m·sec^{-1} (dimensionless 0.409 ± 0.007). Pre-transition COM velocity has not been reported previously for comparison. Negative COM work W_{HS} during the step-to-step transition for normal walking was 0.088 ± 0.016 J·kg^{-1}·step^{-1} (dimensionless work 0.023 ± 0.004 step^{-1}). As expected, this is slightly more negative work than the 0.085 J·kg^{-1}·step^{-1} (dimensionless work 0.0218 step^{-1}) observed by Donelan (2002b) during the shorter period of double-support. Positive push-off work W_{PO} performed on the COM during the step-to-step transition was 0.102 ± 0.027 J·step^{-1} (dimensionless work 0.026 ± 0.007 step^{-1}) for normal walking.

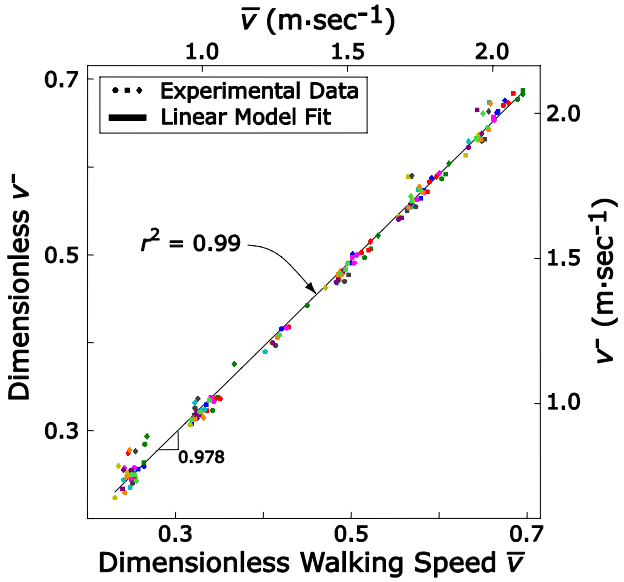

Figure 3.3: Magnitude of the pre-transition COM velocity (v^-) *versus* mean forward walking speed ($\bar{v}$) for experiments NW, CF and CS. Pre-transition COM velocity v^- multiplies with COM direction change to determine the work performed in gait. Walking speed $\bar{v}$ is an exceptional predictor of v^-: the best linear fit is nearly an identity relationship between these variables (slope 0.978, $r^2 = 0.99$). Condition family CV is excluded because it deliberately maintained constant walking speed across conditions.

Pre-transition COM velocity v^- increased with increasing walking speed ($P < 0.05$, Figure 3.3). v^- data were fit extremely well ($r^2 = 0.99$) by the linear prediction of Equation 3.8, with coefficients $C_8 = 0.977 \pm 0.010$ (always dimensionless; all coefficients reported as mean ± 95% confidence interval (CI)) and $D_8 = 0.004 \pm 0.007$. The high r^2 value and slope near unity indicate that forward walking speed strongly dominates the pre-transition COM velocity: $v^- \approx \bar{v}$.

Both the angular direction change in COM velocity and the angle between leg impulses (δ_{vel} and δ_{imp}) significantly increased with increasing step length across all experimental protocols ($P < 0.05$). Angular direction change in COM velocity (δ_{vel}, in radians) was predicted reasonably well ($r^2 = 0.69$) by the linear prediction of Equation 3.9, with coefficients $C_9 = 0.296 \pm 0.035$ and $D_9 = 0.103 \pm 0.036$ (Figure 3.4A). The

angle between leg impulses (δ_{imp}, in radians) was predicted well ($r^2 = 0.91$) by a slightly steeper linear trend per Equation 3.10, with coefficients $C_{10} = 0.485 \pm 0.023$ and $D_{10} = -0.042 \pm 0.023$ (Figure 3.4B). The two measures δ_{vel} and δ_{imp} differ because they rely on different aspects of the body's dynamics. To cause COM velocity changes, leg forces and gravity are all combined and integrated, allowing cancellation of opposing force components. In contrast, leg impulse angle is measured directly and captures both the COM redirection and body weight support actions of each leg. Thus, these measures address different functions within the step-to-step transition, and need not match closely.

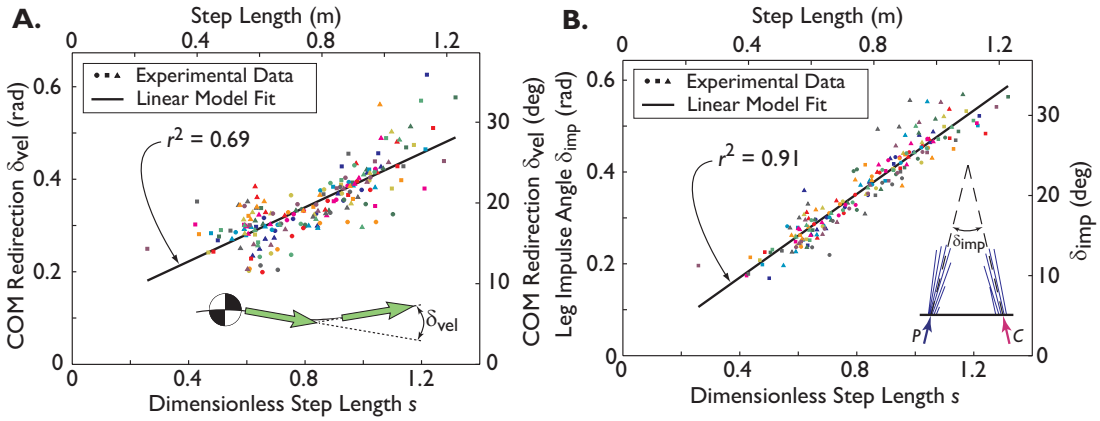

Figure 3.4: A: COM velocity redirection δ_{vel} *versus* measured step length (s) for condition families NW, CF and CV. Here, δ_{vel} is the sagittal-plane angle between the steepest downward and upward COM velocities (see Appendix and Figure 3.7 for other definitions). Despite the potential complexity of gait, Equation 9 predicts the linear trend well, $r^2 = 0.69$. Condition family CS is excluded because it deliberately maintained constant step length across conditions. B: Angle between leg impulses (δ_{imp}) *versus* measured step length (s) for condition families NW, CF and CV. Here, δ_{imp} is measured as the sagittal plane angle between the impulses of the trailing and leading leg GRF (P and C respectively) computed between the times of steepest downward and upward COM velocities. Equation 10 predicts the linear trend very well, $r^2 = 0.91$. Note that for the inverted-pendulum model $\delta_{imp} = \delta_{vel}$ (Figure 3.1), but gravity and leg compliance cause these quantities to differ when measured over the duration of the step-to-step transition in humans. Condition family CS is excluded because it deliberately maintained constant step length across conditions.

The amount of negative COM work (W_{HS}) performed during the step-to-step transition increased significantly with $(v^- \cdot \delta_{vel})^2$ across all conditions ($P < 0.05$, Figure 3.5A). Negative work data agreed ($r^2 = 0.75$) with the linear trend predicted by Equation 3.11, with coefficients $C_{11} = 0.859 \pm 0.069$ and $D_{11} = 0.006 \pm 0.004$. Positive work data (W_{PO}; not shown) also agreed with Equation 3.12 ($P < 0.05$, $r^2 = 0.62$). Coefficients for the positive work fit were $C_{12} = 0.541 \pm 0.062$ and $D_{12} = 0.016 \pm 0.004$.

The amount of negative COM work (W_{HS}) performed during the step-to-step transition also increased significantly with the simplified predictor $(\bar{v} \cdot s)^2$ ($P < 0.05$, Figure 3.5B) across all conditions ($r^2 = 0.82$). The linear trend of Equation 3.13 was best

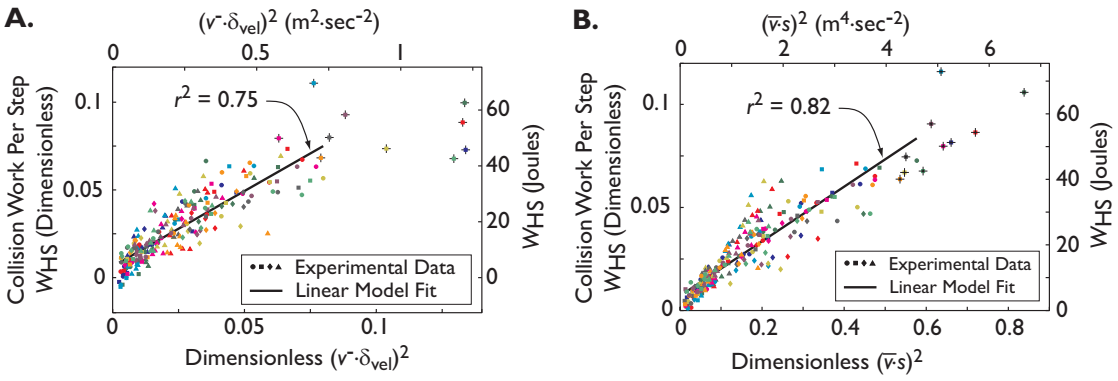

Figure 3.5: Negative COM work performed by the leading leg during the step-to-step transition *versus* (A) its predictor quantity $(v^- \cdot \delta_{vel})^2$ ($r^2 = 0.75$) and (B) the simplified predictor, $(\bar{v} \cdot s)^2$ ($r^2 = 0.82$) for all four condition families. The COM negative work required for gait is well predicted by the trends derived from our simple dynamic walking model. Trials marked (+) have been excluded from model fits (see Figure 3.2).

with coefficients $C_{13} = 0.133 \pm 0.008$ and $D_{13} = 0.007 \pm 0.003$. Positive work data (W_{PO}; not shown) also agreed with Equation 3.14 ($P < 0.05$, $r^2 = 0.66$), with best coefficients $C_{14} = 0.083 \pm 0.009$ and $D_{14} = 0.016 \pm 0.003$.

Discussion

Simple models investigating the mechanisms of energy expenditure in walking have predicted trends in overall center of mass (COM) work and metabolic rate with changes in speed, step length and step width (Donelan, 2001; Donelan, 2002a; Donelan, 2002b). These models are intended to promote understanding of complex human motions in terms of intuitive motion primitives grounded in well-understood principles of physics. To this end, complicated mechanical properties of the body such as distributed mass and compliance of all kinds are simplified into concentrated masses and rigid bodies. A model at this level of abstraction cannot capture the minutiae of locomotion, but it can describe the overarching principles that make walking possible – as long as it captures

them. This study investigated whether the inverted pendulum model's mechanistic description of COM energetics does in fact capture the key actions of a walking human. Previous studies could be criticized for checking only high-level predictions of gait energetics – COM work and metabolic cost trends across speed, step length and step width – without verifying that COM work precursors are also correctly predicted. It could be possible for a subject to alter his control strategy such that he uses a fundamentally different gait than that assumed by the model, even while exhibiting final COM work and metabolic results consistent with model predictions.

This study followed step-by-step as the effects of the gait parameters walking speed and step length propagated through the physics of human gait. We observed that the trends in pre-transition COM speed v^-, COM redirection angle δ_{vel} and angle between leg impulses δ_{imp} are as predicted. COM work appears in proper relationship to variations in v^- and δ_{vel} as well. Therefore, it appears that the simple dynamic walking model does describe the key mechanism leading to COM work during the step-to-step transition of human gait. This key mechanism is the redirection of the COM velocity, which requires the leading and trailing legs to perform work. COM velocity redirection is a more robust predictor of cost than speed and step length, because it also describes body behavior in a wider set of conditions, such as walking with arc-shaped feet (Chapter 2).

Such a simple model of the step-to-step transition is valuable because its limited parameter set and simple dynamics give it an analytically tractable mathematical form. However, even this simple mathematical description lacks an obvious intuitive form to promote understanding of gait. Therefore, a second goal of the present study is to illustrate a simple means by which the energetically significant pre-transition COM

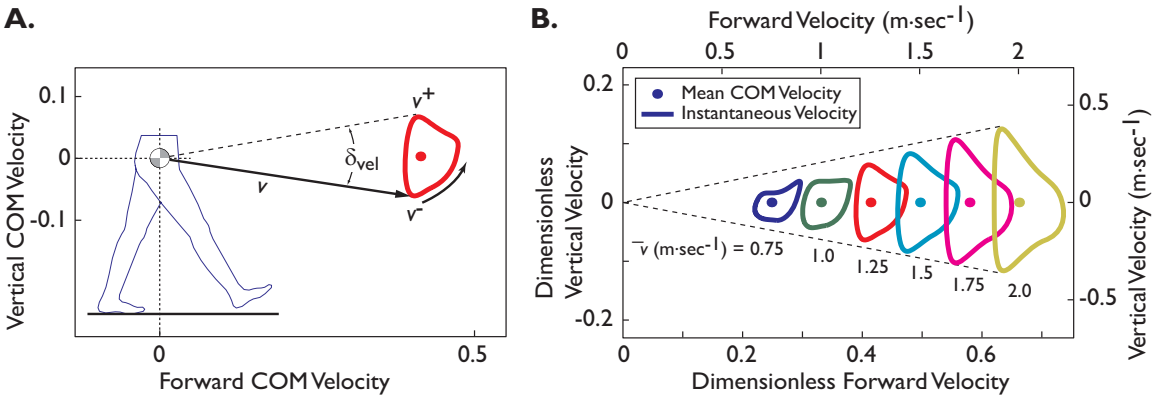

Figure 3.6: A: Construction of a hodograph from forward and vertical components of COM velocity. The hodograph is traced out by the tip of the COM velocity vector over the course of a step. If the COM itself is imagined at the origin, COM velocity at any time can be pictured easily (vector $\mathbf{v}$). Several important metrics of gait, including COM redirection angle (δ_{vel}) and pre- and post-transition COM velocities ($\mathbf{v}^-$ and $\mathbf{v}^+$, respectively), can be measured directly on a hodograph. B: Hodographs of COM velocity during preferred gait at different speeds. Circles mark the mean COM velocity for each condition. Note that both v^- and δ_{vel} increase with speed in preferred gait. COM velocity data are the mean across subjects.

velocity v^- and COM velocity redirection angle δ_{vel} can enhance the understanding of gait. We aim to provide an intuitive view of how various features of gait affect these important variables, and thus how they affect energetic cost.

The two key gait variables in this study, speed and COM velocity redirection, can be visualized using a simple plot of the tip of the COM velocity vector over the course of a step (Figure 3.6A; also see Figure 3.1A-B) or a stride, called a *hodograph*. A hodograph encodes the kinetics of COM motion in a compact graphical format that illustrates relationships among different gaits clearly and quickly, and allows important gait features to be identified and compared. For example, at the start of the step-to-step transition in Figure 3.6A, the marked vector shows that the COM velocity $\mathbf{v} = \mathbf{v}^-$ is down and forward, with dimensionless magnitude roughly 0.4 (1.21 $m \cdot sec^{-1}$). We can also see that $\mathbf{v}^+$ has a similar magnitude but points in a different direction; the angle between them is the COM velocity redirection angle, δ_{vel} (Figure 3.6A). These measurements can be

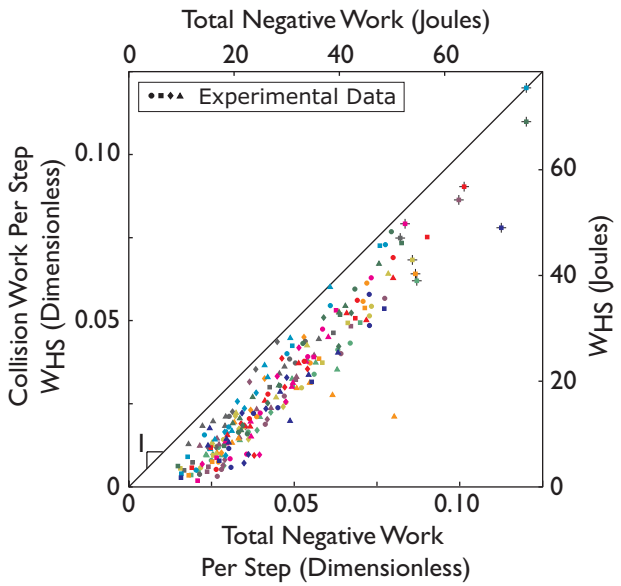

Figure 3.7: Collision accounts for most of the negative work performed during gait, especially at higher work loads. The remainder occurs in the "preload" phase, during which the leg stores energy that will be released in push-off.

compared to other gaits to identify which are likely to have greater COM work and overall energetic cost, as in Figure 3.6B for condition family NW. It is clear that both components of the cost predictor $(v^{-} \cdot \delta_{\text{vel}})^2$ systematically increase with speed in the NW condition family.

The amount of negative COM work (W_{HS}) performed during the step-to-step transition was not a constant fraction of the whole-step negative work. Figure 3.7 shows that in gaits with little total negative work (low speed and step length), there is almost no negative COM work performed in the step-to-step transition. As total negative COM work increases, step-to-step transition negative COM work accounts for nearly all of the gain, with the later "preload" phase of negative work remaining roughly constant. Negative work performed by the leg in the "preload" phase is thought to be stored, perhaps in the Achilles tendon, for subsequent return in the subsequent push-off. Such an energy storage mechanism would be limited by the length of the foot, as the elastic

energy stored in the tendon would produce an ankle moment tending to lift the heel. Our finding of constant preload work would be consistent with this limitation.

Conclusions

This study addressed concerns about the fidelity and applicability of a simple dynamic walking model to human gait. The results demonstrate that COM velocity change during the step-to-step transition is an important determinant of the COM work performed (and its associated metabolic cost), as predicted by this model. Furthermore, the cost of COM velocity change is driven by both the magnitude of COM velocity and the angle through which it is redirected, just as in the model. Greater walking speeds increase COM velocity magnitude, and greater step lengths increase redirection angle. While COM velocity redirection does not provide an *a priori* prediction for the total quantity of COM work in gait, it does allow comparisons across different gaits, which can be facilitated graphically by COM velocity hodographs. Even before measurements are taken, the cost of perturbations from normal gait can be understood in terms of their likely effect on COM velocity redirection angle.

Appendix

Step-to-Step Transition Timing

By our chosen definition, step-to-step transition spans the time from steepest downward to steepest upward COM velocity (see Figure 3.8, circles). However, the fit to our model's predicted trends is not strongly dependent on the choice of step-to-step transition timing limits. Table 3.1 provides coefficients and r^2 values for model fits using data computed with three definitions of step-to-step transition timing, determined from COM velocity, vertical GRF (period of double-support; Figure 3.8, squares) and COM work rate (period spanning push-off work and collision work; Figure 3.8, triangles). Figure 3.8 demonstrates these timing points for a typical trial.

Timing based on the double-support period ("Vertical GRF" in Table 3.1, squares in Figure 3.8) does perform significantly worse than the other two criteria in capturing the COM redirection angle δ_{vel} ($r^2 = 0.31$). This poor fit is caused by the fact that increasing step frequency is associated with a decrease in the fraction of step time spent in double-support; the resulting step-to-step transition capture less of the total COM velocity redirection (see Figure 3.7). This poor measurement of δ_{vel} propagates through Equations 11-12, causing poor fits there as well. In contrast, timing limits from "COM Velocity" and "COM Work Rate" always occur near the top and bottom peaks of the hodograph, effectively capturing COM velocity redirection in all conditions.

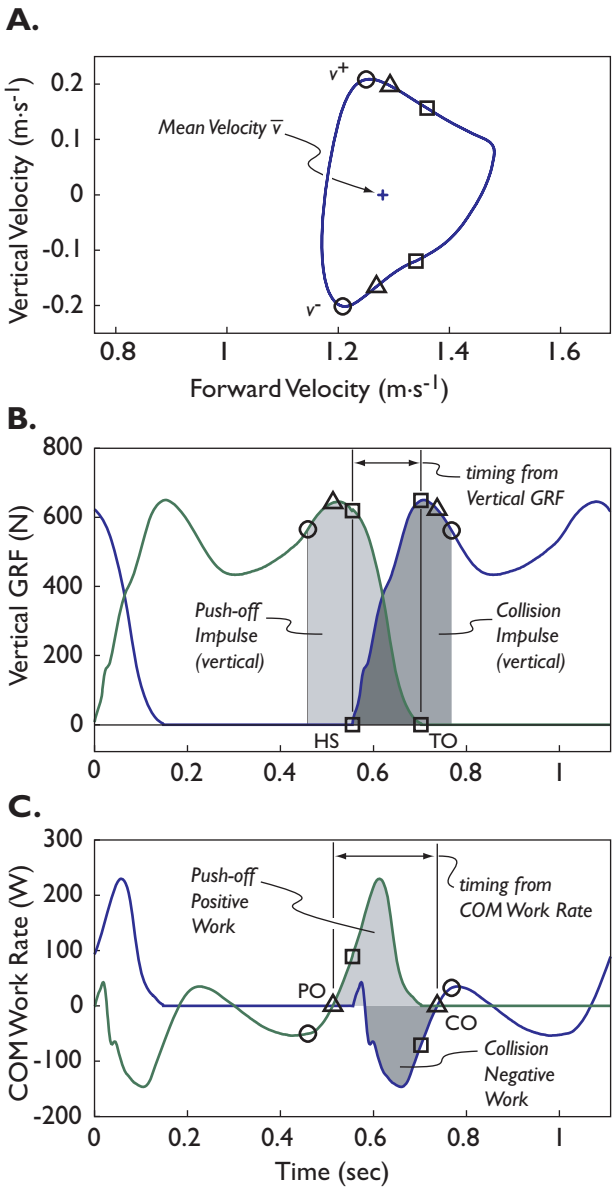

Figure 3.8: Possible definitions for timing of the step-to-step transition, from a typical subject's preferred gait at $1.25\ \mathrm{m \cdot s^{-1}}$. Symbols denote the limits of each time period on all three plots; bold symbols indicate the timing defined on each plot. (A**) Sagittal plane hodograph of COM velocity. Circles define preferred timing, from steepest downward to steepest upward COM velocities ($\mathbf{v}^-$ to $\mathbf{v}^+$). (**B**) Vertical ground reaction force (GRF). Squares denote start (HS: heel-strike) and end (TO: toe-off) of double-support period. Shaded areas represent the step-to-step transition impulse (vertical component) provided by each leg (based on the preferred timing). (**C**) Instantaneous COM work rate. Triangles denote first positive (PO: push-off) and last negative (CO: collision) COM work rate. Shaded areas represent the positive and negative COM work performed by the trailing and leading legs, respectively (based on preferred timing).**

Equation	Timing Signal	Slope C	Offset D	r^2
3.8 $\bar{v} = C_8\overline{v} + D_8$	COM Velocity	0.977 ± 0.010	0.004 ± 0.007	0.99
	Vertical GRF	1.093 ± 0.018	-0.016 ± 0.012	0.98
	COM Work Rate	0.998 ± 0.008	0.005 ± 0.005	0.99
3.9 $\delta_{\text{vel}} = C_9 s + D_9$	COM Velocity	0.296 ± 0.035	0.103 ± 0.036	0.69
	Vertical GRF	0.001 ± 0.038	0.215 ± 0.039	*0.31*
	COM Work Rate	0.267 ± 0.026	0.061 ± 0.026	0.75
3.10 $\delta_{\text{imp}} = C_{10} s + D_{10}$	COM Velocity	0.485 ± 0.023	-0.042 ± 0.023	0.91
	Vertical GRF	0.618 ± 0.025	-0.077 ± 0.025	0.93
	COM Work Rate	0.478 ± 0.020	-0.000 ± 0.020	0.93
3.11 $W_{\text{HS}} = C_{11}(\bar{v} \cdot \delta_{\text{vel}})^2 + D_{11}$	COM Velocity	0.859 ± 0.069	0.006 ± 0.004	0.75
	Vertical GRF	1.394 ± 0.182	0.009 ± 0.004	*0.53*
	COM Work Rate	1.155 ± 0.088	0.008 ± 0.004	0.77
3.12 $W_{\text{PO}} = C_{12}(\bar{v} \cdot \delta_{\text{vel}})^2 + D_{12}$	COM Velocity	0.541 ± 0.062	0.016 ± 0.004	0.62
	Vertical GRF	0.683 ± 0.146	0.019 ± 0.003	*0.40*
	COM Work Rate	0.735 ± 0.088	0.017 ± 0.004	0.60
3.13 $W_{\text{HS}} = C_{13}(\overline{v} \cdot s)^2 + D_{13}$	COM Velocity	0.133 ± 0.008	0.007 ± 0.003	0.82
	Vertical GRF	0.087 ± 0.009	0.010 ± 0.004	0.65
	COM Work Rate	0.129 ± 0.009	0.008 ± 0.003	0.81
3.14 $W_{\text{PO}} = C_{14}(\overline{v} \cdot s)^2 + D_{14}$	COM Velocity	0.083 ± 0.009	0.016 ± 0.003	0.66
	Vertical GRF	0.045 ± 0.007	0.019 ± 0.003	*0.49*
	COM Work Rate	0.081 ± 0.009	0.017 ± 0.004	0.63

Table 3.1: Non-dimensional coefficients and r^2 values for model fits using three different definitions of step-to-step transition timing. r^2 values in italic font reflect poor capture of variations in COM redirection when step-to-step transition timing is based on Vertical GRF.

References

Cavagna, G. A. (1975). Force platforms as ergometers. *Journal of Applied Physiology* **39**, 174-179.

Donelan, J. M., R. Kram and A. D. Kuo. (2001). Mechanical and metabolic determinants of the preferred step width in human walking. *Proceedings of the Royal Society of London, Series B* **268**, 1985-92.

Donelan, J. M., R. Kram and A. D. Kuo. (2002a). Mechanical work for step-to-step transitions is a major determinant of the metabolic cost of human walking. *Journal of Experimental Biology* **205**, 3717-27.

Donelan, J. M., R. Kram and A. D. Kuo. (2002b). Simultaneous positive and negative external work in human walking. *Journal of Biomechanics* **35**, 117-24.

Garcia, M., A. Ruina, A. Chatterjee, and M. Coleman. (1998). The simplest walking model: stability, complexity, and scaling. *ASME Journal of Biomechanical Engineering* **120**, 281-288.

Grieve, D. W. (1968). Gait patterns and the speed of walking. *Bio-Medical Engineering* **3**, 119-122.

Kuo, A. D. (2001). A simple model predicts the speed - step length relationship in human walking. *Journal of Biomechanical Engineering* **123**, 264-9.

Kuo, A. D. (2002). Energetics of actively powered locomotion using the simplest walking model. *Journal of Biomechanical Engineering* **124**, 113-20.

Kuo, A. D., J. M. Donelan and A. Ruina. (2005). Energetic consequences of walking like an inverted pendulum: step-to-step transitions. *Exercise Science and Sports Reviews* **33**, 88-97.

Chapter 4

Analysis of Amputee Gait Using Center of Mass Velocity

Introduction

Clinical gait evaluation in a laboratory produces abundant data regarding kinematics, moments, and powers at the joints of the leg. These data enable clinicians to quantify specific pathologies and prescribe appropriate therapies and walking aids for each individual (Narayanan, 2007). Patients can be encouraged to train specific joints or muscle groups, to change their posture, to use orthoses or other tools to make walking easier, or to seek surgical intervention. However, the use of gait analysis is not universally accepted (Narayanan, 2007). Furthermore, in much practical gait therapy a full laboratory analysis is not available and clinicians must rely on observational gait analysis instead (McGinley, 2003). This approach can be effective, but it also tends to have low repeatability, low inter-observer reliability and, in some cases, low correlation with laboratory measurements (McGinley, 2003; Wren, 2008). In addition, it is primarily qualitative, and as such is difficult to use for measuring changes in gait over time (Narayanan, 2007). It would be valuable for clinicians outside the gait laboratory to have a simple quantitative tool for measuring each patient's gait and comparing changes over time (McGinley, 2003).

Some aspects of gait that are evaluated visually can also be understood biomechanically through the motion of the body's center of mass (COM). For example, the cyclic rise and fall of the body visible to the eye reflects a smooth upward and downward oscillation in vertical COM velocity. Similarly, the visible forward-backward relative motion of the trunk reflects cyclic changes in forward COM velocity. In abnormal gait, asymmetry appearing as a limp represents differences in center of mass motion during left and right steps. In addition, jerky motion implies that the center of mass is accelerating more abruptly than usual at times. Understanding gait through center of mass motion is convenient because COM motion corresponds well to these and other visually apparent gait features, and because COM motion is remarkably simple to quantify and study (Orendurff, 2004). Center of mass motion is also closely linked to gait energetics (Donelan, 2002a,b; Adamczyk, 2006; and see Chapter 3).

We propose the use of a cyclic trajectory plot of center of mass (COM) velocity, called a COM *hodograph*, to visually represent – as well as to quantify – normal and abnormal walking gait and enhance the clinical understanding of individuals' motion patterns. Using as little as one force plate embedded in a walkway, COM acceleration and velocity throughout a stride can be estimated with a simple algorithm (Cavagna, 1975; Whittle, 1997; Donelan, 2002b). A sagittal plane COM hodograph is formed by plotting the vertical component of COM velocity against its forward component at each point in a stride (Figure 4.1; Greenwood, 1988). The COM hodograph for a walking stride has a double-loop structure in which a stride progresses counterclockwise, with one loop representing the stance phase of each leg. The position and contour of the two loops contain a great deal of information about the body's behavior during the stride.

In the present study we used COM hodographs to quantify the differences in center of mass motion between unilateral transtibial amputees and non-amputees. Amputees are known to exhibit asymmetry in step time and ground reaction forces (Nolan, 2003; Zmitrewicz, 2007). We hypothesized that amputees would exhibit gait asymmetry that would appear as differences between hodograph loops for the prosthetic side and the intact side. Because differences in COM velocity imply differences in translational kinetic energy, we further hypothesized that asymmetry in the COM hodograph would correspond to asymmetry in work production by the two legs. Specifically, we hypothesized that less positive work would be performed by the prosthetic side leg in push-off, due to the absence of plantarflexor muscles (Zmitrewicz, 2007). We quantified these asymmetries by measuring forward COM velocity at mid-stance and COM vertical acceleration at the time of opposite heel strike during the stance phase of each leg, and by estimating positive and negative work performed by each leg on the center of mass during each step-to-step transition. We therefore sought to test the utility of the COM hodograph in evaluating asymmetry in the gait of amputees.

Methods

Experiment

We measured center of mass (COM) velocity fluctuation while unilateral transtibial amputees and non-amputees walked over ground in order to determine the effects of transtibial amputation on the motion of the COM. We measured ground reaction forces (GRF) while subjects walked over two force plates mounted in the floor. We used these

GRF date to compute the COM velocity over the course of a stride (left heel strike to left heel strike; Cavagna, 1975; Whittle, 1997; Donelan, 2002b). We plotted a *COM hodograph* as the vertical component of COM velocity *versus* its horizontal component in order to visualize the differences between amputee and non-amputee COM motion (Greenwood, 1988). To quantify distinct asymmetries in the function of an individual's two legs, we estimated the COM velocity at mid-stance on each leg and the vertical COM acceleration at the time of each heel strike. For amputees, we also estimated the instantaneous rate of work performed on the COM by each leg, and total positive work performed in push-off and negative work performed in collision for each leg (Donelan, 2002b; Chapter 3). This computation could not be made for non-amputees because they often stepped on the first force plate with both feet, and single-limb forces could not be recorded during this double-support period.

Walking trials were performed at either a prescribed speed of 1.00 $m \cdot s^{-1}$ (10 non-amputees, body mass M = 68.7 ± 11.9 kg, L = 0.93 ± 0.05 m, mean ± standard deviation; same data set as Chapter 3 (from Donelan 2002a, 2002b)), a prescribed speed of 1.10 $m \cdot s^{-1}$ (4 amputees, mass including prosthesis M = 79 to 104 kg, leg length L unknown), or a prescribed speed of 1.25 $m \cdot s^{-1}$ (4 amputees, M = 79 to 86 kg, L = 0.95 to 1.03 m; and same 10 non-amputees). Walking speed in each trial was measured by photogates placed before and after the force plates. Three trials with clean force plate contact were collected for each condition. Additionally, controlled-speed trials were retaken if speed was not within 0.10 $m \cdot s^{-1}$ of the target speed. All subjects signed informed consent documents before participating, and the protocol was approved by appropriate institutional review boards.

Calculations

We used GRF data to estimate center of mass (COM) velocity as well as gait metrics of mid-stance forward speed, vertical acceleration at opposite heel strike, and push-off and collision COM work. We calculated COM kinematics (linear acceleration and velocity, *v*) from mean three dimensional GRF data using the method of Whittle (1997). We took the dot product of three-dimensional COM velocity *v* with the ground reaction force from each leg to compute the rate of COM work performance by each leg (Donelan, 2002b). We recorded COM forward velocity at mid-stance on each leg, which we defined as the time during single-support when COM vertical velocity passes through zero. We also recorded COM vertical acceleration during each side's stance phase at the time of opposite heel strike. Finally, we integrated the COM work rate curve for each leg from the time of steepest COM velocity declination angle to the subsequent steepest inclination angle to find COM work performed in the step-to-step transition (see Figure 3.8C). We recorded the quantity of positive work performed by the push-off leg and the amount of negative work performed by the landing leg during each step-to-step transition.

Data Analysis

We computed baseline metrics for non-amputees to establish normal levels of variability and asymmetry. We quantified variability in mid-stance COM forward velocity, COM vertical acceleration at opposite heel strike, and push-off and collision COM work by computing the mean and standard deviation of each, treating left and right sides together. We quantified normal asymmetry in these metrics by computing the

absolute difference between left and right for each individual and plotting a histogram of the results. We combined left and right and used absolute difference between sides because the two sides were not expected to differ systematically.

We computed outcome metrics for amputees in order to identify significant differences between amputee and non-amputee gait. We compared mid-stance COM forward velocity, COM vertical acceleration at opposite heel strike, and COM work performed during push-off and collision for the amputees against baseline data, treating prosthetic and intact sides separately. We also compared asymmetry in amputees against baseline asymmetry by computing the difference between metrics for the two sides.

Results

A typical COM hodograph for a non-amputee is shaped like a rounded letter D, with one counter-clockwise loop for each leg's stance phase (Figure 4.1). Double support spans the right (highest-speed) portion of each loop and single support spans the left portion. Just before heel strike, the trailing leg commences push-off, reducing the downward COM velocity and giving the bottom of the D an upward slope. During double-support both legs redirect the COM velocity upward, forming the rounded portion of the D. The maximum upward COM velocity occurs after toe-off as a "rebound" from leg compression. Finally, the middle portion of single-support is characterized by a smooth downward acceleration.

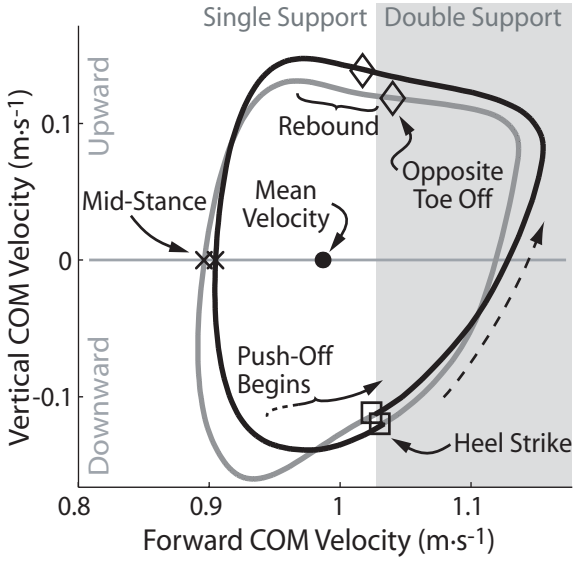

Figure 4.1: Sample COM hodograph for a complete stride cycle of a non-amputee walking at 1.0 m·s^{-1} (from Figure 4.2F). A stride cycle begins at heel strike, and the hodograph progresses counterclockwise for walking. Labels indicate mean velocity and the timing of heel strike, opposite toe off, rebound, mid-stance (defined as zero vertical velocity), and early push-off. Light: Left Stance; Dark: Right Stance. For timing of other gait events, see Figure 3.8.

Non-amputees exhibited no significant asymmetry in any outcome measure (see Figures 4.2, 4.4-4.6). Mid-stance COM forward velocity across both sides was 0.92 ± 0.01 m·s^{-1} (mean ± standard deviation) at 1.00 m·s^{-1}, and 1.18 ± 0.01 m·s^{-1} at 1.25 m·s^{-1}. At both walking speeds this mid-stance forward speed was 92-93% of the walking speed. Absolute asymmetry in mid-stance velocity was 0.01 ± 0.01 m·s^{-1} (mean ± s.d.) at 1.00 m·s^{-1} and 0.02 ± 0.01 m·s^{-1} at 1.25 m·s^{-1}, and samples were most concentrated near zero asymmetry (Figure 4.4). This baseline asymmetry represented 0.013 ± 0.012 times actual walking speed. COM vertical acceleration at opposite heel strike across both sides was 0.40 ± 0.63 m·s^{-2} (mean ± s.d.) at 1.00 m·s^{-1}, and 0.76 ± 0.78 m·s^{-2} at 1.25 m·s^{-1}. Both values were significantly different from zero (P = 0.01 and 4×10^{-4} respectively; *t*-test), indicating that in normal walking the COM experiences some upward acceleration prior to each heel strike. Absolute asymmetry in COM vertical

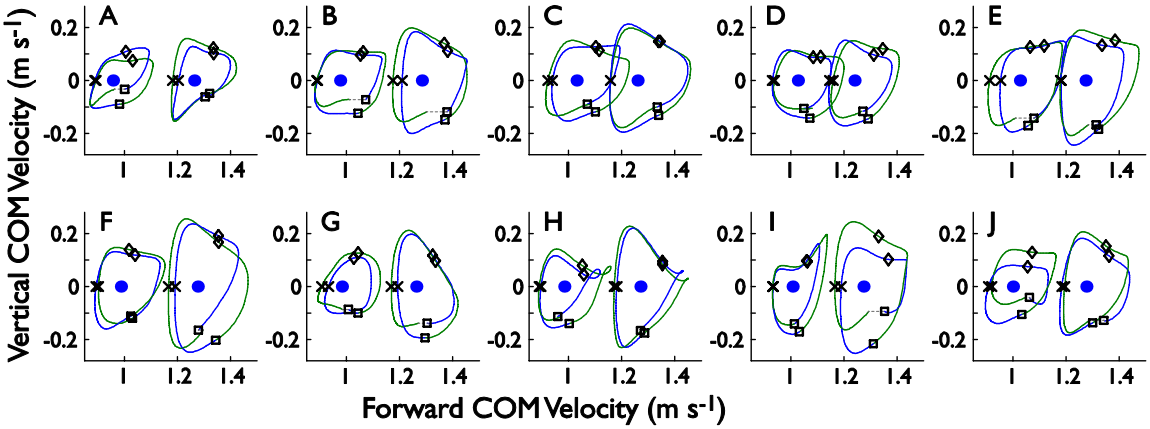

Figure 4.2: Hodographs for ten non-amputee comparison subjects. Mid-stance forward COM velocity is denoted by x's (x) in each loop. Vertical COM acceleration at opposite heel strike is related to hodograph slope; timing is indicated by squares (□). Diamonds (◊) indicate toe-off. Dashed sections connect the end and beginning of strides that are not perfectly periodic as measured.

acceleration at opposite heel strike was 0.49 ± 0.64 $m \cdot s^{-2}$ (mean ± s.d.) at 1.00 $m \cdot s^{-1}$ and 0.81 ± 0.65 at 1.25 $m \cdot s^{-1}$, and again the samples were most concentrated near zero asymmetry (Figure 4.5). Work performed on the center of mass could not be quantified separately for the two legs in non-amputees because subjects stepped on the first force plate with both feet. For the one step-to-step transition with separate force records for the two feet at 1.00 $m \cdot s^{-1}$, positive push-off work performed in each stride was 0.215 ± 0.032 $J \cdot kg^{-1}$ (mean ± s.d.) and negative collision work was 0.122 ± 0.037 $J \cdot kg^{-1}$ (Figure 4.6). At the higher speed of 1.25 $m \cdot s^{-1}$, positive push-off work was 0.244 ± 0.044 $J \cdot kg^{-1}$ and negative collision work was 0.203 ± 0.032 $J \cdot kg^{-1}$.

Unilateral transtibial amputees exhibited significant and substantial asymmetry in mid-stance COM forward velocity, COM vertical acceleration at opposite heel strike, and COM work during push-off and collision. Mid-stance forward COM velocity was substantially higher during prosthetic stance than during intact stance at both speeds (1.05 ± 0.02 $m \cdot s^{-1}$ *versus* 0.96 ± 0.04 $m \cdot s^{-1}$ at 1.10 $m \cdot s^{-1}$; 1.29 ± 0.06 $m \cdot s^{-1}$ *versus* 1.15 ± 0.04 $m \cdot s^{-1}$ at 1.25 $m \cdot s^{-1}$). These speeds represented on average 0.98 and 0.89 times actual

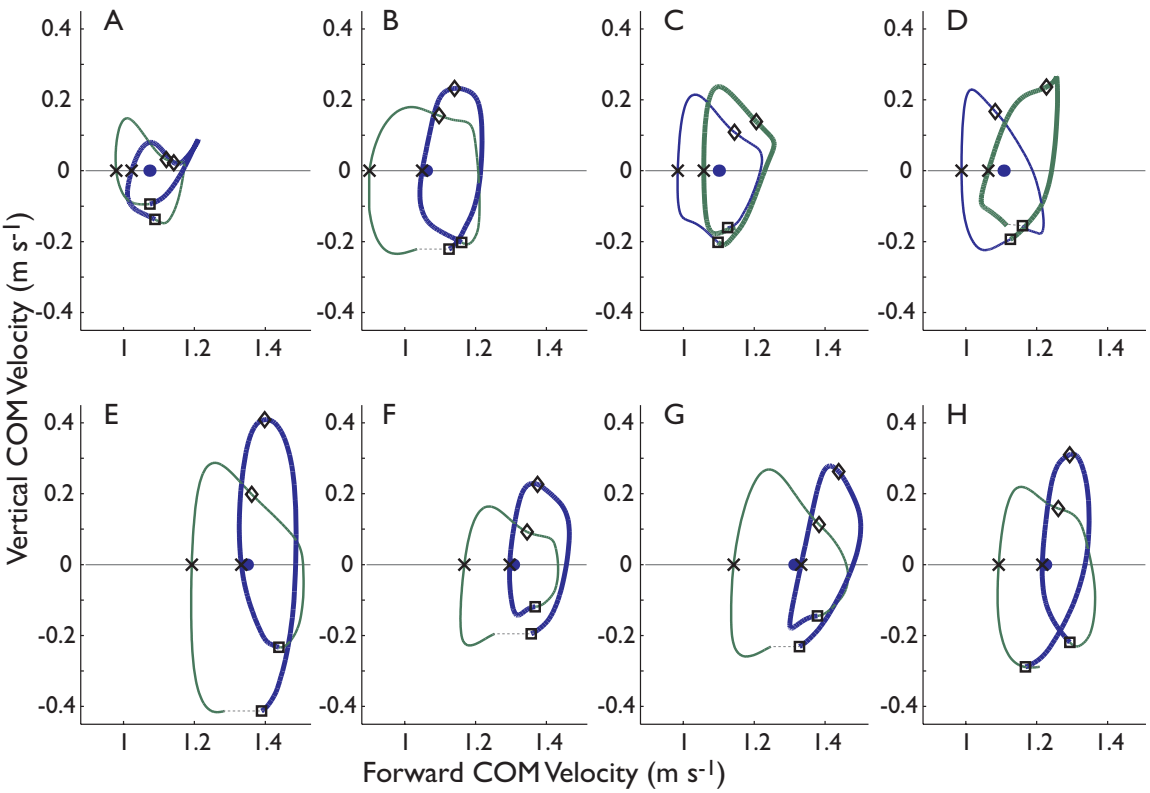

Figure 4.3: Hodographs for eight unilateral transtibial amputees. Bold lines represent the time from prosthetic heel strike to intact heel strike. Significant asymmetry exists in mid-stance forward COM velocity and COM vertical acceleration at opposite heel strike. Individual subjects exhibit further nuance, which may elucidate additional details of their individual walking strategies. See Figure 4.2 for symbol definitions.

walking speed (1.09 and 1.30 m·s^{-1}, different from the specified 1.10 and 1.25 m·s^{-1}) on the prosthetic and intact sides, respectively. The difference between the two sides (0.09 ± 0.04, normalized to walking speed; prosthetic minus intact) was much larger than baseline absolute asymmetry of 0.013 times walking speed (Figure 4.4) and significantly different from zero ($P = 3\times10^{-4}$; paired *t*-test). However, since the baseline mid-stance forward speed (~0.93 times walking speed) is between the two mid-stance speeds of amputee gait, amputees do not appear to alter their strategy in a way that disturbs the overall relationship of mid-stance speed to walking speed.

COM vertical acceleration at opposite heel strike for the amputees was substantially lower and of opposite sign during prosthetic stance (-0.43 ± 0.53; mean ± s.d.;

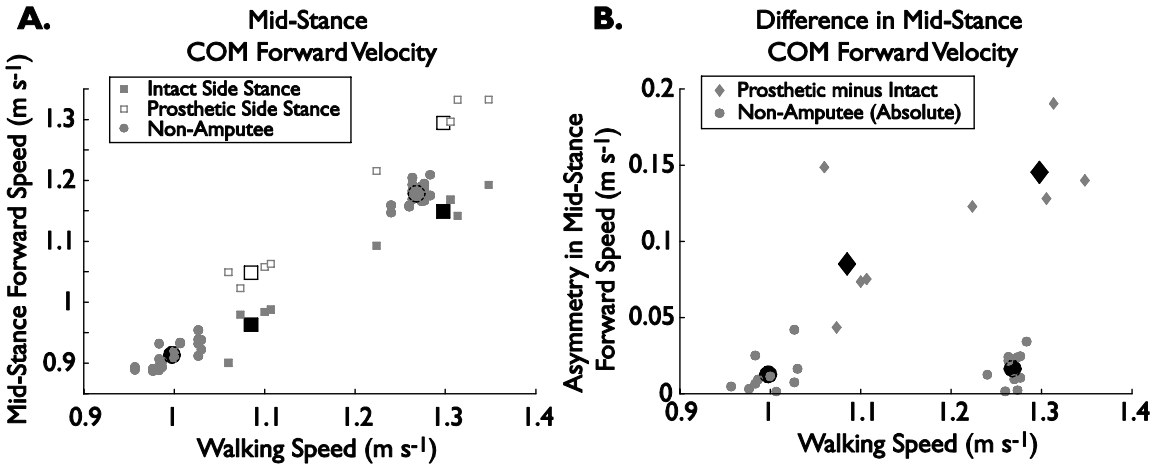

Figure 4.4: Asymmetry in mid-stance forward COM velocity. A) Mid-stance forward speed increases with walking speed, as expected. Amputees have higher speed during prosthetic stance than during intact leg stance. B) Amputees exhibit much larger asymmetry than non-amputees. Data for non-amputees are absolute value of the difference between left and right. Amputee data are computed as prosthetic minus intact. Mid-stance speed asymmetry for amputees also appears to increase with walking speed. In both plots, large black symbols are the mean across subjects for each condition.

normalized to gravity) than during intact stance (0.33 ± 0.52). The difference between the two sides (0.75 ± 0.82; intact minus prosthetic) was larger than baseline absolute asymmetry (Figure 4.5) and significantly different from zero ($P = 0.04$; paired *t*-test), though there was substantial scatter in this measure. COM vertical acceleration at opposite heel strike during intact stance was not different from either baseline case ($P > 0.5$, *t*-test), suggesting that the intact limb performed somewhat normally even though the prosthetic limb did not.

COM work performed by the two legs during the step-to-step transition for unilateral transtibial amputees exhibited significant asymmetry, with both positive push-off work ($P = 0.005$; paired *t*-test) and negative collision work ($P = 0.003$) substantially greater on the intact side than on the amputated side (Figure 4.6). At 1.10 $m \cdot s^{-1}$, positive push-off work performed in each stride was 0.239 ± 0.098 $J \cdot kg^{-1}$ (mean ± s.d.) on the intact side, but only 0.104 ± 0.026 $J \cdot kg^{-1}$ on the prosthetic side. At the higher speed of 1.25 $m \cdot s^{-1}$, positive push-off work was 0.245 ± 0.036 $J \cdot kg^{-1}$ on the intact side, but only 0.120 ± 0.017

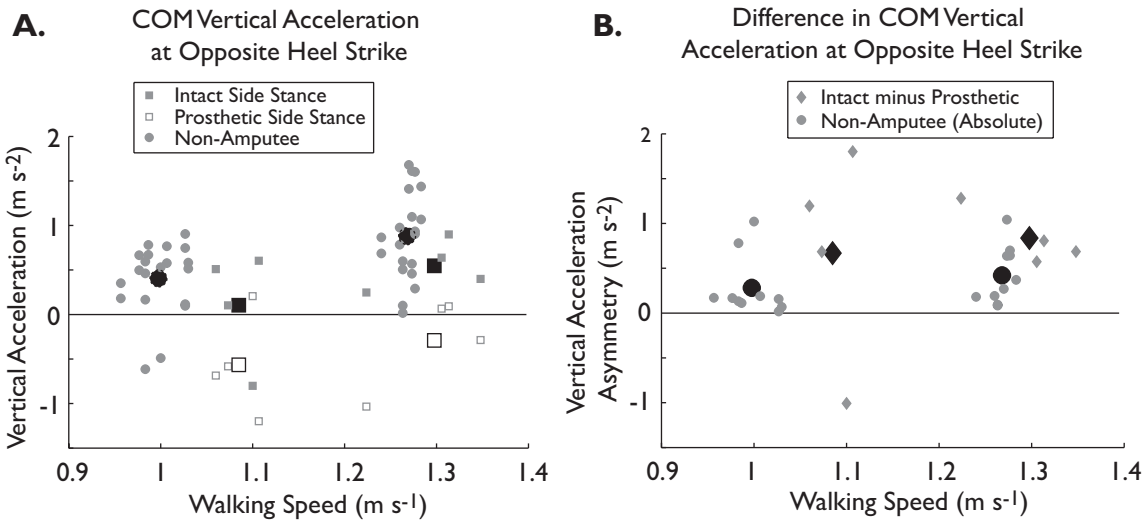

Figure 4.5: COM vertical acceleration at opposite heel strike. A) Results are variable, but COM vertical acceleration at opposite heel strike was generally positive for non-amputees. Similarly, amputees exhibited positive vertical acceleration at prosthetic heel strike (during intact stance) indicating effective push-off by the intact leg. However, vertical acceleration at intact heel strike (prosthetic stance) was generally negative on the prosthetic side, indicating weak prosthetic push-off. B) Asymmetry in vertical acceleration at opposite heel strike is greater in amputees than in non-amputees. In both plots, large black symbols are the mean across subjects for each condition.

$J \cdot kg^{-1}$ on the prosthetic side. At each speed, the intact leg positive push-off work is similar to the value for non-amputees, while the prosthetic leg push-off work is much lower. Negative collision work performed in each stride at 1.10 $m \cdot s^{-1}$ was 0.183 ± 0.041 $J \cdot kg^{-1}$ on the intact side, but only 0.101 ± 0.033 $J \cdot kg^{-1}$ on the prosthetic side. At 1.25 $m \cdot s^{-1}$, negative collision work was 0.220 ± 0.019 $J \cdot kg^{-1}$ on the intact side, but only 0.126 ± 0.065 $J \cdot kg^{-1}$ on the prosthetic side. These results are consistent with principles and models of dynamic walking, which show that push-off on one side acts to mitigate the ensuing contralateral collision by preemptively redirecting the COM (see Chapters 2-3).

Discussion

We proposed the use of center of mass hodographs to help understand gait abnormalities because it is a simple and convenient visualization tool that puts the

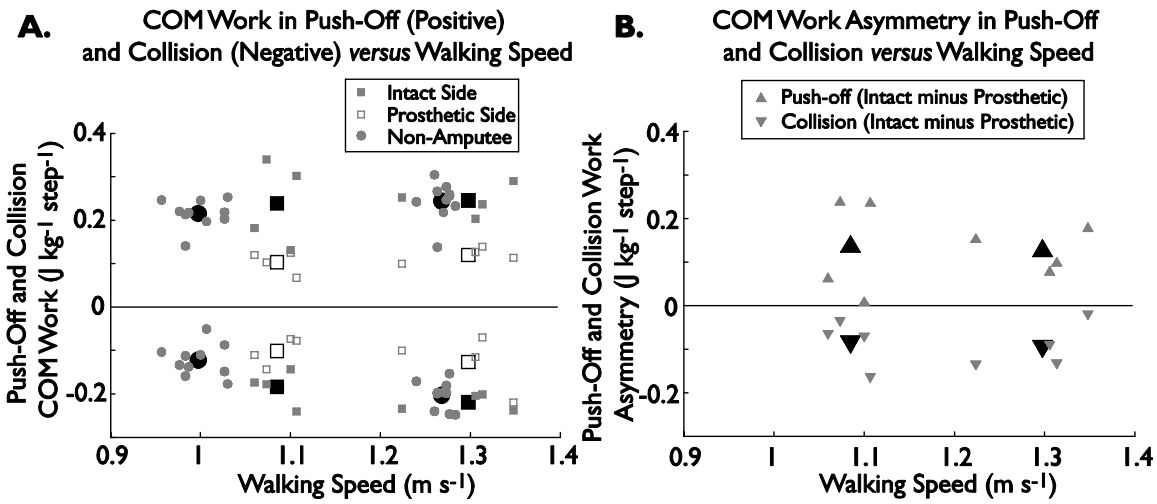

Figure 4.6: COM Work performed during the step-to-step transition for amputees and non-amputees. A) Work performed in push-off by the trailing leg (positive) and in collision by the leading leg (negative) are significantly greater for the intact leg than for the prosthetic leg. B) The difference in push-off and collision work between prosthetic and intact legs shows that the intact leg performed both push-off work and collision work in greater quantity than the prosthetic leg did. For comparison subjects, only one leg could be measured, so no difference could be calculated. In both plots, large black symbols are the mean across subjects for each condition. See Figure 3.8C for measure definitions.

motions of gait into a meaningful context in velocity space. Viewing gait through fluctuations in COM velocity helps illustrate the link between COM motion and the work and forces it requires. Because the kinetic energy of COM motion is proportional to the square of COM velocity magnitude, any change in velocity magnitude implies that work has been performed on the center of mass. Because COM velocity is the integral of the body's net acceleration and acceleration is net force divided by mass, the net force acting on the body is proportional to the rate of change of COM velocity – the slope and arc speed of the hodograph at any point. These relationships inform our interpretation of the present results for unilateral transtibial amputees.

The asymmetry in mid-stance COM forward velocity between amputees' two sides indicates that the two legs have different roles in facilitating the body's forward motion. Since COM forward velocity is higher during prosthetic side stance than during intact

side stance, net work must be performed on the center of mass between these two times: positive work during the time from intact to prosthetic mid-stance, and negative work from prosthetic to intact mid-stance. The observed asymmetry in step-to-step transition COM work confirms these effects. In the prosthetic-to-intact transition, more negative work is performed than positive; in the intact-to-prosthetic transition, there is more positive than negative work. The fore-aft forces that must perform this work are greatest near double support as the trailing leg pushes-off in a forward and up direction while the leading leg pushes backward and up to accept the load of the body. Therefore, the negative work between prosthetic and intact mid-stance must be due to abnormally low forward push-off forces on the prosthetic side and/or abnormally high rearward load-acceptance forces on the intact side. Similarly, positive work between intact and prosthetic mid-stance must be due to abnormally high forward push-off forces on the intact side and/or abnormally low rearward load-acceptance forces on the prosthetic side. Our analysis suggests that the abnormal actions are mostly localized on the prosthetic side, because the COM vertical acceleration at prosthetic heel strike indicates that at least in early push-off, the intact leg performs very similarly to normal while the prosthetic side leg does not.

Our finding of asymmetric mid-stance COM forward velocity in amputees is complicated somewhat by the difference in mass between the two legs. A prosthetic lower leg typically weighs about 0.015 times body mass less than the intact leg (Selles, 2003). During the stance phase of walking at 1.10 $m \cdot s^{-1}$ each foot moves with near zero velocity, but during swing phase the foot moves at roughly 3.5 $m \cdot s^{-1}$. Because each body segment contributes to COM velocity in proportion to its mass, the missing mass on the

prosthetic side would cause an asymmetry of roughly 0.05 $m \cdot s^{-1}$ for 1.10 $m \cdot s^{-1}$ walking, even with perfectly symmetric body kinematics. This effect could explain roughly half of the observed asymmetry in mid-stance forward COM velocity. Nevertheless, if we account for this effect by adding 0.05 $m \cdot s^{-1}$ to the measured intact side mid-stance forward COM velocity, significant asymmetry remains ($P = 0.01$, paired *t*-test).

The deviation in COM vertical acceleration at opposite heel strike on the prosthetic side indicates that the prosthetic leg is unable to produce sufficient vertical force to begin push-off in late single stance. Simple models of bipedal walking (Kuo, 2002; Ruina, 2005) have shown that pre-emptive push-off – starting push-off with the trailing leg before the leading leg accepts the load of the body – reduces the work (and presumably the metabolic energy) required for gait in comparison with later push-off timing. Push-off by the trailing leg begins redirecting COM velocity upward, and the leading leg can continue this redirection without having to stop downward COM motion first. In the amputees we studied, early stage prosthetic side push-off appears insufficient, which causes the intact leg to perform more negative work than normal in load acceptance. This mechanism could contribute to the increased metabolic cost of walking observed in amputees (Waters, 1999).

We computed COM vertical acceleration at opposite heel strike directly from acceleration data in this study, but the meaningful information in this metric can be read directly from a COM hodograph as well. COM vertical acceleration is the rate of change of COM vertical velocity, so any time the COM hodograph trace is moving upward, the COM is accelerating vertically upward. Near the time of heel strike, the COM is nearly always accelerating forward, so positive or negative vertical COM acceleration gives the

hodograph a positive or negative slope. Therefore, the slope of the COM hodograph at the time of opposite heel strike indicates the amount of pre-emptive push-off by the leg in question. Furthermore, in addition to the direction of COM acceleration, magnitude can be estimated from a hodograph if the curve is plotted with markers spaced at regular intervals in time.

In addition to mid-stance COM forward velocity and COM vertical acceleration at the time of opposite heel strike, we observed other distinct qualitative features of individual intact and amputee COM hodographs. For example, two amputees (Figure 4.3 A,D) and one non-amputee (Figure 4.2 H) exhibited a point or loop in the upper-right section of the COM hodograph. For another example, five amputees (B, E-H) seemed to have lower overall range in COM forward velocity during prosthetic stance than during intact stance. It is unknown what causes these behaviors and why particular subjects exhibit them, but they are nonetheless distinct from other, more typical gait hodographs, and it may be helpful to view them in terms of their impact on center of mass motion.

The utility of the COM hodograph is greatly enhanced by the simplicity of its construction. The only data necessary for constructing a basic hodograph are whole-body ground reaction forces for a complete stride. In clinical settings outside a complete gait laboratory, or wherever there is a limited equipment budget, the single large force plate necessary to obtain whole-body GRF data is an economical and compact way to enhance visual observation and diagnosis with quantitative measurements of gait. In addition, the COM hodograph is useful in time-constrained situations because it can be produced quickly by a simple computer program from reliable force plate data, in contrast to the interactive modeling and expensive software needed to process motion capture data in a

gait laboratory. The force plate can be used for over-ground trials as in this study, or a treadmill can be placed on top of it to provide a true steady-state COM hodograph. Finally, the COM hodograph can be enhanced as circumstances allow, by additional equipment such as a second force plate for individual limb GRF measurements or foot switches to better detect ground contact timing on each side.

Conclusions

The center of mass (COM) hodograph is a useful tool to help understand gait abnormalities in terms of their impact on the motion of the body's center of mass. We used the COM hodograph to identify systematic asymmetry in the gait of amputees. Unilateral transtibial amputees exhibit a significantly lower COM forward velocity during intact *versus* prosthetic stance, implying a difference in mechanical energetic state between these times. The amputees also usually exhibit a downward COM vertical acceleration during prosthetic stance at the time of intact heel strike, rather than the upward acceleration observed during intact stance and in non-amputees. Further analysis of the COM hodograph can reveal additional gait features that may reflect nuances of each individual's impairment or coping strategy. We propose the center of mass hodograph as a simple, convenient visualization tool for enhancing clinical understanding of each patient's gait.

References

Adamczyk, P. G., S. H. Collins and A. D. Kuo. (2006). The advantages of a rolling foot in human walking. *Journal of Experimental Biology* **209**, 3953-3963.

Cavagna, G. A. (1975). Force platforms as ergometers. *Journal of Applied Physiology* **39**, 174-179.

Donelan, J. M., R. Kram and A. D. Kuo. (2002a). Mechanical work for step-to-step transitions is a major determinant of the metabolic cost of human walking. *Journal of Experimental Biology* **205**, 3717-27.

Donelan, J. M., R. Kram and A. D. Kuo. (2002b). Simultaneous positive and negative external work in human walking. *Journal of Biomechanics* **35**, 117-24.

Garcia, M., A. Ruina, A. Chatterjee, and M. Coleman. (1998). The simplest walking model: stability, complexity, and scaling. *ASME Journal of Biomechanical Engineering* **120**, 281-288.

Greenwood, D. T. (1988). *Principles of Dynamics*. Prentice-Hall, Englewood Cliffs, NJ.

Kuo, A. D. (2002). Energetics of actively powered locomotion using the simplest walking model. *Journal of Biomechanical Engineering* **124**, 113-20.

McGinley J. L., Goldie P. A., Greenwood K. M., and Olney S. J. (2003). Accuracy and reliability of observational gait analysis data: judgments of push-off in gait after stroke. *Physical Therapy* **83**, 146 –160.

Narayanan, U. G. (2007). The role of gait analysis in the orthopaedic management of ambulatory cerebral palsy. *Current Opinion in Pediatrics* **19**, 38-43.

Nolan, L. et al. (2003). Adjustments in gait symmetry with walking speed in TF and TT amputees. *Gait and Posture* **17**, 142-151.

Orendurff M. S., A. D. Segal, G. K. Klute, J. S. Berge, et al. (2004) The effect of walking speed on center of mass displacement. *Journal of Rehabilitation Research and Development* **41**, 829-34.

Ruina, A., J. E. A. Bertram and M. Srinivasan. (2005). A collisional model of the energetic cost of support work qualitatively explains leg sequencing in walking and galloping, pseudo-elastic leg behavior in running and the walk-to-run transition. *Journal of Theoretical Biology* **237**, 170-92.

Waters, R. L. and S. Mulroy (1999). The energy expenditure of normal and pathologic gait. *Gait & Posture* 9(3):207-231.

Whittle, M. W. (1997). Three-dimensional motion of the center of gravity of the body during walking. *Human Movement Science* **16**, 347-355.

Wren, T. A. L., K. P. Do, R. Hara, F. J. Dorey, R. M. Kay, and N. Y. Otsuka. (2007). Gillette Gait Index as a gait analysis summary measure: comparison with qualitative visual assessments of overall gait. *Journal of Pediatric Orthopedics* **27**, 765-768.

Zmitrewicz R. J., R. R. Neptune, J. G. Walden, W. E. Rogers, and G. W. Bosker. (2006). The effect of foot and ankle prosthetic components on braking and propulsive impulses during transtibial amputee gait. *Archives of Physical Medicine and Rehabilitation* **87**, 1334-1339.

Chapter 5

Design and Testing of the Rock'N'Lock Foot: A Reconfigurable Prosthesis for Walking and Standing

Introduction

In our study of the effects of arc radius of curvature on the energetics of walking, we demonstrated that in walking with fixed ankles, an arc-shaped foot can reduce the amount of work performed on the center of mass (COM) to levels considerably below the work of normal gait, and can strongly influence the metabolic cost of walking (Adamczyk, 2006; Chapter 2). There are many situations in which humans walk without their usual ankle motion, ranging from sports (e.g., ice skates and ski boots) to injury (e.g., casts and orthoses) to amputation (foot prostheses). Our prior results lead us to believe that in such situations, a well-chosen rigid arc shape on the bottom of the foot may benefit users by reducing the energetic costs of walking. Use of a good rigid foot shape may be particularly helpful to wearers of orthoses and prostheses, for whom the underlying cause of ankle fixation is usually permanent and inescapable, and affects every aspect of their lives.

The natural human foot and ankle move and deform during walking so that their behavior with respect to the rest of the body strongly resembles that of a rigid arc (Hansen, 2004a, 2004b, 2005). This arc, termed the "roll-over shape," suggests that the body makes use of the kind of rolling dynamics that occur in fixed-ankle gait, even when the ankle could behave differently. The natural roll-over shape is also robust to changes in walking speed, shoe heel height and carried load (Hansen, 2004a, 2004b, 2005), suggesting that the shape may provide some benefit that the body tries to conserve. Existing prosthetic feet also behave somewhat like arcs, bending into dorsiflexion as the body advances through the stance phase of gait (Hansen, 2000). Researchers have proposed that an important effect of prosthetic foot alignment procedures is to align the roll-over shape of a unilateral amputee's prosthesis to match the roll-over shape of the intact side. In this manner an amputee's gait can be optimized for symmetry (Hansen, 2000), though symmetry may not necessarily be best goal (Hansen, 2007). However, there has been no investigation of the energetic effects of variations in roll-over shape on amputee gait.

Our prior results suggest that a simple match to the intact side may not be the best shape for a prosthesis, since a larger radius of foot curvature always led to lower mechanical work requirements in our experiment (Adamczyk, 2006; Chaper 2). There may exist a foot shape that provides additional energetic benefits to an amputee, even though it may cause less symmetric gait. Furthermore, a roll-over shape produced by material deformation in a prosthesis may not be optimal, because deformation necessarily leads to energy dissipation within the prosthesis material (Geil, 2001). In contrast, a rigid arc can provide the same roll-over shape without dissipating energy. To investigate these

possible advantages, we decided to design a prosthetic foot that provides the benefits of an optimized rigid foot shape to amputees. We hypothesized that a well-designed rigid foot shape would reduce the metabolic cost of walking in comparison to other prostheses.

A foot prosthesis designed for daily use must be helpful for more than just walking, however. Among other requirements, a prosthesis must be comfortable and stable for standing, and unobtrusive in appearance. A rigid arc-shaped prosthesis is neither. As subjects in our arc-foot study discovered, it is very difficult to stand still with a fixed ankle and a rounded foot bottom, because ankle moment cannot be used to adjust the center of pressure underfoot. In addition, a rigid arc-shaped foot is markedly different in appearance from a natural foot. Because of these limitations of an arc-shaped walking foot, we sought to design a reconfigurable prosthesis, called the Rock'N'Lock foot, which would exploit a rigid arc shape for energetic benefits during walking, but change into more a stable and natural-looking shape while standing still or sitting down.

Design Features of the Rock'N'Lock Foot

The key feature of the Rock'N'Lock Foot (Figure 5.1) is the ability to reconfigure into two modes, while always retaining the strength to stably support the user's weight. This mode-switching is enabled by a simple linkage, in which a base link attaches to the user's tibial pylon, and moving links on the bottom of the foot pivot into two positions. In walking position the foot bottom is convex for an easy rolling effect (Figure 5.1, 5.2A). In standing position the rolling effect is removed, and there is stable ground contact at the

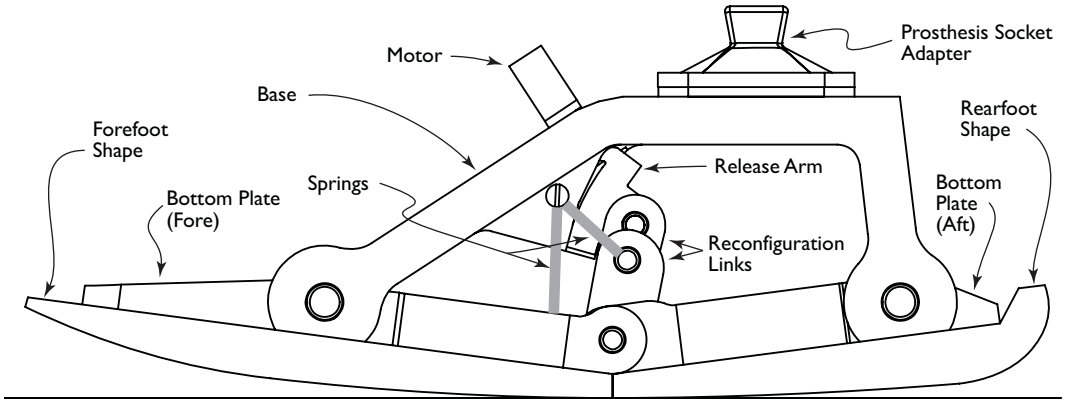

Figure 5.1: The Rock'N'Lock foot, here shown in the rounded, walking configuration.

heel and the toe (Figure 5.2D). The foot is locked firmly into both positions to support the user's weight in any task.

There are four load-bearing links that move to reconfigure the foot bottom (Figure 5.1). Fore and aft foot bottom sections pivot with respect to the base about joint axes at the ball of the foot and below the ankle. These two sections also share an axis near the middle of the foot, which is allowed to slide relative to the aft section in a slot. A load-bearing chain of two reconfiguration links connects this axis to the base, also near mid-foot (Figure 5.1). This chain accomplishes reconfiguration of the bottom sections by either sequential alignment or nested alignment of the two links in a kinematic singularity. If the two links are aligned sequentially, the mid-foot axis between the bottom segments assumes a "down" position, which allows a smooth arc shape to be formed on the bottom of the foot for walking (Figure 5.1, 5.2A). In this configuration, mid-foot forces are transferred to the base through compression or tension in both reconfiguration links. If the two links are nested, the mid-foot axis between the bottom segments assumes an "up" position, causing the fore and aft foot bottom sections to rotate 15 degrees from their orientation in walking mode and lower the heel and toe (Figure

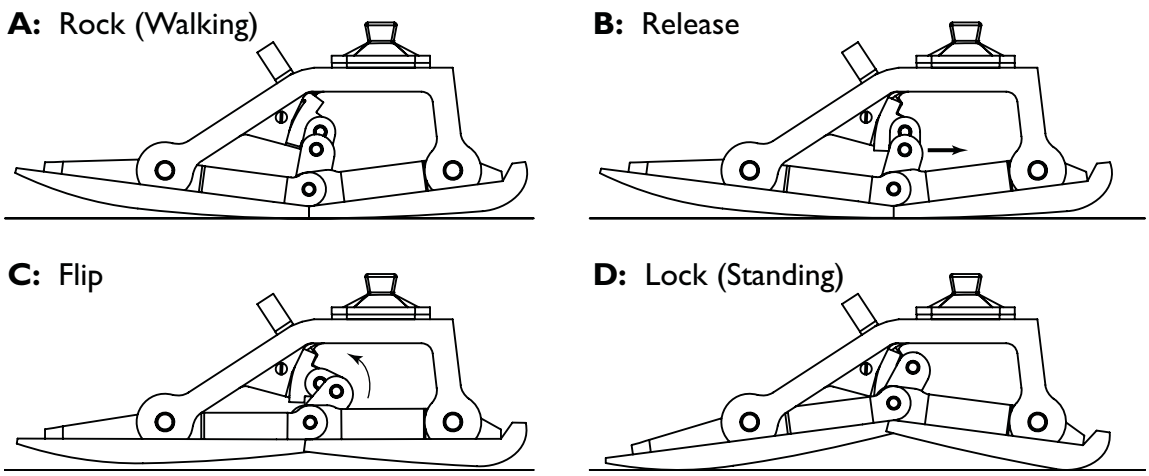

Figure 5.2: Reconfiguration of the Rock'N'Lock foot from walking mode to standing mode. A: Walking mode has a smoothly contoured foot bottom shape for economical locomotion. B: To initiate mode switching, the release arm pushes the mid-reconfiguration chain axis out of its kinematic singularity. C: Once out of the singularity, a spring from the base to the forefoot plate (see Figure 5.1) pulls the forefoot up, folding up the reconfiguration chain simultaneously. D: In standing mode, the reconfiguration links take a nested configuration and the foot bottom establishes heel and toe contact with the ground.

5.2B-D). With heel and toe lowered, the foot establishes two-line contact with the ground, providing a long base of support for standing. In this configuration, loads are transmitted through one reconfiguration link in compression and through the other in tension.

The two positions of the reconfiguration links are strong and stable because they represent a kinematic singularity in the linkage. With three axes aligned (the mid-foot-bottom axis, the mid-reconfiguration-chain axis and the chain-to-base axis), the whole reconfiguration chain acts as a single member transmitting loads from foot bottom to base. The mechanism is held stably in these positions by hard stops on the base that prevent the mid-chain axis from moving forward, and by a bias spring that pulls the mid-chain axis to rest against the hard stops (Figure 5.1).

Mode switching is accomplished by perturbing the reconfiguration links out of their kinematic singularity and allowing other forces to move the pieces. The mechanism to

perturb the reconfiguration links consists of an irregular aluminum release arm mounted on the chain-to-base axis, having arms that contact the proximal reconfiguration link on the same surface that rests against the hard stop, near the mid-reconfiguration-chain axis (Figure 5.1). To switch modes, this release arm rotates 23 degrees under force from an actuator attached at its upper end, so that one of its arms pushes the mid-chain axis out of the kinematic singularity (Figure 5.2B). Then, a force in the correct direction along the distal link causes the proximal link to flip over and settle in the opposite singularity.

To switch from rounded walking mode to flat standing mode, a spring from the bottom forefoot link to the base produces a compressive force in the distal reconfiguration link, which is no longer balanced by the proximal link in alignment. This force causes the proximal link to rotate up around its axis with the base (Figure 5.2C). Then, the reconfiguration chain settles into standing mode. This switch only occurs if the foot is off the ground, because body weight forces dominate the effects of the spring.

The switch from flat standing mode to rounded walking mode is powered by external forces from heel strike or toe push-off. Once the proximal reconfiguration link is pushed out of its “up” position by the release arm, either of these forces produces a tensile force in the distal reconfiguration link. This force is not balanced by the proximal link in alignment, so it causes the proximal link to rotate down around its axis with the base. Then the reconfiguration chain settles into walking mode.

Using a kinematic singularity to support external loads and a perturbation mechanism for mode-switching removes the Rock’N’Lock actuator from the path of external loads, allowing it to be small, lightweight, and low in energy consumption. The

actuator for the release arm is a preloaded spring (preload about 4 N) attached to the arm of a servomotor (length 0.0125 m). The servomotor axis intersects the reconfiguration chain-to-base axis at a right angle. As the servomotor rotates its arm 180 degrees, it stretches the spring by only about 0.009 m, while reversing the force the spring applies to the release arm. When the force applied by the actuator spring overcomes the bias spring force pulling the mid-chain axis against the hard stop, the axis is pushed out of its singularity. This out-of-plane, series-elastic design allows most of the actuator force to be supplied by a simple spring pre-load rather than the motor, and prevents damage to the motor if the reconfiguration links are back-driven by external forces.

The particular shape taken by the Rock'N'Lock foot in walking and standing modes is determined by the contour of two foam rubber pieces attached to the foot-bottom links. These are shaped from ethylene-vinyl acetate (EVA) foam, commonly known as "crepe" (SoleTech, Salem, MA). The two pieces are interleaved at mid-foot to eliminate any gap in walking configuration, while still allowing the foot to fold up into standing mode. We originally designed these shapes so that the foot would have the same height and inclination in both modes (shown in Figure 5.2A,D). However, the preferred orientation is different for walking and standing; users prefer a slightly plantar-flexed orientation for walking, and a more dorsiflexed orientation to allow slight knee flexion while standing still. The second-generation foot bottom shape changes this angle by 5 degrees when switching between modes in order to accommodate this preference.

The first prototype of the Rock'N'Lock Foot also includes many other basic design features that are crucial to a usable prosthetic foot. It is lightweight, at about 1.1 kg including batteries, and can easily be reduced further with revision. It is strong enough

for users over 100 kg. It runs for 3-4 days on 4 AAA batteries. And, it can fit inside a shoe in some configurations. Therefore, we believe this first prototype can be developed further into a marketable prosthesis if it proves effective and useful for amputees.

Prototype 1 Testing

Methods

In order to determine the effectiveness of using a simple rigid arc shape to reduce metabolic cost, we performed pilot testing of the Rock'N'Lock foot on unilateral transtibial amputees. We measured metabolic energy expenditure and ground reaction forces while subjects walked wearing their usual prostheses and shoes, and wearing the Rock'N'Lock foot. We compared the cost of walking in the two conditions to determine whether one was energetically superior. We also compared body center of mass (COM) velocity fluctuations using a full-stride COM hodograph to understand the effects of the two prostheses on the motion of the body center of mass.

Subjects walked on a treadmill at 1.25 $m \cdot s^{-1}$ while we collected respiratory gas exchange data to estimate energy expenditure. Four unilateral transtibial amputees (all male; body mass including prosthesis, M = 79 to 86 kg; leg length, floor to greater trochanter, L = 0.95 to 1.03 m) performed metabolic trials on a standard treadmill. In addition, two of the subjects performed metabolic tests at the higher speed of 1.5 $m \cdot s^{-1}$ to help clarify the effect of speed. The amputees also performed speed-matched mechanics measurement trials, in which they walked across two force plates (Bertec, Columbus, OH) in a walkway while we measured ground reaction forces (GRF). In these trials,

speed was measured with photogates and trials were discarded if speed was not within 0.1 $m \cdot s^{-1}$ of the target speed. We collected at least six good trials in each condition. All subjects signed an informed consent document approved by the local Institutional Review Board prior to participating in this experiment.

We estimated metabolic energy expenditure rate from respiratory gas exchange data collected during the treadmill trials. We used a portable open-circuit respirometry system (Viasys Respiratory Care, Yorba Linda, CA) to measure the volume rates of oxygen consumption and carbon dioxide production ($\dot{V}_{O_2}$ and $\dot{V}_{CO_2}$, $mL \cdot sec^{-1}$). Following a 3-minute transient period to allow subjects to reach steady state, we collected and averaged volume rates over at least 3 minutes of each trial. Metabolic energy expenditure rate $\dot{E}_{met}$ was estimated using the formula

$$\dot{E}_{met}(W) = 16.48 \tfrac{J}{ml} \cdot \dot{V}_{O_2} + 4.48 \tfrac{J}{ml} \cdot \dot{V}_{CO_2}, \quad (5.1)$$

after Brockway (1987) and Weir (1949). Finally, we calculated net metabolic rate by subtracting the metabolic rate of quiet standing. The quiet standing data collection procedure was similar to that of the walking tests, but was performed before any other trials.

We used GRF data to estimate the COM velocity changes that occurred throughout the stride cycle for each amputee. We calculated COM kinematics (linear acceleration, velocity, and position) from average three-dimensional GRF data from all acceptable trials (6-7 per subject) (Whittle, 1997; Donelan, 2002b). The velocity data were then used to plot a COM hodograph, illustrating the changes in COM velocity over the course of a

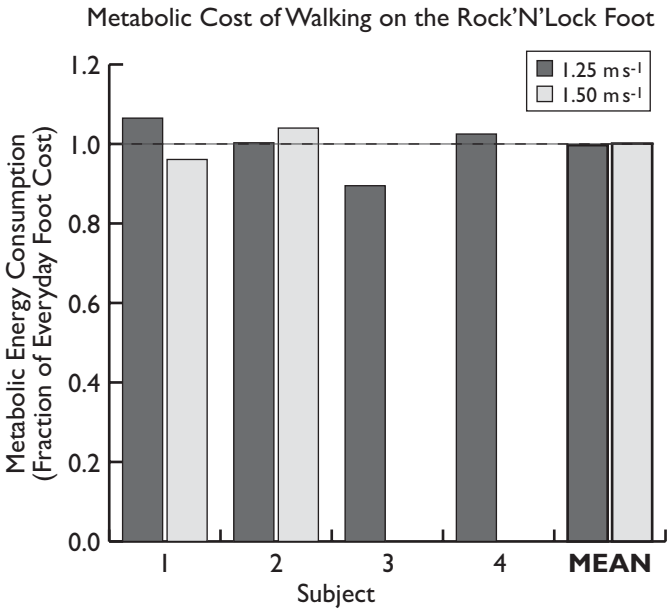

Figure 5.3: Metabolic cost for walking on the Rock'N'Lock for four amputees, at 1.25 and 1.50 meters per second. Mean cost across subjects is indistinguishable from the cost of the subjects' everyday foot at both speeds.

stride. One subject (Subject 4) was excluded from the hodograph analysis because his steps using the Rock'N'Lock foot did not contact the force plates cleanly.

Results

The four amputees exhibited no mean difference in cost when walking on the Rock'N'Lock foot *versus* their usual prostheses, though subject-specific results were variable (Figure 5.3). At 1.25 $m \cdot s^{-1}$, two amputees (Subjects 1 and 4) had slightly higher walking cost with the Rock'N'Lock foot than with their usual prostheses (7% and 2%), while one amputee had no difference and one amputee (Subject 3) had substantially lower cost (10%). At the higher speed of 1.5 $m \cdot s^{-1}$, one amputee (Subject 2) had greater cost (4%) in walking with the Rock'N'Lock foot, while one amputee (Subject 1) had lower cost (4%). On average, there was less than 0.5% difference between the costs of the two feet, at both speeds.

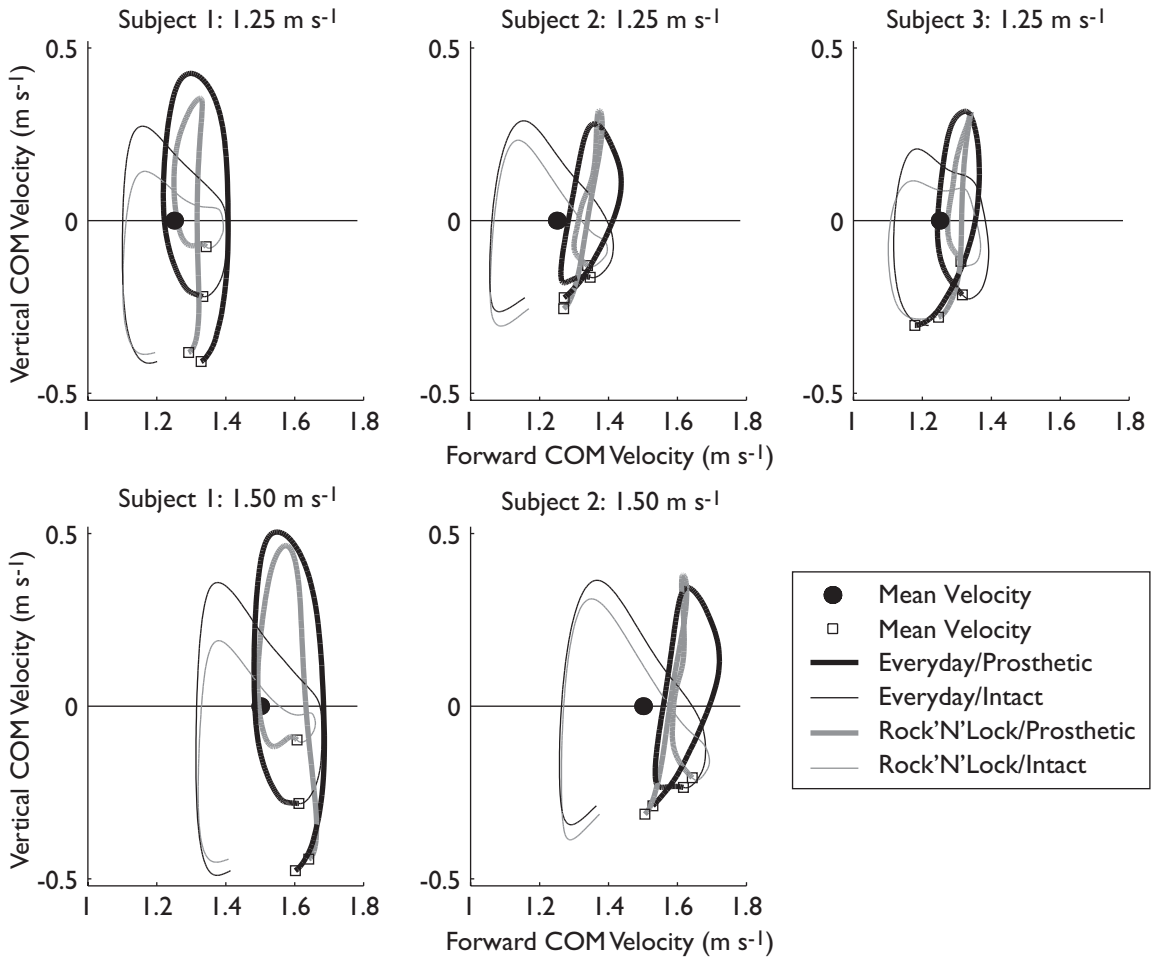

Figure 5.4: Hodographs for three subjects walking with their everyday prosthesis and with the Rock'N'Lock foot. COM vertical velocity is greater (less negative) at the time of intact-leg heel strike in the Rock'N'Lock case, suggesting that the Rock'N'Lock foot provides more support of body weight during late stance that the subjects' usual feet. Also note that asymmetry between the two hodograph loops is also greater in the Rock'N'Lock case.

The amputees' hodographs changed substantially with condition (Figure 5.4). In all three subjects analyzed, the prosthetic-side loop of the hodograph was narrower for the Rock'N'Lock foot than for the subject's own foot. All three subjects also showed a substantial increase in COM vertical velocity at the time of intact heel strike (late prosthetic-side stance) when wearing the Rock'N'Lock foot versus their own usual foot, suggesting that the prosthetic side provides stronger support against gravity with the Rock'N'Lock foot. All subjects also had lower vertical COM velocity in the intact-side "rebound" phase when wearing the Rock'N'Lock foot. Finally, the two hodograph loops

are less similar when wearing the Rock'N'Lock foot, indicating that COM motion is less symmetric overall in that condition.

Discussion

The variety of metabolic responses to the Rock'N'Lock foot suggests that the different strategies amputees adopt for controlling and powering their gait have substantial influence on the cost of walking with any particular prosthesis. The fact that some amputees had increased cost while others had equal or lower cost suggests that the Rock'N'Lock foot fit better into the gait of some subjects than others. Learning and adaptation must take place in order for each individual to minimize the cost of gait with a new prosthesis, and this learning is probably even more important if the new prosthesis behaves very differently from others that are more familiar. Our results showing equal cost between the novel Rock'N'Lock foot and other feet to which subjects were fully habituated should be considered promising, because it is likely that the cost of walking on the Rock'N'Lock would decrease further if subjects were allowed to adapt to it completely.

We also expect to achieve further metabolic improvements in future versions of the Rock'N'Lock foot through better design of the foot bottom shape. The shape we tested was designed to maintain constant height and foot inclination with a low profile, rather than to minimize cost. In fact, the best shape for minimizing cost was unknown at the time of this pilot test. We also had not yet eliminated the gap between the fore and aft segments of the sole, so the subjects experienced a slight bump between them during

every step. In addition, we received feedback from subjects after the test that the heel of the foot felt too stiff, and caused an uncomfortable, jarring bump at heel strike. It is likely that subjects modified their gait to minimize this effect, incurring greater cost in the process. More careful design of the foot bottom shape and stiffness will help improve the performance of the Rock'N'Lock foot.

It appears that the walking speed can also affect how well a foot prosthesis performs for an individual. For example, subject 1 required more energy to walk with the Rock'N'Lock foot than with his own foot at 1.25 $m \cdot s^{-1}$, but less energy at 1.5 $m \cdot s^{-1}$ (Figure 5.3). In contrast, subject 2 had the same cost for both feet at 1.25 $m \cdot s^{-1}$, but had a higher cost for the Rock'N'Lock at 1.5 $m \cdot s^{-1}$. The variability of this response may make it more difficult to choose a favorable static shape, because the same shape may not be best for all walking speeds. However, this problem is not unlike the challenge of specifying a conventional foot prosthesis, in which a constant foot stiffness is chosen based on an individual's activity level. The chosen foot stiffness is very effective for the specified activity (e.g. walking slowly), but may not be optimal for others (e.g. fast walking).

Increased asymmetry does not appear to increase the metabolic cost of walking directly. All three hodographs showed more asymmetry in COM motion when the subjects wore the Rock'N'Lock foot than when they wore their usual prostheses, but only one of these three subjects (two of four overall) had a substantial increase in cost. Enhancing symmetry for its own sake does not appear to be a good driving goal for prosthesis design, and it could even be harmful (Hansen, 2007). In the case of the

Rock’N’Lock foot, it is very likely that the best design will still lead to some asymmetry. We hope to choose features that make this asymmetry beneficial.

References

Adamczyk, P. G., S. H. Collins and A. D. Kuo. (2006). The advantages of a rolling foot in human walking. *Journal of Experimental Biology* **209**, 3953-3963.

Brockway, J. M. (1987). Derivation of formulae used to calculate energy expenditure in man. *Human Nutrition: Clinical Nutrition* **41C, 463-471.**

Donelan, J. M., R. Kram and A. D. Kuo. (2002). Simultaneous positive and negative external work in human walking. *Journal of Biomechanics* **35**, 117-24.

Geil, M. D. (2001). Energy loss and stiffness properties of dynamic elastic response prosthetic feet. *Journal of Prosthetics and Orthotics* **13**, 70.

Hansen, A. D. (2000). Prosthetic foot roll-over shapes with implications for alignment of trans-tibial prostheses. *Prosthetics and Orthotics International* **24**, 205-215.

Hansen, A. D., and D. S. Childress. (2004a). Effects of shoe heel height on biologic rollover characteristics during walking. *Journal of Rehabilitation Research and Development* **41**, 547-54.

Hansen, A. D., and D. S. Childress. (2005). Effects of adding weight to the torso on roll-over characteristics in walking. *Journal of Rehabilitation Research and Development* **42**, 381-90.

Hansen, A. D., D. S. Childress and E. H. Knox. (2004b). Roll-over shapes of human locomotor systems: effects of walking speed. *Clinical Biomechanics* **19**.

Hansen, A. D., M. R. Meier, P. H. Sessoms, and D. S. Childress. (2007). The effects of prosthetic foot roll-over shape arc length on the gait of trans-tibial prosthesis users. *Prosthetics and Orthotics International* **30**, 286-299.

Weir, J. B. de V. (1949). New methods for calculating metabolic rate with special reference to protein metabolism. *Journal of Physiology* **109**, 1-9.

Whittle, M. W. (1997). Three-dimensional motion of the center of gravity of the body during walking. *Human Movement Science* **16**, 347-355.

Chapter 6

The Metabolically Optimal Foot Shape for Fixed-Ankle Walking

Introduction

Walking with rigidly constrained ankles is a surprisingly common task, resulting from a variety of injuries from sprains and fractures to leg amputation. Whenever the ankle is held fixed, as in the case of casts, orthoses and prostheses, the body loses its natural ability to control ankle moment and vary the center of pressure underfoot. The intact ankle-foot system uses this ability to act like a rolling wheel during the stance phase of walking, with the radius of the wheel roughly 30% of leg length. The shape of this effective wheel is maintained across a wide range of speeds, shoe heel heights, and carried loads (Hansen, 2004a; 2005; 2004b). However, without ankle motion, the lower leg's contact with the ground is determined entirely by the shape and deformation of the bottom of the foot.

Our prior results show that if the foot bottom is rigid and shaped like a circular arc in the sagittal plane, the work performed by the legs on the center of mass (COM work) and the metabolic cost of walking depend strongly upon the arc's radius of curvature (Adamczyk, 2006; Chapter 2). When we varied the curvature of a foot-bottom arc

experimentally, subjects' COM work decreased steadily as the arc's radius of curvature increased, as predicted by a simple dynamic walking model. Metabolic cost was high for small-radius arcs and decreased until moderate radii (about 30% of leg length), but increased again for larger radii. We suspect that COM work and metabolic cost measures differed because the foot shapes we used became very long (fore-aft) for large radii. The extra foot length likely caused a large knee hyperextension moment due to the high moment arm of the ground reaction force about the knee during late stance. This moment would be balanced by extra activity in the hamstrings, which would not affect COM work performed by the legs but would increase metabolic cost.

The dynamic walking model we used to predict how COM work decreases with arc radius of curvature also shows that the cause of the reduced work is actually increasing foot length, not arc radius per se. In fact, Ruina (2005) argued that the model should have similar COM work for any foot contour as long as it is convex, and that the determining factor for COM work is the length of the foot. In our original model and experiment these parameters were linked in order to avoid pivoting on the ends of the foot (Adamczyk, 2006; Chapter 2). However, foot length and arc radius can be varied independently.

The purpose of this study was to differentiate the effects of foot length and foot bottom curvature on the work performed on the COM during human walking, and on the associated metabolic cost. Additionally, this study aimed to determine the most economical length and radius to use for a circular foot bottom shape in fixed-ankle walking. We imposed a rigid, curved foot surface on human subjects, manipulating the radius of curvature and overall length experimentally. We prevented subjects from preserving their usual effective roll-over shapes by rigidly constraining the ankles. We

hypothesized that longer foot shapes would reduce the angular redirection of the center of mass, and would require the least work to be performed on the COM. We hypothesized that shapes of medium length would lead to the lowest metabolic cost, as in our original study (Adamczyk, 2006; Chapter 2). We further hypothesized that the foot shape's radius of curvature would not affect COM work or metabolic cost significantly. We therefore sought to test the hypothesis of step-to-step transitions and center of mass dynamics, as well as to find the best foot bottom shape for fixed-ankle walking.

Methods

We designed an experiment to rigidly constrain ankle motion and impose different arc shapes on subjects' feet, and observed the impact of these changes on COM work and the metabolic cost of walking. We used a simple boot apparatus to fix subjects' ankles in a neutral position. The boot restricted the ankle's dynamic action, allowing us to impose different static shapes on the foot bottom as an experimental manipulation. We measured ground reaction forces (GRF) and metabolic rate while subjects walked on an instrumented treadmill wearing different foot shapes. We compared these data sets to elucidate how changes in foot length and curvature affect work performed on the body center of mass (COM), and how in turn these quantities affect the metabolic cost of walking. Before describing the experiments in more detail, we use a simple model of walking to predict the effects of changes to foot length and radius of curvature.

Model

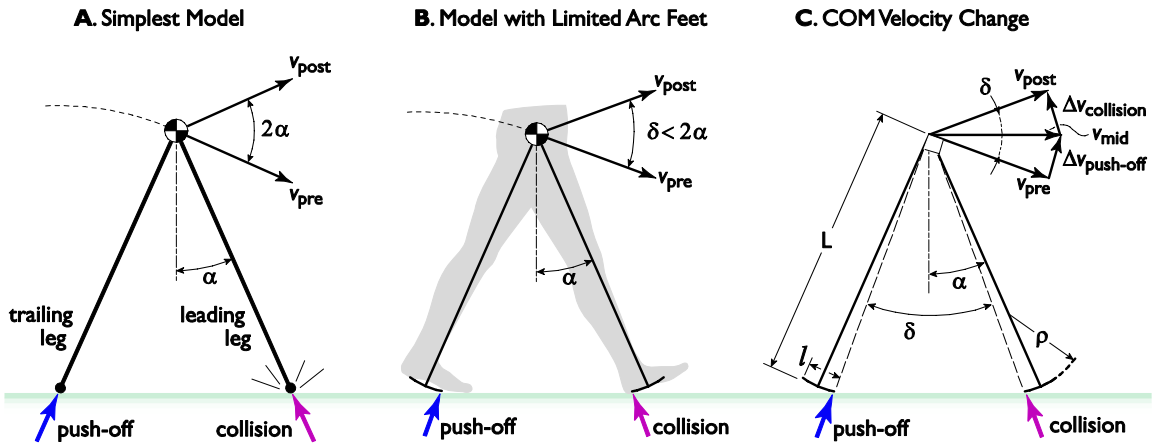

Figure 6.1: Step-to-step transitions in a dynamic walking model with limited foot length. A: The Simplest Model of walking on level ground has all mass concentrated at the pelvis, and only infinitessimal mass in the legs. This model walks with a conservative stance and swing phase, but performs both positive and negative work through push-off *P* and collision *C* at the step-to-step transition in order to redirect the COM velocity from a downward to an upward direction. B: In human walking, or in a model with feet of nonzero length, the angular change in COM velocity is reduced by forces at the toe and heel, away from the axis of the leg. C: The model for analysis has leg length *L* = 1, and feet of length *l* and curvature ρ, expressed as fractions of *L*.

A simple dynamic walking model illustrates the influence of foot length and curvature on step-to-step transitions (Figure 6.1). This model is very similar to a model of walking with arc-shaped feet we have described previously (Adamczyk, 2006; Chapter 2), which is based on the *Simplest Model* of walking on level ground (Kuo, 2001, Figure 6.1A). The model has a point mass at the pelvis, with infinitesimally small point masses at the bases of the feet (Figure 6.1A). Arc-shaped feet are rigidly attached to the leg without an ankle, so that through mid-stance the foot rolls on the ground like a wheel. However, the present model limits the fore-aft length of the foot, so that for leg angles far from vertical the foot ceases rolling and instead pivots on its front or rear edge (Figure 6.1B,C). Whereas the earlier model linked foot length and curvature to avoid pivoting, the present limited-length foot allows us to separate the effects of foot length and curvature.

The dynamic walking model can be powered by an instantaneous push-off impulse applied under the stance foot just before contralateral heelstrike (Figure 6.1B) (Kuo,

2001). This push-off impulse performs positive work on the COM, of magnitude W^+. Immediately thereafter, the collision of swing leg with ground performs negative work, of magnitude W^-. For a periodic gait at steady speed, $W^+ = W^-$.

The step-to-step transitions may be computed as a function of the foot's overall length, l. Push-off and heelstrike impulses are directed from the ground contact points to the COM. These impulses successively redirect the COM velocity. The push-off impulse redirects the COM from its pre-transition velocity v_{pre} to a mid-transition velocity v_{mid}; then the heelstrike impulse redirects the COM to a post-transition velocity v_{post}. A foot of nonzero length reduces the directional change in COM velocity, and the work performed to redirect the COM (Figure 6.1B). For legs at angle $\pm\alpha$ with respect to vertical at the step-to-step transition, and feet with positive radius of curvature ρ and length l (represented by the angle subtended by the foot, λ), the pre-to-post angular direction change δ in COM velocity is less than the angle between the legs 2α. A periodic gait is produced (Kuo, 2002) if this net directional change is shared equally between the push-off and collision impulses (Figure 6.1C). From the geometry of these impulses,

$$\tan\frac{\delta}{2} = \frac{\rho\sin\left(\alpha-\frac{\lambda}{2}\right)+(1-\rho)\sin\alpha}{\rho\cos\left(\alpha-\frac{\lambda}{2}\right)+(1-\rho)\cos\alpha}. \qquad (6.2)$$

A small angle approximation for α and λ and the foot length relationship $\rho\lambda \approx l$ yield

$$\tan\frac{\delta}{2} \approx \alpha - \frac{l}{2}. \qquad (6.3)$$

Note that the foot length term subsumes the effect of arc radius ρ in this linear approximation.

The magnitude W^- of the negative work performed each step by the heelstrike collision is equal to the change in kinetic energy:

$$W^- = \frac{1}{2}Mv_{\text{mid}}^2 - \frac{1}{2}Mv_{\text{post}}^2 . \qquad (6.4)$$

The geometric relationship between v_{mid} and v_{post} (see Figure 6.1C) yields

$$W^- = \frac{1}{2}Mv_{\text{post}}^2 \tan^2\frac{\delta}{2} . \qquad (6.5)$$

The overall trend is revealed by substituting Equation 6.3 into Equation 6.5:

$$W^- = \frac{1}{2}Mv_{\text{post}}^2 \left(\alpha - \frac{l}{2}\right)^2 . \qquad (6.6)$$

The model therefore predicts the trends in COM velocity change and step-to-step transition work as a function of foot length l. Keeping step length fixed, the step-to-step transition leg angle α is nearly constant over the range of ρ and l applied in our experiment. Keeping walking speed fixed, the post-transition velocity v_{post} is also approximately constant. Again assuming small angles, Equation 6.3 reduces to show that the angular direction change δ in COM velocity decreases approximately linearly with foot length l,

$$\delta \propto C_\delta - l \qquad (6.7)$$

where C_δ is a constant offset. The trend in the magnitude of negative COM work performed simplifies to a similar form,

$$W^- \propto (C_W - l)^2 \qquad (6.8)$$

where C_W is the foot length at minimum negative COM work. For a constant-speed gait, $W^- = W^+$, allowing Equation 6.8 to predict the trend for positive COM work as well. This prediction forms the basis for comparisons to measured data.

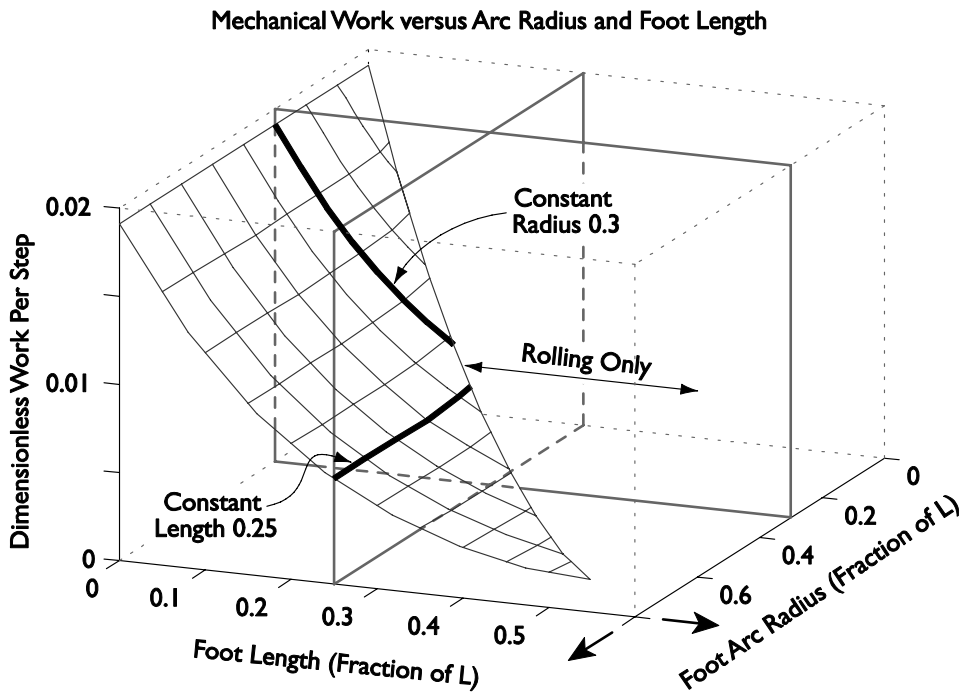

Figure 6.2: The simulation model matches the analytical model's results very closely: the effect of arc radius of curvature is very slight, but work cost decreases dramatically with increasing foot length. At longer foot lengths than required for rolling, cost is constant because the extended heel and toe never contact the ground.

We used numerical simulations to verify the analytical prediction of Equation 6.8. The simulation model includes anthropomorphic leg mass and inertia, as well as a spring about the hip joint in order to produce human-like step frequencies (Kuo, 2001; McGeer, 1990). We examined the model's gait across variations in foot radius of curvature ρ and length l, keeping speed, step length, and other model parameters fixed. We limited our model investigation to foot lengths that lead to pivoting on the corners of the foot, $\lambda \leq 2\alpha$, and to radius of curvature below 0.8 times leg length. For larger foot angles, there is no pivoting at the heel or toe, and the model is identical to that analyzed in (Adamczyk, 2006; Chapter 2).

The model exhibits a consistent decrease in work (i.e., energy cost) with increasing foot length l at constant radius of curvature ρ, but there is no substantial change in cost with varying radius at constant foot length (Figure 6.2). Simulations show that the model

closely follows the curve of Equation 6.8 as foot length increases from zero until the heel and toe edges are not reached during rolling. For feet of constant length, radius of curvature has no meaningful effect on work requirements.

Based on the results of the model, we hypothesized that COM work in human walking would follow the trend of Equation 6.8. We expected COM work to decrease steadily with increasing foot length, but we expected no effect from changes to foot radius of curvature. This expectation is reasonable given that the model in our previous study was a very effective predictor of COM work (Adamczyk, 2006; Chapter 2). However, based on our previous study in which very long foot shapes led to increased metabolic cost in spite of decreased COM work, we expected to observe a minimum in metabolic cost for a foot of intermediate length. We expected no trend in metabolic cost over changes in foot radius of curvature in the modest range tested, though intuition suggests that extremely high radius of curvature (e.g. flat feet) should lead to a higher cost.

Experiment

We measured mechanical work performed on the body's center of mass (COM work) and metabolic rate while 8 adult human subjects walked in rigid boots with soles of different length and curvature. Walking speed was fixed at 1.275 $m.s^{-1}$. All subjects (4 male, 4 female; body mass 72.8 ± 12.5 kg (mean ± standard deviation) ; leg length 0.904 ± 0.062 m) were healthy and had no known gait abnormalities. The study was approved by the local Institutional Review Board and all subjects gave their informed consent prior to participation.

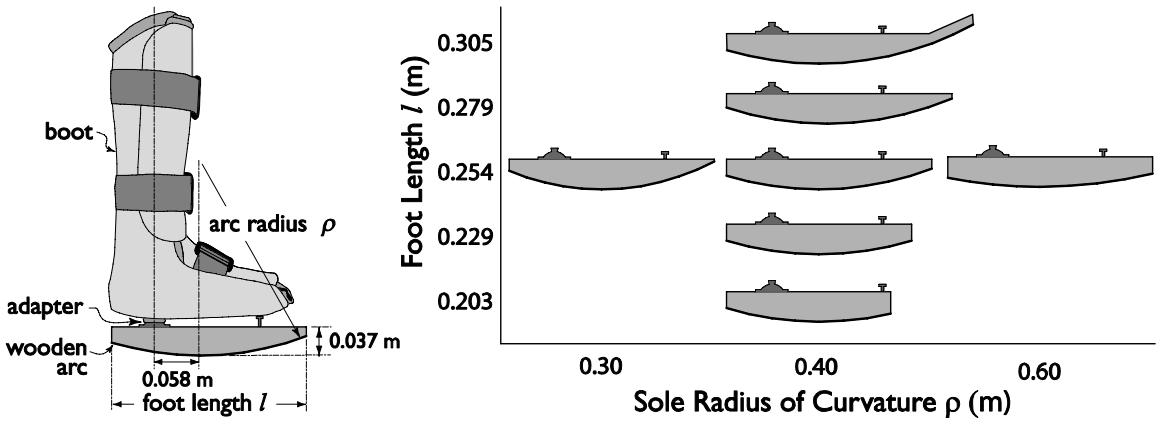

Figure 6.3: Apparatus used to immobilize the ankle and change the roll-over shape of the foot. Wooden arcs were cut in five lengths and three radii of curvature. We hypothesized minimum cost for the medium length and radius.

The experimental apparatus (Adamczyk, 2006; Chapter 2) consisted of a pair of rigid walking boots (PneumaticWalker; Aircast, Inc.; Summit, NJ) modified to accept interchangeable foot surfaces in place of their standard soles (Figure 6.3). The bottom of each boot was replaced with an aluminum plate and pyramidal prosthesis adapter socket. The adapters allowed attachment of foot surfaces (referred to as *arcs*), circular segments as viewed in the sagittal profile, cut from pine wood 0.086 m wide and covered on the bottom surface with SoleFlex shoe sole material 0.0015 m thick (SoleTech, Salem, MA). Pairs of arcs were constructed in seven shapes of different length and/or radius of curvature (see Figure 6.3). Five pairs had radius of curvature 0.40 m, with different heel-to-toe lengths (0.203, 0.229, 0.254, 0.279, and 0.305 m). Two additional pairs had length 0.254 m, with different radius of curvature (0.30 and 0.60 m). Arcs were matched in weight (0.45 ± 0.01 kg, mean ± limits) and standing height (0.037 ± 0.003 m), although moment of inertia could not be precisely matched. All arcs were attached to the same pair of boots for a given subject (boot mass 0.85 kg medium, 1.05 kg large). Arcs were positioned relative to the leg so that the arc center was 0.058 m anterior to the tibial axis (Figure 6.3). This dimension is slightly less than in our previous study (Adamczyk, 2006;

Chapter 2) because of the different geometry of the arcs. Subjects walked with each pair of arcs and in normal street shoes (*normal walking*), with the order of arc conditions randomized for each subject.

Walking speed was held constant at 1.275 $m.s^{-1}$ for all trials. Subjects were allowed to choose their step frequency freely in each condition, in order to ensure that the measured metabolic rate represented the subject's preferred gait in each condition. The freedom to choose step frequency could allow a confounding metabolic effect from the choice to force leg motion differently between conditions (Doke, 2005), but since all the conditions differed only subtly we expected this effect to be small. The mean observed step frequency for experimental conditions ranged from 94% to 100% of the frequency for normal walking.

We measured ground reaction forces (GRFs, see Figure 6.4) and metabolic energy consumption while subjects walked at 1.275 $m.s^{-1}$ for at least 7 minutes on a custom-built split-belt instrumented treadmill. We recorded multiple 30 second trials of GRF data to ensure recording of several clean ground contact periods of each foot on a single side of the treadmill at steady-state. Among the good steps, we kept the seven with the most similar vertical GRF signal on each side and averaged them (processing in MATLAB, The MathWorks, Inc., Natick, MA). We reassembled the average right and left steps of GRF data into a single average stride, beginning with left heel strike and ending with the next left heel strike.

We used GRF data to estimate the COM velocity changes and the average rate of negative mechanical work performed on the COM over the step cycle. We calculated COM kinematics (linear acceleration, velocity, and position) from three-dimensional

GRF data, assuming periodic gait (Whittle, 1997; Donelan, 2002b). The velocity data were then used to derive the maximum angular change δ_{COM} in the direction of COM velocity in the sagittal plane (see Figure 6.5). The COM velocity data were also plotted as a COM hodograph for each condition (Greenwood, 1988). The instantaneous rate of mechanical work performed by each leg on the COM was calculated according to the *individual limbs method* of Donelan (2002b), as the dot product of each leg's GRF and the COM velocity (Figure 6.6). We integrated the combined negative portions of the individual limbs' work rate to find the total negative work W^{-}_{mech} (J) performed during one step. Finally, we multiplied this work by step frequency (Hz) to yield the average rate of negative mechanical work $\dot{W}^{-}_{\mathrm{mech}}$ (in W) performed by the subject on the COM.

We estimated metabolic energy expenditure rate from respiratory gas exchange data collected during the treadmill trials. We used an open-circuit respirometry system (Physio-Dyne Instrument Corp., Quogue, NY) to measure the volume rates of oxygen consumption and carbon dioxide production ($\dot{V}_{\mathrm{O_2}}$ and $\dot{V}_{\mathrm{CO_2}}$, mL·sec^{-1}). Following a 3-minute transient period to allow subjects to reach steady state, we collected and averaged volume rates over at least 3 minutes of each trial. Metabolic energy expenditure rate $\dot{E}_{\mathrm{met}}$ was estimated using the formula

$$\dot{E}_{\mathrm{met}} = 16.48\tfrac{\mathrm{J}}{\mathrm{mL}}\dot{V}_{\mathrm{O_2}} + 4.48\tfrac{\mathrm{J}}{\mathrm{mL}}\dot{V}_{\mathrm{CO_2}}, \quad (6.9)$$

after Brockway (1987) and Weir (1949). Finally, we calculated net metabolic rate by subtracting the metabolic rate of quiet standing. The quiet standing data collection procedure was similar to that of the walking tests, but was performed before any other trials.

Data Analysis

We used angular change in COM velocity, average COM work rate, and metabolic rate to test the simple model's predictions for changes in foot length and arc radius. First, we performed a least-squares fit to the model of Equation 6.7, regressing COM velocity direction change δ_{COM} against foot length l according to

$$\delta_{\mathrm{COM}} = c_{\mathrm{COM}} \cdot l + d_{\mathrm{COM}} \,. \qquad (6.10)$$

Coefficients c_{COM} and d_{COM} accommodate differences between humans and the model, such as knee flexion and duration of step-to-step transition, that can affect measured δ_{COM}.

We regressed subjects' mechanical and metabolic costs against foot length (for conditions with constant arc radius 0.40 m) using a general second order curve fit inspired by the model (Equation 6.8):

$$\text{Curve Fit: } a_l l^2 + b_l + c_l \,. \qquad (6.11)$$

We also regressed mechanical and metabolic costs against arc radius (for conditions with constant foot length 0.254 m) in the same manner, using coefficients a_ρ, b_ρ, and c_ρ. We applied the same form of fit to both mechanical and metabolic costs, $\dot{W}^{-}_{\mathrm{mech}}$and $\dot{E}_{\mathrm{met}}$, adding subscripts "mech" and "met" respectively to distinguish the various coefficients. Finally, we converted the coefficients for each fit into a form similar to Equation 6.8,

$$A(C - x)^2 + G \,, \qquad (1)$$

where x represents the parameter foot length l or arc radius ρ, A is a scaling coefficient and G identifies the curve minimum value at parameter value C.

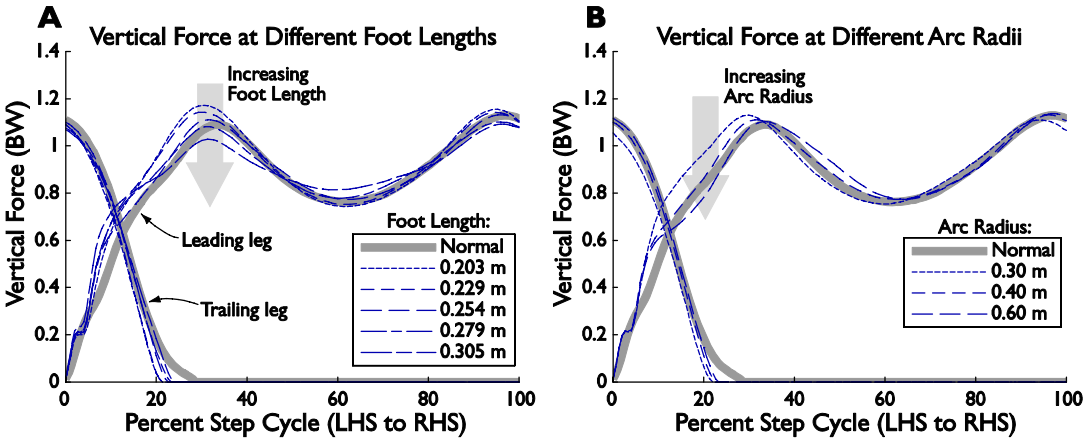

Figure 6.4: Ground Reaction Forces (GRF) across varying foot length and arc radius. A: First peak ground reaction force was reduced as foot length increased. B: Early rate of increase in GRF was reduced by increasing radius.

To account for differences in subjects' body size, we performed all analyses with non-dimensionalized variables. We used base units of total mass M (body plus apparatus), gravitational acceleration g, and natural standing leg length L. Work rate and energy rate were therefore made dimensionless by the divisor $Mg^{1.5}L^{0.5}$; work, energy and moment by MgL; and force by Mg. Foot length and arc radius were non-dimensionalized by L. Work rate and energy rate graphs and model fits are presented in both dimensionless units and in the more common units of W·kg^{-1}. Conversion between these units was performed with the mean factor $g^{1.5}L^{0.5} \approx 29.2$ W·kg^{-1}. We also accounted for inter-subject kinematic and energetic variations by computing offsets d_{COM} and c separately for each subject and then averaging them.

Results

The mechanics and energetics of walking changed significantly as a function of foot length, and slightly with arc radius of curvature. Peak ground reaction forces were reduced with increases in both foot length l and arc radius ρ. The angular direction

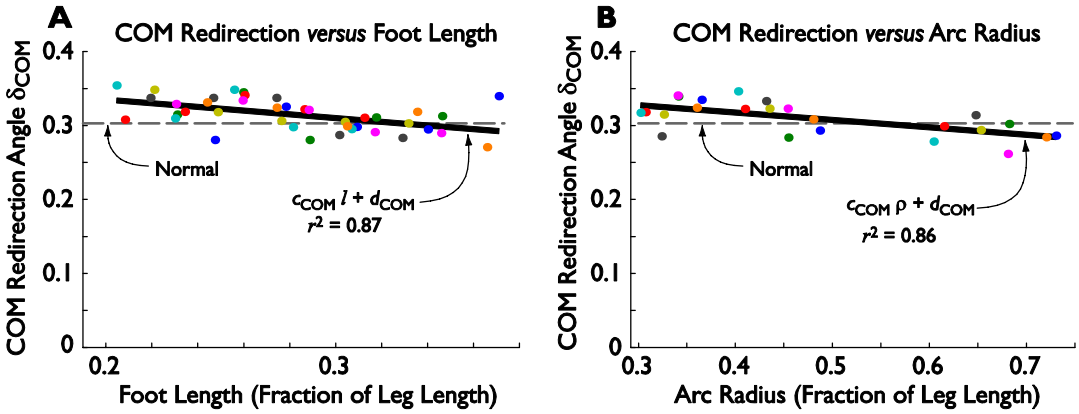

Figure 6.5: Angular redirection of COM velocity *versus* foot length (A) and arc radius of curvature (B). The linear trend is significant in both cases. In previous studies, angular redirection of COM velocity has been a strong predictor of COM work.

change in COM velocity occurring each step also decreased with increasing foot length and arc radius, though the effect was very small across arc radius. The average rate of negative mechanical work performed on the COM also decreased significantly with increasing foot length. Net metabolic rate exhibited a statistically significant minimum as foot length increased. Results for ground reaction forces, COM velocity direction change, COM work rate, and metabolic rate during normal walking and walking with arcs are compared below.

We first verified that the measured mechanical work rate and metabolic rate of normal walking were comparable to values found in previous literature. In normal walking at 1.275 m/s with preferred step frequency 1.86 ± 0.09 Hz, the angular direction change δ_{COM} in COM velocity was 17.3 ± 2.6 deg. Subjects performed negative COM work $\dot{W}^{-}_{\mathrm{mech}}$ at an average rate of 0.543 W·kg^{-1} (non-dimensional value, 0.019). This is equivalent to 0.291 J·kg^{-1} per step, which is slightly lower than previous estimates of 0.31 to 0.36 J·kg^{-1} per step from previous studies (Donelan, 2002a; 2002b), possibly because of differences between over-ground and treadmill walking during mechanics trials.

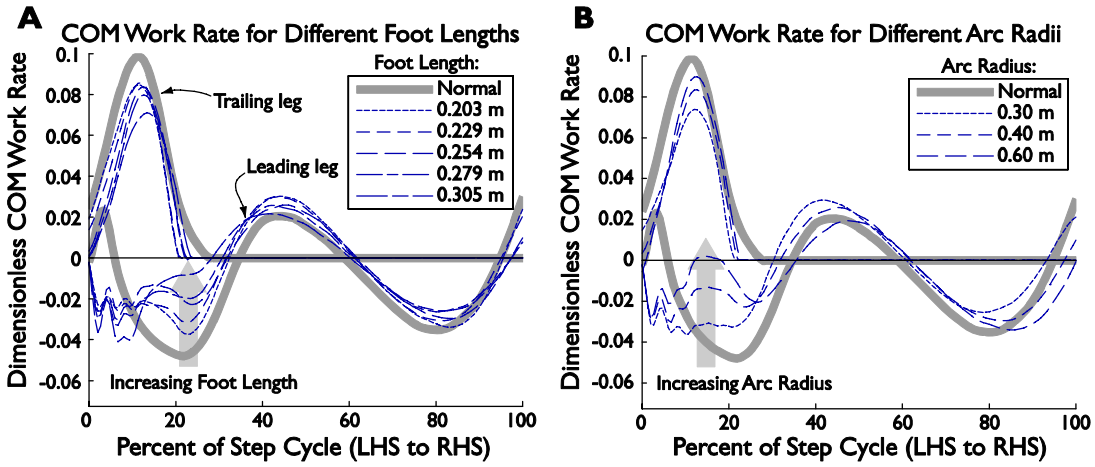

Figure 6.6: COM work rate performed by the two legs over the course of a stride at different foot lengths and arc radii. A: With increasing foot length, positive push-off work and negative collision work both decline. B: With increasing radius, negative collision work declines, but positive push-off work increases. Also, negative work is shifted toward the later "preload" phase of gait.

Average net metabolic rate $\dot{E}_{\text{met}}$ for normal walking was 2.96 W·kg^{-1} (non-dimensional value, 0.101), slightly higher than previous published results (Adamczyk, 2006; Chapter 2), possibly due to the different test conditions required to walk on a split-belt *versus* a single-belt treadmill.

Measured ground reaction forces changed with foot length and with arc radius, and differed from those of normal walking. Vertical forces (Figure 6.4) exhibited slightly greater overlap with higher length and radius, expanding the duration of double support from about 10.5% of the stride (two steps) for the shortest feet (0.203 m length) to 12% for the longest feet (0.305 m), and from 11% for 0.30 m radius feet to 11.5% for 0.60 m radius feet. Vertical force peaks (Figure 6.4) declined with both increasing foot length and increasing arc radius. The early force peak, about 1.17 BW (body weight) for the shortest foot length, decreased to about 1.03 BW for the longest foot length. At constant foot length of 0.254 m, the first peak fell slightly from 1.13 to 1.10 BW as arc radius increased from 0.30 to 0.60 m. The second vertical GRF peak's magnitude also fell slightly with increasing foot length from 1.15 BW to 1.09 BW, but had no distinct trend

with changes in arc radius. In addition, the mid-stance force trough became shallower with increasing foot length, rising from 0.74 BW to 0.81 BW. The trough showed no clear trend with changes in arc radius. Reflecting the relative rigidity of the boot-arc apparatus compared to a normal foot and ankle, the force increased more quickly than normal at the beginning of stance, though the rate decreased thereafter and the first peak vertical GRF occurred only slightly earlier than normal (16.5% versus 17% of the stride cycle). The vertical GRF most similar to normal walking occurred in feet of length 0.254 m and radius 0.40 m.

The observed angular direction change in COM velocity, δ_{COM}, decreased with increasing foot length l ($P < 0.05$, Figure 6.5A) at constant arc radius of curvature ρ = 0.40 m. These data were fit well (r^2 = 0.87) by the linear prediction of Equation 6.10, with coefficients c_{COM} = -14.4 ± 9.5 deg (mean ± 95% Confidence Interval, CI), and d_{COM} = 22.1 ± 2.9 deg. The COM direction change for normal walking intersected with the observed trend at a foot length of about 0.33 times leg length. Angular direction change δ_{COM} in COM velocity also decreased with increasing arc radius ρ ($P < 0.05$) at constant foot length l = 0.254 m, though the trend was much shallower. Angular direction change *versus* arc radius data were fit well (r^2 = 0.86) by a linear trend similar to Equation 6.10, with curve fit slope -6.7 ± 3.8 deg (mean ± 95% Confidence Interval, CI) and intercept 20.5 ± 2.4 deg (Figure 6.5B). The curve fit intersected the angular direction change of normal walking at an arc radius of about 0.55 times leg length.

The relative distribution of COM work throughout the step also changed with foot length (Figure 6.6). We define the collision as the first phase of negative COM work in a step, and push-off as the first phase of positive work starting near the end of the

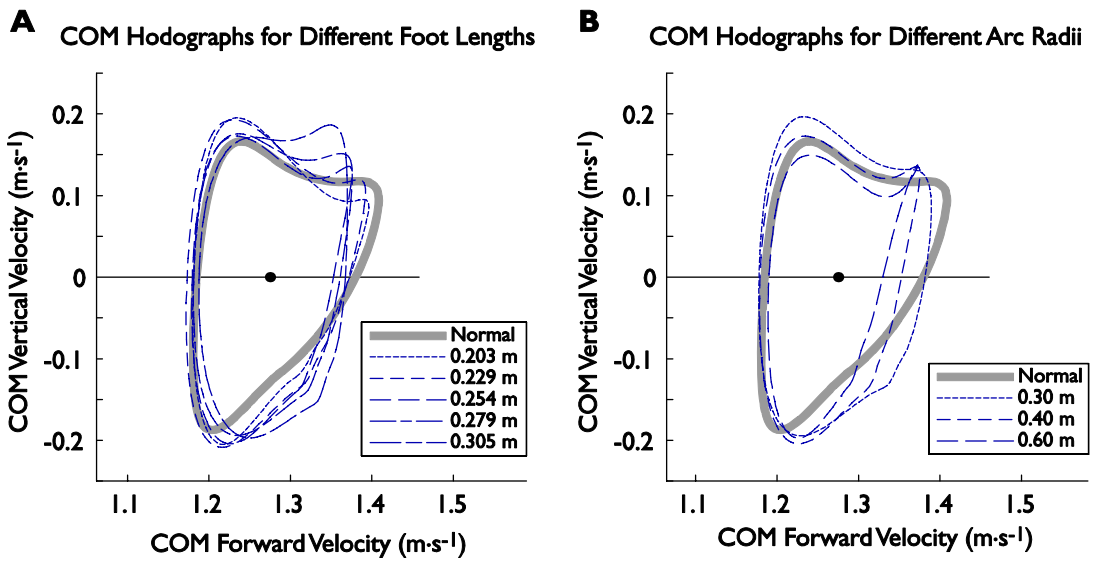

Figure 6.7: COM hodographs for walking in arc feet. A: With increasing foot length hodographs morphed gradually from a pointy, arrow-shaped loop for the shortest feet to a more rectangular loop for the longest feet. Total height of the hodograph also decreased. B: With increasing arc radius, total hodograph height was reduced, but the loop became more pointed in the upper-right section (near toe-off).

preceding step and extending through double support (Kuo, 2005; also see Figure 3.8). Collision negative work performed by the leading leg decreased with increasing foot length l, with early collision work relatively constant and late collision work decreasing such that the collision period ended earlier with longer feet (Figure 6.6A). Push-off positive work rate by the trailing leg also decreased with increasing foot length l, and shifted later for longer feet, possibly helping to lessen the late collision COM work in the leading leg. Subjects performed about the same amount of work during push-off and during collision, allowing single-support positive and negative work in the stance leg to remain roughly constant. Collision negative work also decreased with increasing arc radius of curvature. In this case, however, the work was merely shifted to the later "preload" phase of negative work. Positive push-off work increased with increasing arc radius, the opposite effect from increasing foot length.

COM hodographs changed steadily with increasing foot length and arc radius (Figure 6.7). With increasing foot length, the hodographs decreased in total height and width,

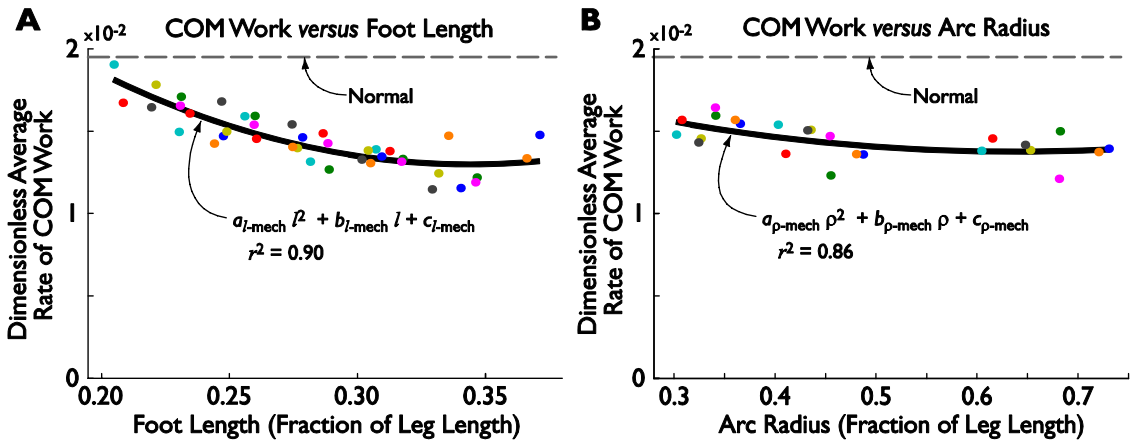

Figure 6.8: Average rate of negative COM work performed by the legs. All arc conditions had work cost considerably lower than Normal. A: Average COM work rate was predicted very well by the model for foot length, $r^2 = 0.90$, and exhibited an apparent minimum within the range of arcs tested. B: Average COM work rate had a shallower relationship with arc radius, decreasing slightly but having very little change overall.

indicating overall smaller changes in COM velocity. The shape of the hodograph also changed from a relatively pointed structure for the shortest feet to a more rectangular contour for the longest feet. With increasing arc radius, total hodograph height and width also decreased, but the hodograph became more pointed as well.

In relation to normal walking, walking on arc feet resulted in a lower average COM work rate but a considerably higher metabolic rate. COM work rate with arcs at 1.275 $m \cdot s^{-1}$ ranged from a high of 0.484 $W \cdot kg^{-1}$ (dimensionless 0.017) for the shortest feet (l = 0.203 m, ρ = 0.40 m) to a low of 0.379 $W \cdot kg^{-1}$ (0.013) for the longest feet (l = 0.305 m, ρ = 0.40 m; Figure 6.8). All arc feet resulted in lower average negative COM work rates than normal walking. However, the Curve Fit to metabolic rate for walking on arcs was always at least 30% higher than the rate for normal walking (Figure 6.9). Net metabolic rate ranged from 3.99 $W \cdot kg^{-1}$ (dimensionless 0.137) for the longest feet (l = 0.305 m, ρ = 0.40 m) to 3.93 $W \cdot kg^{-1}$ (0.130) for the mid-length feet at radius 0.40 m (l = 0.254 m). The curve fit to metabolic cost demonstrated a shallow minimum near arc radius ρ = 0.563

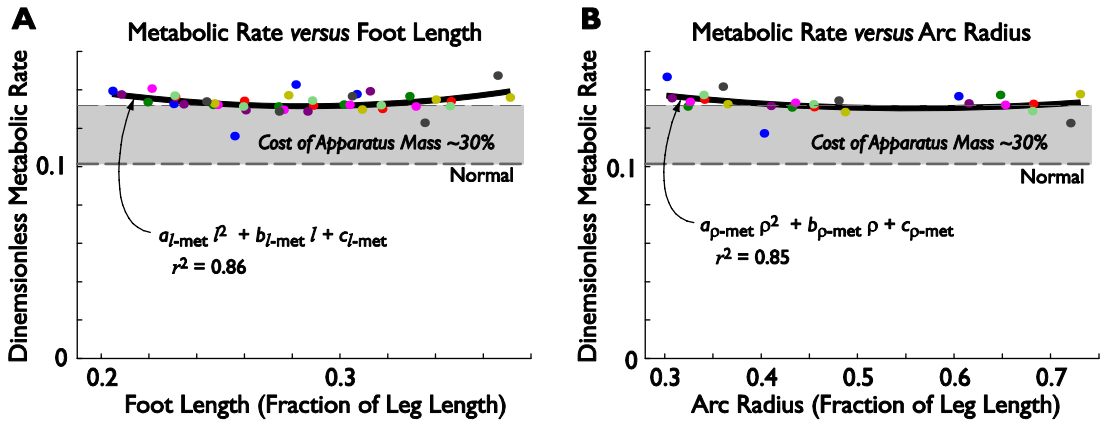

Figure 6.9: Metabolic cost changed significantly with foot length (A) and slightly with arc radius (B). The curve minimum costs indicate that the metabolically optimal circular foot shape for walking with fixed ankles in these conditions is l=0.284, ρ = 0.563. Shaded regions indicate the added cost expected due to apparatus mass and mass distribution, about 30% of the normal walking cost.

times leg length (average dimensional length 0.509 m) and foot length l = 0.284 times leg length (average dimensional length 0.255 m).

The amount of negative COM work performed ($\dot{W}^-_{\text{mech}}$) agreed well with the decreasing quadratic trend across foot length predicted by the dynamic walking model (Figure 6.8, Equation 6.8), and also decreased with increasing arc radius. Overall negative work rate decreased with increasing foot length l ($P < 0.05$), fitting the Curve Fit of Equation 6.11 with an r^2 value of 0.90. The curve fit showed a decline in overall negative COM work rate from 0.529 W·kg^{-1} to a minimum of 0.380 W·kg^{-1} (dimensionless 0.018 to 0.013) as foot length l increased from 0.20 to 0.37 (Figure 6.8). The coefficients of the curve fit are $a_{l\text{-mech}}$ = 7.75 ± 4.83 W·kg^{-1} (mean ± CI, dimensionless 0.265 ± 0.165), $b_{l\text{-mech}}$= -6.32 ± 2.76 W·kg^{-1} (-0.182 ± 0.095), and $c_{l\text{-mech}}$ = 1.29 ± 0.39 W·kg^{-1} (0.044 ± 0.013). The model form (Equation 6.12) of this curve is $\dot{W}^-_{\text{mech}} = 7.75(0.344 - l)^2 + 0.38$ W·kg^{-1}, or in dimensionless form, $0.265(0.344 - l)^2 + 0.013$. Negative work rate did not change significantly with increasing arc radius of curvature ρ (P = 0.33), although the cost did trend downward slightly (Figure 6.8).

Metabolic energy expenditure rate $\dot{E}_{\text{met}}$ also changed quadratically with increasing foot length as predicted (Figure 6.9, Equation 6.8), and exhibited a shallow downward trend with increasing arc radius. Metabolic rate exhibited a significant minimum at moderate foot length l ($P < 0.05$), fitting the Curve Fit of Equation 6.11 with an r^2 value of 0.86. The curve fit showed a decline in metabolic rate (Figure 6.9) from 4.03 W·kg^{-1} at dimensionless foot length 0.20 to a minimum of 3.85 W·kg^{-1} at foot length 0.285, then rose again to 4.06 W·kg^{-1} at foot length 0.37 (dimensionless metabolic rate 0.138, 0.132 and 0.139, respectively). The coefficients of the curve fit are $a_{l\text{-met}}$ = 29.5 ± 26.1 W·kg^{-1} (mean ± CI, dimensionless 1.009 ± 0.894), $b_{l\text{-met}}$= -16.7 ± 14.9 W·kg^{-1} (-0.574 ± 0.511), and $c_{l\text{-met}}$ = 6.22 ± 2.10 W·kg^{-1} (0.213 ± 0.072). The model form (Equation 6.12) of this curve is $\dot{E}_{\text{met}} = 29.5(0.284 - l)^2 + 3.84$ W·kg^{-1}, or in dimensionless form, $1.009(0.284 - l)^2 + 0.132$. Metabolic energy expenditure rate did not change significantly with increasing arc radius of curvature ρ (P = 0.31), though there was a shallow quadratic term in the curve fit, with a minimum cost 3.81 W·kg^{-1} (dimensionless 0. 130) at ρ = 0.563.

Discussion

We investigated the effects of foot length l and foot arc radius of curvature ρ on the mechanical and metabolic costs of walking. Our model of walking with arc-shaped feet predicted an energetic cost based on the work performed on the center of mass (COM) in each step-to-step transition. We predicted that the average rate of COM work would fall with increasing foot length according to Equation 6.8, but arc radius would have no

significant effect. Based on prior results, we also predicted that there would be a minimum in metabolic cost at intermediate foot length.

Foot length does appear to be as important as hypothesized in determining the cost of walking. Even in the limited range of foot lengths we tested, we found a statistically significant trend in both COM work and metabolic cost. The metabolically optimal foot length was found to be 0.284 times leg length, or 0.255 meters on average for these subjects. This length is nearly identical to the mid-length (0.254 m) foot arc in this study. Therefore, we expect that the results measured from the 0.254 m foot arc represent a best-case scenario for walking on rigid circular arcs similar to those used here.

Variation in foot arc radius of curvature does not appear to influence the cost of walking significantly independent of foot length within the range of foot shapes we studied. Arc radius is still important, however, because it interacts geometrically with foot length to determine overall foot shape. At the best foot length in this study (l = 0.254 m), the lowest foot radius that could reach full length in the available height was $\rho_{\min} \approx$ 0.30 m. For radii smaller than $\rho_{\min}$, the foot arc would have to be taller in order to reach the full foot length. In the intended use of the present results in the Rock'N'Lock foot prosthesis, the same effect will influence the overall height of the foot, and this height is constrained by the requirement to match the anatomical foot.

Despite our finding that metabolic cost is not sensitive to arc radius in the roughly anthropomorphic radius range, radius of curvature is still relevant to cost. We tested two additional foot shapes to demonstrate the effect of extremely high arc radius. One shape was nearly flat but slightly convex, having radius of curvature $\rho \approx 5.0$ m, nearly ten times that of any of the other arcs (foot length was 0.229 m). This foot shape let to metabolic

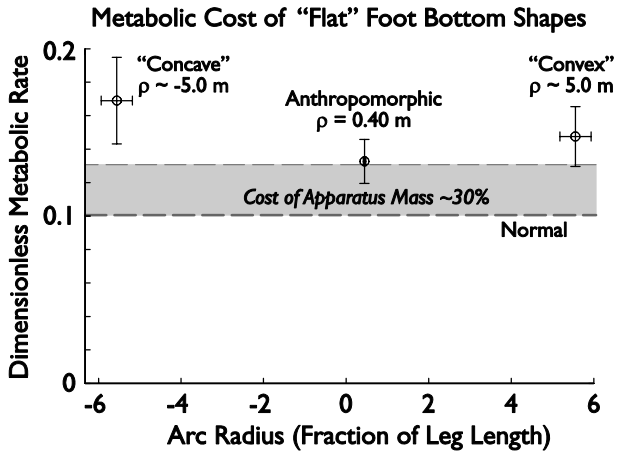

Figure 6.10: Metabolic cost of walking with "nearly flat" foot shapes. Barely convex shapes ($\rho \approx 5.0$ m) led to substantially increased cost from the smooth, anthropomorphic arcs tested in the main experiment. Barely concave shapes ($\rho \approx -5.0$ m) led to even higher cost. Data are mean and standard deviation for each condition, across all subjects. Results show that a smooth rolling effect is important, even though cost is not very sensitive to variations in foot radius near the anthropomorphic region (Figure 6.9). The three conditions shown had foot length 0.229 m.

cost of 4.31 ± 0.52 $W \cdot kg^{-1}$ (dimensionless 0.148 ± 0.018), which is 46% greater than the cost of normal walking, and 14% and 8% greater than the cost of the best and worst smooth arc conditions, respectively (Figure 6.10, "Convex"). The other shape had the same foot length and curvature but was cut to be concave instead ($\rho \approx$ -5.0 m), so that it achieved contact with the ground only at heel and toe (Figure 6.10, "Concave"). This foot shape led to metabolic cost of 4.94 ± 0.76 $W \cdot kg^{-1}$ (dimensionless 0.169 ± 0.026), which is 67% greater than the cost of normal walking, and 30% and 24% greater than the cost of the best and worst smooth arc conditions. These additional tests demonstrate that conspicuously unfavorable curvature does substantially increase walking cost. Thus, the smooth rolling effect noted by Hansen in natural systems (2000, 2004a, 2004b, 2005) and mimicked in our main experiment is beneficial in comparison to an excessively rapid transition from heel to toe contact.

This study did not address the use of foot bottom shapes in which arc radius is not constant – that is, shapes that are not circular arcs. Research has shown that the human

ankle-foot roll-over shape is very well approximated by a circle (Hansen, 2004a, 2005, 2004b), so a circular arc is a good choice for a prosthesis roll over shape. Indeed, many available prostheses have roll-over shapes that are circular (Hansen, 2000). However, our results show that the cost of walking is insensitive to changes in radius of a circular foot, so it is unlikely that varying radius of curvature within a single foot will affect cost dramatically. Nonetheless, it may be possible to find a foot bottom shape that uses varying radius of curvature to perform better than a circular arc. Our mechanical model of walking suggests that foot length almost exclusively determines the work required for walking with a convex foot, so more subtle changes in foot shape applied to a human are only likely to affect non-work contributors to energetic cost, such as joint moments. However, similar dynamic walking models predict additional work costs for any feet that are not convex, such as the "concave" condition described above.

The results of this study demonstrate a clear minimum metabolic cost for walking on foot arcs of a certain shape, but it is not clear that walking on arcs can reduce or even approach the cost of normal walking. In this study, the minimum cost predicted by curve fits is about 30% higher than the cost of normal walking (see Figure 6.9), despite the arcs' advantage in lowering mechanical work. One factor that could contribute to this offset is the added mass of the experimental apparatus. The boot and foot arc together added about 1.5 kg at each foot in arc conditions. Considering many studies that measured the cost of adding weight to the legs (see Adamczyk, 2006; Chapter 2), we estimate that a hypothetical mass at the feet could explain an increase of up 30% in cost compared with normal walking. The independent influence of boot and foot arc moment of inertia is estimated to be negligible, on the order of 1% (Adamczyk, 2006; Chapter 2).

An additional factor may have been the novelty of walking on arc-shaped feet. After brief practice sessions, subjects may not have fully adapted to the added mass, restricted ankle motion, smaller ground contact patch, and rigid arcs. Practice may help subjects to improve balance and control, reducing metabolic cost. Novelty may therefore have contributed to the overall cost of walking on arcs, but it did not contribute to the observed trends in cost due to randomized trial order. Factors such as added mass, increased moment of inertia, decreased double-support time, difficulty of balancing on the arcs, the need to compensate for restricted ankle motion, and incomplete adaptation could all contribute to the higher overall cost we measured for walking with arc feet.

References

Adamczyk, P. G., S. H. Collins and A. D. Kuo. (2006). The advantages of a rolling foot in human walking. *Journal of Experimental Biology* **209**, 3953-3963.

Brockway, J. M. (1987). Derivation of formulae used to calculate energy expenditure in man. *Human Nutrition: Clinical Nutrition* **41C, 463-471.**

Doke, J., J. M. Donelan and A. D. Kuo. (2005). Mechanics and energetics of swinging the human leg. *Journal of Experimental Biology* **208**, 439-446.

Donelan, J. M., R. Kram and A. D. Kuo. (2002a). Mechanical work for step-to-step transitions is a major determinant of the metabolic cost of human walking. *Journal of Experimental Biology* **205**, 3717-27.

Donelan, J. M., R. Kram and A. D. Kuo. (2002b). Simultaneous positive and negative external work in human walking. *Journal of Biomechanics* **35**, 117-24.

Greenwood, D. T. (1988). *Principles of Dynamics*. Prentice-Hall, Englewood Cliffs, NJ.

Hansen, A. D. (2000). Prosthetic foot roll-over shapes with implications for alignment of trans-tibial prostheses. *Prosthetics and Orthotics International* **24**, 205-216.

Hansen, A. D., and D. S. Childress. (2004a). Effects of shoe heel height on biologic rollover characteristics during walking. *Journal of Rehabilitation Research and Development* **41**, 547-54.

Hansen, A. D., D. S. Childress and E. H. Knox. (2004b). Roll-over shapes of human locomotor systems: effects of walking speed. *Clinical Biomechanics* **19**.

Hansen, A. D., and D. S. Childress. (2005). Effects of adding weight to the torso on roll-over characteristics in walking. *Journal of Rehabilitation Research and Development* **42**, 381-90.

Kuo, A. D. (2001). A simple model predicts the speed - step length relationship in human walking. *Journal of Biomechanical Engineering* **123**, 264-9.

Kuo, A. D. (2002). Energetics of actively powered locomotion using the simplest walking model. *Journal of Biomechanical Engineering* **124**, 113-20.

Kuo, A. D., J. M. Donelan and A. Ruina. (2005). Energetic consequences of walking like an inverted pendulum: step-to-step transitions. *Exercise Science and Sports Reviews* **33**, 88-97.

McGeer, T. (1990). Passive dynamic walking. *International Journal of Robotics Research* **9**, 68-82.

Ruina, A., J. E. A. Bertram and M. Srinivasan. (2005). A collisional model of the energetic cost of support work qualitatively explains leg sequencing in walking and galloping, pseudo-elastic leg behavior in running and the walk-to-run transition. *Journal of Theoretical Biology* **237**, 170-92.

Weir, J. B. de V. (1949). New methods for calculating metabolic rate with special reference to protein metabolism. *Journal of Physiology* **109**, 1-9.

Whittle, M. W. (1997). Three-dimensional motion of the center of gravity of the body during walking. *Human Movement Science* **16**, 347-356.

Chapter 7

Conclusions

The purpose of this work was to investigate the limits of center of mass work models and computations in determining and predicting the metabolic cost of walking. Very simple models of complex phenomena such as walking are by their nature limited in scope, but they are also helpful in their clarity. In contrast to more complicated musculoskeletal models of walking, which can sometimes include hundreds of parameters and states, the equations for these simple models can be understood in every term. It is this property that allows us to make testable analytical predictions about the properties of human walking.

The two arc foot experiments (Chapters 2 and 6) sought to test what appeared to be an outlandish prediction at the time: that through simple variation of the foot bottom shape, the locomotion cost of an entire person could be affected systematically. Our result that COM work fell substantially below the amount required for normal gait was surprising because the intact body is already so good at minimizing unnecessary work, for example by timing push-off to lead collision in the step-to-step transition. We did not expect that such a simple manipulation could improve on the mechanical cost required

just to move around. The work savings implies that in a hypothetical animal evolved to use a rolling foot, walking could be achieved more cheaply than it is by humans. The caveat is that by fixating the ankle joint we substantially reduced the stability and versatility of the overall locomotor system: subjects could neither run, nor jump, nor even stand still with the boot and arc apparatus on their feet. It appears that in this comparison, the human body is willing to compromise some locomotor energy economy to improve its performance in other tasks (Adamczyk, 2006; Chapter 2).

The second set of arc feet (Chapter 6) were specified in a narrow range of speeds and foot lengths primarily so that we could determine the metabolically optimal foot bottom arc to implement on the Rock'N'Lock foot. Our results indicate that humans exhibit a shallow bowl in metabolic cost with respect to foot length and roll-over radius in the vicinity of anthropomorphic values (Hansen, 2004a). Because only foot length appears to have substantial influence over cost (Figure 6.9), the Rock'N'Lock foot is likely to perform similarly across a wide range of bottom shape designs with constant or variable curvature. The freedom to choose the foot bottom radius of curvature gives designers flexibility, particularly with respect to fitting a Rock'N'Lock mechanism into the dimensions of a human foot. However, the additional results from "nearly flat" feet (Figure 6.10) make it clear that this flexibility has limits – care must be taken to ensure a comfortable, smooth rolling effect in order to achieve a favorable cost.

The match between the predictions of all our dynamic walking models and human experiments in terms of work performed on the center of mass (COM work) suggests that the mechanical behavior of the body in powering gait is well described by these simple models. However, if we seek to apply these results to the gait of amputees, they are

incomplete. Most amputees have lost only one of the two legs, and are left with a structural asymmetry that allows them to power walking in ways our symmetric model and bilateral experiments did not allow. For example, an amputee can use increased push-off by the intact ankle to lower the collision cost on the prosthetic side, or take steps of different length on the two sides. Asymmetric step length is known to occur, and is sometimes actively countered in physical therapy (Nolan, 2003; Hansen, 2007). Because of the asymmetry, it is unclear exactly how well the results of our bilateral experiments transfer to amputees.

Hansen (2007) studied some of the mechanical effects of changing the effective length of a prosthetic foot by cutting gaps in the keel material of an experimental prosthesis to eliminate the stiffness of the toe and forefoot area. As the length of the remaining stiff portion increased from a mid-foot gap to no gap (full-length stiffness), the prosthesis ankle moment and ground reaction force during late stance increased dramatically. Contralateral ground reaction forces in early stance ("collision" forces) decreased with a longer stiff section, as did step length asymmetry in some instances. The decrease in the early vertical ground reaction force (GRF) is consistent with our findings in bilateral non-amputee experiments (Chapter 6), although we did not find higher late GRF for longer feet, possibly because of differences in curvature and rigidity between our wooden arcs and the experimental prosthesis used by Hansen (2007). Comparison of the results from these two studies suggests that some mechanical features of walking on bilateral arc feet, perhaps including reduced COM work, are likely to be observed in unilateral amputees wearing the Rock'N'Lock with a long, favorable arc shape.

Our findings of no average metabolic difference between the Rock'N'Lock foot and the everyday prostheses of our pilot subjects give us hope that with design improvements and full acclimatization, a prosthesis with fixed curvature and appropriate length can lead to energy savings for amputees. Future design improvements should incorporate our findings of an optimal foot length and insensitivity to foot radius of curvature. There will also be improvements in response to feedback from our pilot subjects regarding heel cushioning, prosthesis alignment and ankle flexibility.

We found in Chapter 3 that center of mass velocity change during the step-to-step transition is a quantitative determinant of the work performed on the COM by the legs. Thinking about the work cost of gait in this way should represent a significant step forward in the common understanding of gait energetics. Gait is often viewed in terms of the position or excursion of the center of mass, or alternatively as a set of limb segment and joint trajectories. COM velocity analysis and COM position or excursion analysis are both far simpler than joint and segment analysis. However, COM velocity is also one step closer to the forces and work production that drive gait than COM position is. Changes in COM velocity imply changes in the energetic state of the system, whereas changes in position do not. Therefore it is helpful to think of gait perturbations such as limb weakness or joint fixation in terms of their impact on COM velocity rather than on COM position or excursion, especially if the perturbation's impact on gait energetics is under consideration.

Considering the gait of the amputees in Chapter 4 according to this paradigm, the mid-stance COM forward velocity asymmetry makes it clear that these amputees are using more work than non-amputees to accelerate and decelerate the COM between

alternate mid-stance phases. The ongoing negative vertical acceleration at the time of intact heel strike also leads directly to increased work on the COM, as the intact limb has to stop a faster fall of the COM than it normally would. This negative acceleration is the result of weak push-off on the prosthetic side. Any intervention that can replace this push-off, or otherwise stop or reverse the fall of the COM prior to heel strike, is likely to decrease COM work for amputees, specifically in the collision phase on the intact side.

The Rock'N'Lock foot appears to perform this function. All subjects in Figure 5.4 have vertical COM velocity that is less negative at the time of intact heel strike when walking on the Rock'N'Lock foot as compared to their everyday prosthesis. Though there are other features of the hodograph that are very strange and need to be better understood, this feature should help lower the work requirements of the intact limb. The likely mechanism for this decrease in falling velocity is simply the rigidity of the forefoot and toe of the Rock'N'Lock foot, which support the weight of the body better than other feet do. When the ground reaction force moves out to this extreme end of a prosthetic foot, compliant feet flex substantially and provide less support. The Rock'N'Lock foot does not give way, but rather prevents the COM from falling more steeply.

It is our hope that future design refinement of the Rock'N'Lock foot can eliminate its unhelpful features and optimize its energetic benefits. We hope to replace the energetic benefits of the amputated leg's lost push-off work just by offering improved body weight support throughout the late stance period and the step-to-step transition.

References

Adamczyk, P. G., S. H. Collins and A. D. Kuo. (2006). The advantages of a rolling foot in human walking. *Journal of Experimental Biology* **209**, 3953-3963.

Hansen, A. D., and D. S. Childress. (2004a). Effects of shoe heel height on biologic rollover characteristics during walking. *Journal of Rehabilitation Research and Development* **41**, 547-54.

Hansen, A. D., M. R. Meier, P. H. Sessoms, and D. S. Childress. (2007). The effects of prosthetic foot roll-over shape arc length on the gait of trans-tibial prosthesis users. *Prosthetics and Orthotics International* **30**, 286-299.

Nolan, L. et al. (2003). Adjustments in gait symmetry with walking speed in TF and TT amputees. *Gait and Posture* **17**, 142-151.